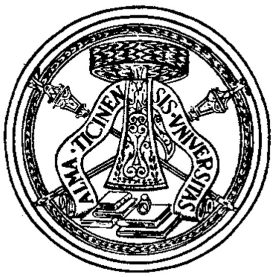

RESPONSE STATISTICS OF UNCERTAIN DYNAMICAL SYSTEMS SUBJECTED TO STOCHASTIC LOADING USING SPARSE GRID COLLOCATION TECHNIQUES

A Dissertation Submitted in Partial Fulfilment of the Requirements for the Master Degree in

Earthquake Engineering and Engineering Seismology

By

JORGE CREMPIEN DE LA CARRERA

Supervisors:
Prof. FERDINANDO AURICCHIO
Prof. CARLO G. LAI
Prof. FABIO NOBILE

December, 2008

Istituto Universitario di Studi Superiori, Università degli Studi di Pavia

The dissertation entitled “Response statistics of uncertain dynamical systems subjected to stochastic loading using sparse grid collocation techniques”, by Jorge Crempien de la Carrera, has been approved in partial fulfilment of the requirements for the Master Degree in Earthquake Engineering.

Ferdinando Auricchio _____

Carlo G. Lai _____

Fabio Nobile _____

ABSTRACT

The objective of this work is to develop robust numerical methods to compute probabilistic response of dynamical systems with uncertain state parameters and uncertain loadings, using the stochastic collocation method. This method is used due to the many advantages it has over Monte Carlo simulations and the straightforward way to parallelize the problem at hand. By probabilistic response, we mean the moments of the problem, as well as probability distribution functions. The stochastic tensor collocation method suffers from the *curse of dimensionality*, which is the exponential growth of the approximating space due to the increase of dimensions in the same. To overcome this problem, it is possible to show that stochastic sparse collocation method converges to the full tensor approximation, as the number of dimensions used grows. This is a great advantage to avoid the computation of large number of realizations.

In this work we did several numerical examples, such as the statistical response of a cantilever beam subjected to a tip force and with material uncertainty. In the range of dynamical mechanical problems, a linear oscillator with uncertain stiffness and damping subjected to a Gaussian stochastic process was solved using random vibration theory. Also a non linear oscillator subjected to a random pulse and a 1d site response analysis considering a random shear velocity profile where problems approached in this work.

ACKNOWLEDGEMENTS

I would like to express my most sincere gratitude to many people, starting from professor Ferdinando Auricchio, for his constant enthusiasm and support in this interesting field of numerical analysis, also for the human qualities that he has shown me during this stay in Pavia. Thank you very much.

To professor Carlo G. Lai, for encouraging me to go further in this topic and for his valuable comments.

This work would not have been possible to achieve withought the seminal inspiration and the help of professor Fabio Nobile. His assistance in the understanding and interpretation was essential.

To Alessandro Reali, for assisting me in many crucial steps during this thesis.

Mom, Dad, Claudia and Christian, I just want to mention that it would have been extremely difficult to continue this work withought your constant support.

Annika, thanks for your patience and understanding during the moments in which this work took away my attention from you.

Last but not least, a special mention to all the friends that I have made in this program. You have been a fountain of inspiration during this time, and I learned many things from you.

TABLE OF CONTENTS

ABSTRACT i

ACKNOWLEDGEMENTS ii

TABLE OF CONTENTS iii

LIST OF FIGURES vii

LIST OF TABLES xii

1. INTRODUCTION 1

1.1 Uncertainties in dynamical systems 1

1.2 Objectives and outline of this dissertation 4

1.3 Brief literature review 4

2. GENERAL PROBABILITY CONCEPTS 7

2.1 Probability spaces 7

2.2 Probability measure 9

2.3 Continuous random variables and vectors 10

2.3.1 Functions of random variables 12

2.3.2 Random vectors 12

2.4 Stochastic processes and random fields 14

2.4.1 Stationary stochastic processes 15

2.4.2 Non stationary separable stochastic processes 15

2.4.3 Modulation functions 17

2.4.4 Simulation of separable processes 18

2.4.5 Evolutionary stochastic processes 19

3. APPROXIMATION AND QUADRATURE OF FUNCTIONS 20

3.1 The space of square integrable functions 20

3.2 Approximation of square integrable functions 21

3.2.1 Polynomial approximation of functions 21

3.3 Quadrature of square integrable functions in $\mathbb{R}$ 26

3.3.1 Gauss formula 26

3.3.2 Gauss-Radau formula 26

3.3.3 Gauss-Lobatto formula 26

3.3.4 Clenshaw-Curtis formula 27

3.4 Interpolation of square integrable functions in $\mathbb{R}^N$ 28

3.4.1 Polynomial approximation of functions 28

3.4.2 Sparse interpolation 30

3.5 Quadrature of square integrable functions in $\mathbb{R}^N$ 31

4. DISCRETIZATION OF RANDOM FIELDS 32

4.1 Series expansion methods 32

4.2 Karhunen-Loève expansion 32

4.3 Galerkin expansion method 34

4.4 Orthogonal series expansion method 38

4.5 Optimal linear estimation method 38

4.6 Expansion optimal linear estimation method 39

5. METHODS TO SOLVE STOCHASTIC DIFFERENTIAL EQUATIONS 41

5.1 Standard definitions 42

5.2 Stochastic collocation approximation 43

5.3 Stochastic Galerkin approximation using double orthogonal polynomials . 44

5.4 Monte Carlo approximation 46

6. SPARSE GRID COLLOCATION METHODS FOR STATIC PROBLEMS 47

6.1 Beams with uncertain mechanical properties 47

6.1.1 Finite elements for beams using a residual formulation 48

7. SPARSE GRID COLLOCATION METHODS FOR DYNAMIC PROBLEMS 58

7.1 Response of linear systems subjected to stochastic Gaussian processes . . . 58

7.1.1 Response of a simple oscillator 59

7.1.2 Response to a stationary process 60

7.1.3 Response of a non-stationary separable process 61

7.2 Response of Bouc-Wen SDOF to random pulses 67

7.3 Site response using 1d SEM 73

8. CONCLUDING REMARKS AND FUTURE RESEARCH 80

8.1 Concluding remarks 80

8.2 Future research 80

REFERENCES 82

LIST OF FIGURES

1.1 Proposed methodology to perform analysis and design of systems with uncertainty. 3

2.1 This figure corresponds to the realization of a Gaussian random field with a Gaussian covariance function in 2D, with $\mu = 0$, $\sigma = 1$ and $L = 10$. 16

3.1 Barycentric Lagrange interpolation of a Saragoni function using only 10 CC nodes. 25

3.2 Barycentric Lagrange interpolation of a Saragoni function using 100 CC nodes. 25

4.1 The first 4 eigenfunctions are plotted along the domain for a exponential covariance function with a correlation length of 1. This was done using a piecewise Galerkin method. 35

4.2 The corresponding eigenvalues are plotted for the exponential covariance function with a correlation length of 1. 35

4.3 The first 4 eigenfunctions are plotted along the domain for a Gaussian covariance function with a correlation length of 1. This was done using a piecewise Galerkin method. 37

4.4 The corresponding eigenvalues are plotted for the Gaussian covariance function with a correlation length of 1. 37

6.1 The beam has a unit length and is loaded at the tip with a concentrated force P. . 48

6.2 The sparse grid using Clenshaw-Curtis nodes for $N = 2$, $L = 2$, $w = 3$. 50

6.3 The realization of the elastic Young modulus along the length of the beam of each point of the previous sparse grid is shown. 51

6.4 The absolute value of the weights assigned to each sparse grid point used before. 51

6.5 Mean (in solid blue) plus minus the standard deviation (in red dashed) of the deflection at the tip of the beam due to a load of $P = 1.5$ (MN). the beam is considered to be elastic. 52

6.6 Mean (in solid blue) plus minus the standard deviation (in red dashed) of the deflection at the tip of the beam due to a load of $P = 1.5$ (MN). the beam is considered to be inelastic, with $\sigma_y = 250$ (MPa). 52

6.7 The surface response of the deflection of the tip of the beam with a load of $P = 1.5$ (MN) for the elastic case. This surface was computed using sparse interpolation techniques and the previous sparse grid where the black dots are the realizations of the sparse grid points. 53

6.8 The surface response of the deflection of the tip of the beam with a load of $P = 1.5$ (MN) for the inelastic case, with $\sigma_y = 250$ (MPa). This surface was computed using sparse interpolation techniques and the previous sparse grid where the black dots are the realizations of the sparse grid points. 53

6.9 The PDF of the deflection at the tip of the beam using a fitting scheme with Beta function with the moments and limits, the K-S density estimation with Monte Carlo simulation using the response surface and finally a Monte Carlo simulation from scratch, also using K-S density estimation. All of these for the elastic case and loaded with $P = 1.5$ (MN). 54

6.10 The PDF of the deflection at the tip of the beam using a fitting scheme with Beta function with the moments and limits, the K-S density estimation with Monte Carlo simulation using the response surface and finally a Monte Carlo simulation from scratch, also using K-S density estimation. All of these for the inelastic case and loaded with $P = 1.5$ (MN) and $\sigma_y = 250$ (MPa). 55

6.11 The 3d sparse grid for the previous problem with the addition of uncertain loading, the load $P \sim \mathcal{U}$ between the values of 1 and 1.5 (MN). $N = 3$ and $w = 5$. . 55

6.12 Expected value (solid blue line) plus minus the standard deviation (dashed red line) of the tip deflection. 56

6.13 Beta PDF estimation, using the first 2 moments as well as the limits and K-S density estimation with the straight forward Monte Carlo simulation, the inelastic case, with $\sigma_y = 250$ (MPa). 56

7.1 SDOF subjected to a dynamic force modelled as a stochastic process. 64

7.2 Sparse grid plot for the possible values of the circular natural frequency and the critical damping ratio with $N = 2$ and $w = 3$. 64

7.3 Realizations of the mean square displacement response in time for each point in the previous sparse grid where the linear oscillator was subjected to a Gaussian process with a gamma envelope. The coefficients of the envelope are $\alpha = 0.18$, $\beta = 0.5$ and $\gamma = 3.55$. 65

7.4 Mean square displacement response in time of a linear SDOF subjected to a nonstationary Gaussian process with uncertain circular natural frequency and critical damping ratio (both distribute uniformly). The coefficients of the envelope gamma are $\alpha = 0.18$, $\beta = 0.5$ and $\gamma = 3.55$. 65

7.5 The absolute value of the weights for every sparse grid point that was considered in the original grid. 66

7.6 A SDOF with a bilinear Bouc Wen model of hysteresis subjected to random pulses. 69

7.7 Possible acceleration pulses applied at the base of the SDOF in figure (7.6). . . 69

7.8 Normalized force-displacement curves of a SDOF oscillator with a Bouc-Wen nonlinear rule due to the previous pulses (in accordance by colors). 70

7.9 Displacement response in time of a SDOF oscillator with a Bouc-Wen nonlinear rule due to the previous pulses (in accordance by colors). 70

7.10 Sparse grid plot of the possible maximum amplitudes and pulse durations using $N = 2$ and $w = 6$. 71

7.11 The expected value (solid blue line), plus minus the standard deviation (dashed red line) of the normalized internal energy due to the random pulses stated before. 71

7.12 Sparse interpolation of the final normalized internal energy where the black dots are the realizations of the sparse grid points. 72

7.13 The estimation of PDF using a Beta fitting method, K-S density estimation combined with Monte Carlo simulation with the response surface and K-S density estimation with straightforward Monte Carlo simulation for the normalized internal energy. 72

7.14 The 1d site conditions and the respective uncertainty in the shear wave speed of each layer. 75

7.15 The 1d soil column is subjected to this Ricker wavelet at the base. 76

7.16 Sparse grid for the possible shear wave velocities of the bi-medium 1d soil column with $N = 2$ and $w = 6$. 76

7.17 Mean (solid blue line), plus minus the standard deviation (dashed red line) of the evolutionary Arias intensity at the free surface due to a Ricker wavelet at the base of the medium. 77

7.18 Response surface of the Arias intensity at the free end using sparse interpolation where the black dots are the realizations of the sparse grid points. 77

7.19 PDF estimation using a Beta fitting method using the first 2 moments and the limits, Monte Carlo simulation combined with K-S density estimation using both the response surface and simulation from scratch. All of witch are due to a Ricker wavelet at the base of the medium. 78

7.20 Absolute value of the weights for each sparse grid point. 78

LIST OF TABLES

3.1 Classical weight functions. 21

3.2 Modified weight functions. 22

1. INTRODUCTION

1.1 UNCERTAINTIES IN DYNAMICAL SYSTEMS

In modern days, there has been a dramatic increase in the numerical capacity of computers, and due to this fact, many numerical methods to solve models of deterministic dynamical problems in the field of mechanics. Since this numerical capacity continues to grow, many researchers have seen the chance to incorporate uncertainty into these dynamical problems, in a attempt to generalize the previous deterministic cases.

Mathematically, a dynamic problem in mechanics can be modelled with a partial differential equation

$$\mathcal{L}u = f \tag{1.1}$$

where $\mathcal{L}$ is a partial differential operator, that depends on the system properties such as geometry conditions and material properties, f is the external loading and u is the response. Uncertainties may be present in the partial differential operator or in the loading, and if either is uncertain, then the response, u, would also be an uncertain quantity. The case in which f is an uncertain external load has been studied extensively for the particular case of $\mathcal{L}$, linear differential operators [Rice, 1944; Parzen, 1962; Lin, 1965]. Equation (1.1) becomes more complicated to solve when $\mathcal{L}$ is uncertain, and the solution methods used for the case of uncertain external loading no longer is valid. Equation (1.1) is known as a stochastic differential equation, which can be ordinary (stochastic ordinary differential equation, SODE), if it depends only on one variable, or partial (stochastic partial differential equation, SPDE), if the arguments of the equation are beyond one.

Once the response is characterized, it will be much easier to make possible designs for these systems, so that they perform in an optimal way.

Since it is important to characterize the probabilistic response, then it is equally important to model the inherent randomness within the forcing terms, as well as the possible uncertainties

in the physical domain of the problem. Among the possible uncertainties there is for example the material properties, geometry and boundary conditions, etc. It is not a trivial task to find a probabilistic model to account for these uncertainties. Several attempts have been made in the case of geotechnical engineering such as the efforts of E.H.Vanmarcke [1977]; Ghiocel and Ghanem [2002]; Lai, Foti, and Rix [2002]. In the field of Mechanics, many contributions have been maid by Graham and Baxter [2000]; Ostoja-Starzewski and Wang [1989] which are more oriented to the microscale level.

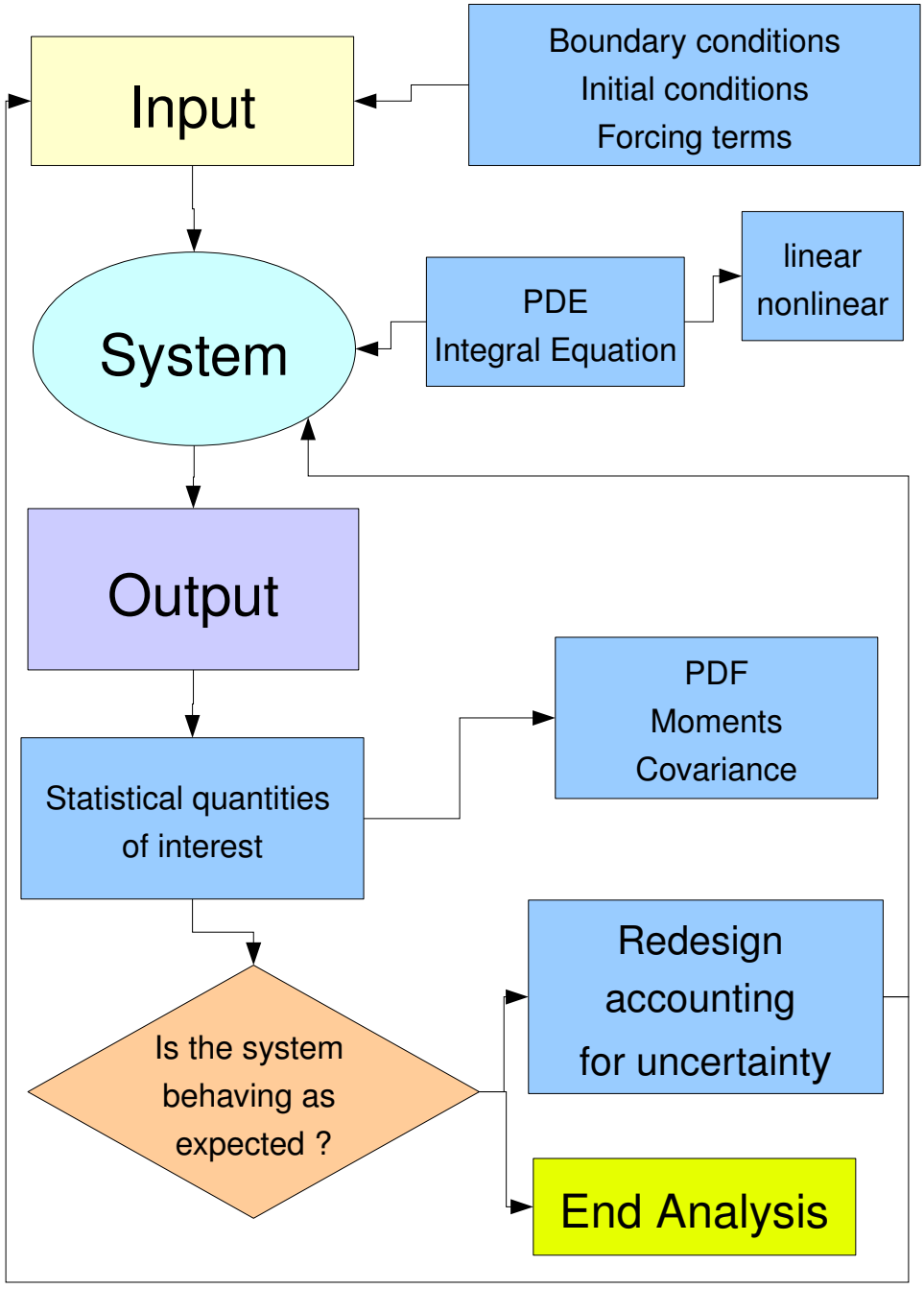

Figure 1.1: Proposed methodology to perform analysis and design of systems with uncertainty.

In figure (1.1) the entire process of analysis considering uncertainties of different types is summarized in this diagram flow. The uncertainty can be present in the Input as well as the System. The system can be a ordinary differential equation, a partial differential equation and a integral equation. The system can also be linear and nonlinear.

1.2 OBJECTIVES AND OUTLINE OF THIS DISSERTATION

The objectives of this dissertation is to develop robust numerical methods to compute the probabilistic response of dynamical systems with uncertain state parameters and uncertain loading, using the sparse collocation technique, because of it's advantages over straightforward Monte Carlo simulation, as well as the easy way to parallelize with the sparse collocation technique. By probabilistic response we mean the probability distribution function of the response, the moments and the covariance or correlation. With this information it is possible to fully characterize the response of systems to later fulfill the ultimate goal, and that is to take an informed decision to improve or optimize the performance of the system at hand.

The organization of this work is started with a brief explanation of general probability concepts in chapter (2) followed by a reminder of the general theory of approximation and quadrature of functions in chapter (3). In chapter (4) there is a review of the different methods present in the literature regarding the methodologies to discretized random fields. In chapter (5) the sparse stochastic collocation method is presented, as well as alternative methods used to solve stochastic differential equations. In chapters (6) and (7) there are several numerical examples using sparse collocation methods to solve static and dynamic problems in the field of mechanics. In chapter (8) final conclusions and possible future topics of research regarding this work are exposed.

1.3 BRIEF LITERATURE REVIEW

In the literature, there are different approaches and uses of numerical solutions intended for the solution of stochastic partial diferential equations. The first problem at hand is to represent the uncertainty of scalar or tensor fields, present in the partial differential operator, or in the forcing terms using random fields. This problem has been tackled by Li and Der Kiureghian [1993], Zhang and Ellingwood [1994], Spanos and Ghanem [1991], etc. All of the methods proposed by these authors assume the knowledge of the autocovariance function of the random field in question.

Most of the numerical approaches that solve stochastic partial differential equations aim at obtaining the moments μ_p (which will be defined in chapter (2)) of the response. Some of the authors that proceed with this methodology are [Ghanem and Spanos, 1991; Babuška, Tempone, and Zouraris, 2004] using a Galerkin approach, and using collocation methods [Babuška, Tempone, and Zouraris, 2004]one can also obtain the moments of the response. These methods perform an approximation in both the physical and probabilistical domain $\mathcal{D} \otimes \Omega$, but the distribution of the response is not obtained, and the only way to obtain it is by performing a Monte Carlo simulation using the obtained approximations, which is already a computational relief compared to a Monte Carlo simulation of the partial differential equation of interest. Nevertheless there are methods that are oriented to obtain the distribution of the response such as the approach of Sett, Jeremić, and Kavvas [2007] and Paez [2006] with the inclusion of nonlinear problems as well.

Galerkin methods were first approached by Jensen and Iwan [1991] and Ghanem and Spanos [1991]. Jensen and Iwan [1991] solved the dynamical response on linear systems, considering a gaussian stochastic process for excitation, and where the system is also characterized with random properties (a random field) Ghanem and Spanos [1991] solved basically for linear static problems. Later on Ghanem [1998] incursioned in different problems such as groundwater flow, etc.

Stochastic collocation methods have the advantage that they are able to solve very easily nonlinear problems because of the decoupling of the SPDE problem, which basically is the computation of N realizations of the SPDE of interest. Many authors have incursioned into this method to solve different problems, where Baldeweck [1999] was the first. Baroth, Bodé, Bressolette, and Fogli [2006]; Baroth, Bressolette, Chauviére, and Fogli [2007] solved it for a nonlinear contact problem, Huang, Mahadevan, and Rebba [2007] used this method to solve a cantilever beam and a plate problem (all linear elastic). Keese and Matthies [2003] have used stochastic collocation methods to solve a stochastic groundwater flow, time varying mechanical problems, etc. Nobile, Tempone, and Webster [2008a] have also solved the problem of ground water flow, but considering a collocation method that incorporate also the influence importance of each random variable in the discretized random field.

There are attempts to solve reliability problems where the limit state function $G(x)$ has as argument the solution of finite element realization problem, and since the general approach in reliability problems is oriented at obtaining the gradient of the limit state function, thus there has been a big effort to compute the sensitivity of the response of finite element models to parameters that define the operator of the partial differential equation. In this field, Zhang and Der Kiureghian [1993]; Haukaas and Der Kiureghian [2005]; Conte and Peng [1997] can be

mentioned as leading researchers of the topic.

2. GENERAL PROBABILITY CONCEPTS

Probabilities are objective measures of the likelihood of occurrence of random events or unknown parameters. The theory of probabilities is a formal way to express typical probability concepts. These formal way is assisted by the rules of mathematics and logic. The first contributers to the theory where Kolmogorov [1956]; Cox [1946].

2.1 PROBABILITY SPACES

The act of performing an experiment to quantify the behavior of a specific random phenomena is defined as a **trial** and the result of the experiment is referred to as an **outcome**. For a given experiment, there is a space of all possible outcomes, which can be determined simply by performing the experiment many times under the same initial conditions. This space will be called a **sample space** (a set), usually represented by Ω in the literature, such that the sample space can be viewed as $\Omega = \{\theta_1, \ldots, \theta_N\}$, where θ_i are all the possible outcomes. It must be noted that the cardinality of the sample space can be discrete or dense and bounded or unbounded, thus if the set is bounded and discrete, then the cardinality of the set will be finite, on the other hand if the set is either unbounded or dense, then the cardinality will be infinite.

Remark 2.1.1. It must be pointed out that since θ_i are just elements that belong to the sample space, $\theta_i \in \Omega$, then $\theta_i \cap \theta_j = \varnothing \; \forall i \neq j$, where $\varnothing$ is the empty set.

There is also the possibility of obtaining more than 1 outcome for each trial that is performed, so it is necessary to define mathematically this possibility in order to group all of these outcomes into a single set.

Definition 2.1.2. An **event** A is defined as a subset of the sample space, $A \subset \Omega$.

An event is allowed to have more than one statement, but in any case it must satisfy that the statements must be connected at all times with logical statements such as **and**, **or**, etc.

Example 2.1.3. Let us observe the random phenomena of coin flipping. There can be 2 outcomes, heads (H) or tails (T). So with no loss of generality, we can define θ_1 as H and θ_2 as T, then $\Omega = \{H, T\}$, which is the sample space.

Example 2.1.4. For a given year, the world cup will only host 3 teams; Italia, Brazil and France. The sample space of the possible champion is $\Omega = \{I, B, F\}$. The sample space for the finalists will be $\Omega = \{IB, BF, IF\}$. If the sample space of the first and second place of the world cup is needed, the sample space increases its cardinality and will become $\Omega = \{IB, BI, BF, FB, IF, FI\}$

Since there are many options to assemble an event A with a given sample space Ω, then it is interesting to define a set that contains all of the possible events.

Definition 2.1.5. A **power set** of Ω is defined as a set that contains as elements of all possible subsets of Ω, and it can be written formally as $\mathcal{P}(\Omega)$. Any subset of $\mathcal{P}(\Omega)$ is called a family of sets of Ω.

Example 2.1.6. If $\Omega = \{A, B\}$, then $\mathcal{P}(\Omega) = \{\{\}, \{A\}, \{B\}, \{A, B\}\}$

So basically, power set can be viewed as an operation over a certain set, and it operates in such a way that it creates a set that contains all the possible combinations of the original set.

Definition 2.1.7. A $\sigma - algebra$ of a given set Ω is a collection Σ of subsets of Ω, that is $A_i \subset \Omega$, such that $\Sigma = \bigcup_{i}^{N} A_i$, that is closed under complementation and satisfies that it's members are countable unions. More formally, a subset $\Sigma \subset \mathcal{P}(\Omega)$ is a $\sigma - algebra$ with the following properties:

1. Σ is nonempty, such that $\varnothing$,$\Omega \in \Sigma$
2. If $A \in \Sigma$, then $A^C \in \Sigma$ is also satisfied, where A^C is the complement of A, that can also be viewed as $\Sigma\ A$.
3. The union of countably many sets in Σ is also in Σ, as well as the intersection.

$$\bigcup_{j=1}^{\infty} A_j, \bigcap_{j=1}^{\infty} A_j \in \Sigma$$

This basically means that a $\sigma - algebra$ is a set that contains some of the possible events that belongs to the power set of the original set, so the definition is not as strong as opposed to the definition of power set.

2.2 PROBABILITY MEASURE

Having in mind the general concepts of power set and $\sigma - algebra$, it is possible to return to the primary interest of measuring certain events.

Definition 2.2.1. Given any set Ω of that represents a sample space, and a $\sigma - algebra$ Σ on Ω, then P is a probability measure if:

1. P is non negative
2. $P(\varnothing) = 0$
3. $P(\Omega) = 1$

Now what rests to do is to define for certain events of interest, the probability measure, taking into account the sample space.

Definition 2.2.2. The probability of an event $A \in \Omega$, such that $A \in \Sigma$ is defined as:

$$P(A) = \sum_{\theta \in A} P(\{\theta\}) \tag{2.1}$$

where P is a measure that needs to be defined a priori taking into account the previous definition and Σ is any of the possible $\sigma - algebra$ that can be formed from the original sample space Ω.

When it comes to quantify the variability of an experiment that is random by nature, then this type of variability is usually referred to as **aleatory variability**, which has to be treated separately from **epistemic variability**. Epistemic variability is the attempt to quantify the variability of a trial that has already taken place, but the results of the trial are unknown. In other words it can be viewed as variability due to the lack of information or knowledge of the system in study.

Example 2.2.3. A very simply yet enlightening example is to roll die in a cup. Before the die are rolled, it would be the case of aleatory uncertainty, but once the die are rolled, the uncertainty turns into epistemic, which can be reduced if you are a cheat, taking little peeks as to gain more knowledge of your hand.

2.3 CONTINUOUS RANDOM VARIABLES AND VECTORS

It is interesting to construct mappings from the sample space Ω to $\mathbb{R}$, given a probability space (Ω, Σ, P), because probability spaces are not directly observable as opposed to the quantifiable values of an experiment.

Definition 2.3.1. A **random variable** η, is a function that maps a sample space into the real numbers and it can be written as follows:

$$\eta : \Omega \to \mathbb{R} \tag{2.2}$$

Since the random variable already has a assigned probability measure P, then it is rather easy to compute the probability of certain simple events, and from there, to define elementary concepts to understand better the behavior of generical random variables.

Definition 2.3.2. The **cumulative distribution function** (CDF) $F_\eta(z)$, is defined as the probability of the event in which the random variable is less or equal than a certain threshold that is in the real numbers, this can be read more formally as:

$$F_\eta(z) = P(\{\theta \colon \eta(\theta) \leq z\}) = P(\eta \leq z) \tag{2.3}$$

with $z \in \mathbb{R}$ and it can be easily checked that this function increases monotonically in the interval of $[0, 1]$ as variable z increases.

From the CDF, another function can be defined, which resembles a "weight" function or mass function, that physically tells where is the value of the random variable more likely to be before the trial is performed.

Definition 2.3.3. The **probability density function function** (PDF) is defined as the derivative of the CDF

$$p_\eta(z) = F'_\eta(z) \tag{2.4}$$

provided that F_η is differentiable at least 1 time.

It can be noted that the PDF is non-negative, and that $\int_{\mathbb{R}} p_\eta(z)dz = 1$, which comes from the previous definition of the P measure.

There is an important operator that maps from the probability space to the real numbers from which many properties of random variables can be defined. This operator is known as **expectation** and it is defined as follows:

$$E[f(x)] = \int_{-\infty}^{\infty} f(x)w(x)dx \tag{2.5}$$

where $w(x)$ is a weight function, that in the future will be assigned as the PDF. With this in mind, the **expected value** of a random variable is:

$$E[\eta] = \mu_1 = \int_{\mathbb{R}} z dF_\eta(z) = \int_{\mathbb{R}} z p_\eta(z) dz \tag{2.6}$$

and a generalization of the **moments** is given by:

$$\mu_p = E[\eta^p], p = 1, 2, \dots \tag{2.7}$$

the **first centered moment**, also known as the variance is:

$$V[\eta] = \mu_2' = E[(\eta - E[\eta])^2] \tag{2.8}$$

and the higher **centered moments** will be:

$$\mu_p' = E[(\eta - E[\eta])^p], p = 1, 2, \dots \tag{2.9}$$

finally, the **standard deviation** is defined as follows:

$$\sigma = \sqrt{V[\eta]} \tag{2.10}$$

with these properties, it is not possible to posses the CDF or PDF of a random variable, but it is possible to have an approximation of the latter functions

Example 2.3.4. A collection of some of the most important distributions is presented.

- Gaussian $\rightarrow \eta \sim N(\mu, \sigma^2)$

$$p_\eta(z) = \varphi(z) = \frac{1}{\sqrt{2\pi\sigma^2}} e^{-\frac{(z-\mu)^2}{2\sigma^2}} \tag{2.11}$$

  $E[\eta] = \mu$ and $V[\eta] = \sigma^2$

- Uniform $\rightarrow \eta \sim \mathcal{U}(a, b)$

$$p_\eta(z) = \begin{cases} \frac{1}{b-a} & \text{for} \quad a \leq z \leq b \\ 0 & \text{otherwise} \end{cases} \tag{2.12}$$

- Exponential $\rightarrow \eta \sim Exp(\lambda)$

$$p_\eta(z) = \begin{cases} \lambda e^{-\lambda z} & \text{for} \quad 0 \leq z \leq \infty \\ 0 & \text{otherwise} \end{cases} \tag{2.13}$$

2.3.1 Functions of random variables

Clearly, a function $g\colon \mathbb{R} \to \mathbb{R}$ that has as an argument a random variable η such that $\zeta = g(\eta)$, then ζ is also a random variable. The CDF is given by:

$$F_\zeta = P(g(\eta) \leq y) = \int_{\mathbb{R}} dF_\zeta(y) = \int_{\mathbb{R}} \mathbf{I}_{[\eta\colon\, g(\eta)\leq y]} dF_\eta(z) \tag{2.14}$$

where $\mathbf{I}_A$ is the **indicator function** of a set $A \subset \mathbb{R}$ such that:

$$\mathbf{I}_A = \begin{cases} 1 & \text{if} \qquad \eta \in A \\ 0 & \text{otherwise} \end{cases} \tag{2.15}$$

from this, the expected value and the variance are respectively:

$$\begin{aligned} E[g(\eta)] &= \textstyle\int_{\mathbb{R}} g(z) dF_\eta(z) \\ V[g(\eta)] &= \textstyle\int_{\mathbb{R}} \left(g(z) - E[g(\eta)]\right)^2 dF_\eta(z) \end{aligned} \tag{2.16}$$

2.3.2 Random vectors

A **random vector** of dimension N, is function $\boldsymbol{\eta}\colon\, [\Omega_1 \times \Omega_2 \ldots \times \Omega_N] \to \mathbb{R}^N$ is defined as a collection of N real valued random variables, such that:

$$\boldsymbol{\eta}(\boldsymbol{\omega}) = \left[\eta_1(\theta_1), \ldots, \eta_N(\theta_N)\right]^T \tag{2.17}$$

Each component of the random vector has a sample space that can be different from each other and to this generic random vector, it is possible to define the **joint cumulative distribution function** (JCDF) as

$$F_\eta(\mathbf{z}) = P(\eta_1 \leq z_1, \ldots, \eta_N \leq z_N) \tag{2.18}$$

The **joint probability distribution function** (JPDF) naturally becomes:

$$p_\eta(\mathbf{z}) = \frac{\partial^N F_\eta(\mathbf{z})}{\partial z_1 \cdots \partial z_N} \tag{2.19}$$

provided that F_η is differentiable. From the previous definitions, it is possible to define the expected value of a random vector.

$$E[\boldsymbol{\eta}] = \int_{\mathbb{R}^N} \boldsymbol{\eta} dF_\eta(\mathbf{z}) \in \mathbb{R}^N \tag{2.20}$$

A useful concept in multivariate analysis is the **covariance matrix**, which is simply:

$$C[\boldsymbol{\eta}] = E[(\boldsymbol{\eta} - E[\boldsymbol{\eta}])(\boldsymbol{\eta} - E[\boldsymbol{\eta}])^T] \in \mathbb{R}^{N \times N} \tag{2.21}$$

this matrix can give information related to two random variables that belong to a random vector. A particular case of this matrix is the variance of each random variable belonging to the random vector, which is basically the diagonal of the covariance matrix.

$$V[\boldsymbol{\eta}] = diag(C[\boldsymbol{\eta}]) \in \mathbb{R}^N \tag{2.22}$$

In multivariate analysis it is very interesting to obtain the CDF or PDF of any component of the random vector, this is referred to as the **marginal distribution function** $F_{\eta_i} : \mathbb{R} \to \mathbb{R}$, which can be computed simply as:

$$F_{\eta_i} = F_{\eta}(\infty, \ldots, \infty, z_i, \infty, \ldots, \infty) \tag{2.23}$$

It is quite clear that $p_{\eta_i} = F'_{\eta_i}$ provided that F_{η_i} is differentiable. The **conditional probability density function**, $\boldsymbol{\eta}_j = [\eta_1, \ldots, \eta_{i-1}, \eta_{i+1}, \ldots, \eta_N]$ can be computed as:

$$p_{\eta_\mathbf{j}|\eta_i}(\mathbf{z_j}|z_i) = \frac{p_\eta(\mathbf{z})}{p_{\eta_i}(z_i)} \tag{2.24}$$

Remark 2.3.5. The random variables $\eta_1, \ldots, \eta_N$ are said to be **independent** if the distribution F_η can be expressed as:

$$F_\eta(z_1, \ldots, z_N) = \prod_{i=1}^{N} F_{\eta_i}(z_i) \tag{2.25}$$

and also the PDF

$$p_\eta(z_1, \ldots, z_N) = \prod_{i=1}^{N} p_{\eta_i}(z_i) \tag{2.26}$$

(a) Change of variables Any random vector $\boldsymbol{\eta}$, with a distribution function $F_\eta(\mathbf{z})$ can be expressed as a deterministic function of N independent random variables ζ_i, $i = 1, 2, \ldots, N$, each with absolutely continuous distribution function $F_\zeta(\mathbf{y})$ i.e. there exists $G : \mathbb{R}^N \to \mathbb{R}^N$ such that $\boldsymbol{\eta} = G(\zeta_1, \ldots, \zeta_N)$ A possible way to construct such a mapping G is by using the **Rosenblatt transformation** [Rosenblatt, 1952]:

$$\begin{aligned}
&F_{\zeta_1}(y_1) = F_{\eta_1}(z_1) \\
&F_{\zeta_2}(y_2) = F_{\eta_2}(z_2|\eta_1 = z_1) \\
&F_{\zeta_3}(y_3) = F_{\eta_3}(z_3|\eta_1 = z_1, \eta_2 = z_2) \\
&\vdots \\
&F_{\zeta_N}(y_N) = F_{\eta_N}(z_N|\eta_1 = z_1, \ldots, \eta_{N-1} = z_{N-1})
\end{aligned} \tag{2.27}$$

From equation (2.27), if the right side is multiplied, as well as the left side and then equated, yields the following result:

$$\prod_{i=1}^{N} F_{\zeta_i}(y_i) = \prod_{i=1}^{N} F_{\eta_N}(z_N|\eta_1 = z_1, \ldots, \eta_{i-1} = z_{i-1}) \tag{2.28}$$

but the right hand side of equation (2.28) is $F_\eta(\mathbf{z})$, the JCDF of $\boldsymbol{\eta}$, and from this result, it is possible to show that every JCDF has a associated at least one transformation such that the JCDF of the transformed random vector $\boldsymbol{\zeta}$ has independent components.

Example 2.3.6.

(b) Diagonalization of the covariance matrix The covariance matrix $C[\boldsymbol{\eta}]$ is a symmetric and positive semi-definite. Hence, it has real eigenvalues $\lambda_1, \ldots, \lambda_N \geq 0$ and a complete set of orthonormal eigenvectors $[\mathbf{v}_1, \ldots, \mathbf{v}_N]$:

$$C[\boldsymbol{\eta}] = VDV^T = \sum_{i=1}^{N} \lambda_i \mathbf{v}_i (\mathbf{v}_i)^T \tag{2.29}$$

with D diagonal and V orthogonal. Assuming that all the eigenvalues λ_i are strictly positive, then it is possible to define the random vector $\boldsymbol{\zeta} = [\zeta_1, \ldots, \zeta_N]$

$$\boldsymbol{\zeta} = D^{-\frac{1}{2}} V^T (\boldsymbol{\eta} - E[\boldsymbol{\eta}]) \Longrightarrow \zeta_i = \frac{1}{\sqrt{\lambda_i}} \mathbf{v}_i \cdot (\boldsymbol{\eta} - E[\boldsymbol{\eta}]) \tag{2.30}$$

It is easy to show that the random variables $\boldsymbol{\zeta}_i$ have zero mean, unit variance and are uncorrelated, but this does not imply that they are independent. A more compact notation of equation (2.30)

$$\Longrightarrow \boldsymbol{\eta} = E[\boldsymbol{\eta}] + VD\boldsymbol{\zeta} \tag{2.31}$$

2.4 STOCHASTIC PROCESSES AND RANDOM FIELDS

Random processes or also known as **Random fields** emerged as a necessity to extend the concept of random variables, because in certain trials, the outcome is not a number, but a function of one or more parameters that posses a certain level of continuity. With this in mind, the definition of a random process is a family of random variables and it can be stated in a more formal way as

Definition 2.4.1. Let $\mathcal{D} \subset \mathbb{R}^d$ be a domain. A **random field** $\kappa(\mathbf{x}, \theta) \colon \mathcal{D} \times \Omega \longrightarrow \mathbb{R}$ is a collection of infinite random variables $\kappa(\mathbf{x}, \theta)$, for each point $\mathbf{x} \in \mathcal{D}$.

Remark 2.4.2. The sample space is considered the same for each random variable assigned to a point in the physical domain, simply for convenience, but in reality, this can clearly change. Another point that can be made out is that the domain is not reserved only to a space domain, it can be any type of domain, such as a time domain, in which the this particular random field is usually denoted as a **stochastic process**, $\kappa(t, \theta)$.

It is clearly quite cumbersome to characterize the infinite collection of random variables that belong to the physical space $\mathcal{D}$, that is why a discrete approach might be more interesting. A random field can be viewed finite dimensional distribution of order n,with n points in the physical domain $\mathcal{D}$ $\mathbf{x}_1, \ldots, \mathbf{x}_n$ or in simple words as a random vector where each component of the vector is associated to a random variable that belongs to the random field. From (2.18) the JCDF is simply

$$F_n(z_1, \ldots, z_n; \mathbf{x}_1, \ldots, \mathbf{x}_n) = P(\kappa(\mathbf{x}_1, \theta_1) \leq z_1, \ldots, \kappa(\mathbf{x}_n, \theta_n) \leq z_n) \tag{2.32}$$

The random process is fully characterized by the distribution functions of any order $n = 1, 2, \ldots$ and any set of points $\mathbf{x}_1, \ldots, \mathbf{x}_n$, provided that they satisfy some consistency and symmetry conditions. The covariance function for two points $\mathbf{x}$ and $\mathbf{y}$ that belong to $\mathcal{D}$ is:

$$C[\kappa(\mathbf{x}), \kappa(\mathbf{y})] = E[(\kappa(\mathbf{x}, \theta) - E[\kappa(\mathbf{x})])(\kappa(\mathbf{y}, \theta) - E[\kappa(\mathbf{y})])] = C_{\kappa\kappa}(\mathbf{x}, \mathbf{y}) \tag{2.33}$$

from (2.33), the variance is simply:

$$V[\kappa(\mathbf{x})] = C[\kappa(\mathbf{x}), \kappa(\mathbf{x})] \tag{2.34}$$

Definition 2.4.3. $\kappa(\mathbf{x}, \theta)$ is said to be a second order random field if

$$V[\kappa(\mathbf{x})] < \infty \tag{2.35}$$

for all $\mathbf{x} \in \mathcal{D}$

Example 2.4.4. In this example, a realization of a random field is performed in figure (2.1), given a Gaussian correlation field function, and considering that the random field is Gaussian.

2.4.1 Stationary stochastic processes

Stationary stochastic models of the gaussian type was first introduced by Housner [1947]. Since then, they have been used by a great number of authors [Bycroft, 1960], [Tajimi, 1960], [Housner and Jennings, 1964] and [Brady, 1966]). Even though these models do not represent accurately what is really happening, they are a good first approximation to estimate the probabilistic response of linear structural systems given that the used frequency content is the predominant of the time history [Tajimi, 1960].

2.4.2 Non stationary separable stochastic processes

Since stationary stochastic processes present limitations, some authors introduced gaussian non stationary stochastic processes, among the ones that can be mentioned are Bolotin [1960], Bogdanoff and Kosin [1961], Goldberg, Bogdanoff, and Sharpe [1964], Amin and Ang [1966],

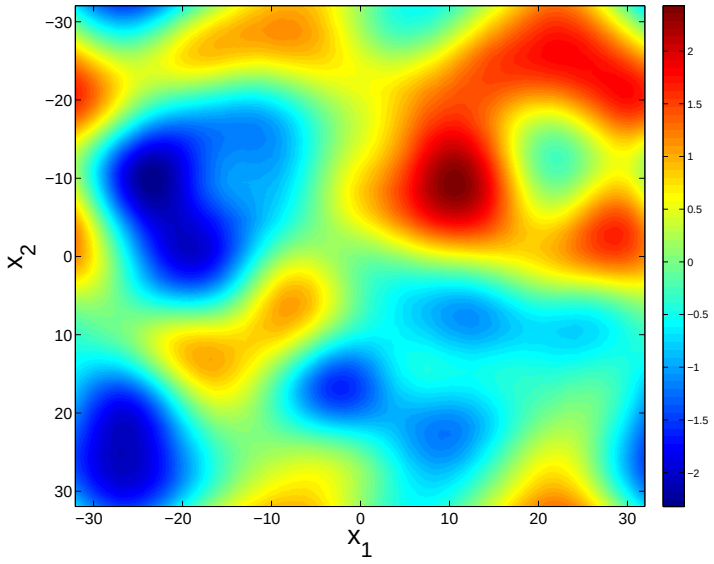

Figure 2.1: This figure corresponds to the realization of a Gaussian random field with a Gaussian covariance function in 2D, with $\mu = 0$, $\sigma = 1$ and $L = 10$.

Shinozuka and Sato [1967], Jennings and Housner [1968] and Iyengar and Iyengar [1969]. It must be noted that these models are just a empirical way to capture the behavior of strong ground motion, based on the observation of real accelerograms. These models are made with a stationary stochastic process, that provides the frequency content, modulated by a deterministic function that multiplies the stationary process to give the amplitude evolution in time.

$$f(t) = \psi(t)s(t,\theta) \tag{2.36}$$

where $\psi(t)$ is the modulating function that provides the variations of amplitude in time, and $s(t)$ is the gaussian stochastic process that provides the frequency content. Some of the basic properties of these processes are as follow:

$$E[s(t,\theta)] = \mu_s(t) = 0 \tag{2.37}$$

$$E[s^2(t,\theta)] = \sigma_s^2(t) = 1 \tag{2.38}$$

The latter yields a non stationary stochastic process $f(t,\theta)$, which in this particular case, is seen as the ground acceleration. Using equations (2.37) and (2.38), the mean of the process can be computed for any moment in time.

$$E[f(t,\theta)] = E[\psi(t)s(t,\theta)] = \psi(t)\mu_s(t) = 0 \tag{2.39}$$

The mean square of the process, that is equal to the variance for each moment is given by:

$$E[f^2(t)] = E[\psi^2(t)s^2(t,\theta)] = \psi^2(t)\sigma_s^2(t) = \psi^2(t) \tag{2.40}$$

This is so because $\sigma_x^2(t) = E[x^2(t,\theta)] - \mu_x^2(t)$ for any process $x(t,\theta)$ and last but not least, the generalized autocorrelation function can be computed as:

$$R_{ff}(t_1,t_2) = E[f(t_1,\theta)f(t_2,\theta)] \tag{2.41}$$

and rearranging the terms yields:sub

$$R_{ff}(t_1,t_2) = \psi(t_1)\psi(t_2)R_{ss}(t_1,t_2) \tag{2.42}$$

where $R_{ss}(t_1,t_2)$ is the autocorrelation function of the stationary process $s(t,\theta)$. Taking the generalized autocorrelation function to the frequency domain, by means of the bivariate Fourier transform, the following can be obtained:

$$\Phi_{ff}(\omega_1,\omega_2) = \frac{1}{4\pi^2}\int_{-\infty}^{+\infty}\int_{-\infty}^{+\infty}\psi(t_1)\psi(t_2)R_{ss}(t_1,t_2)e^{-i(\omega_2 t_2-\omega_1 t_1)}dt_1dt_2 \tag{2.43}$$

and using the Wiener-Kchinchine relationship, the following can be written

$$\Phi_{ff}(\omega_1,\omega_2) = \int_{-\infty}^{+\infty}\Phi_{ss}(\omega)\Psi(\omega_2-\omega)\Psi^*(\omega_1-\omega)d\omega \tag{2.44}$$

where

$$\Psi(\omega) = \frac{1}{2\pi}\int_{-\infty}^{+\infty}\psi(t)e^{-i\omega t}dt \tag{2.45}$$

$\Phi_{ff}(\omega_1,\omega_2)$, determined by equation (2.44) is denoted as the generalized power spectral density function.

2.4.3 Modulation functions

Many modulation functions have been proposed in the literature, and the way to adjust their parameters is also solved differently, depending on the availability and type of the data of the process that needs to be represented.

Bolotin [1984] and Shinozuka [1970], proposed a function that is composed by the difference of two exponential functions.

$$\psi(t) = \sqrt{\beta}(e^{-\alpha t} - e^{-\gamma t}) \tag{2.46}$$

where $\alpha < \gamma$. This function is very inconvenient due to the difficulty to assign the parameters α, β and γ, given any type of data..

A model function that is adjustable to accelerograms is gamma function, proposed by Saragoni and Hart [1974]. This method supposes that the propagation medium can be modeled as a series

of linear oscillators acting in cascade, where each oscillator properties are normally distributed. This model also supposes that the source can be represented by a white noise excitation. Using all of these assumptions, it is possible to arrive to the following expression for the mean square of the process

$$E[f^2(t)] = \psi^2(t) = \beta e^{-\alpha t} t^{\gamma} \tag{2.47}$$

where α, β and γ are constants that can be determined by different ways.

Taking into consideration this model, Arias, Holzapfel, and Saragoni [1976], developed a similar modulating function as the latter, but forcing the condition that the function reaches zero once the process duration time is over. This is why the beta function was selected to represent some random phenomena.

$$\psi(t) = \begin{cases} \sqrt{\beta} \left(\frac{t}{t_f}\right)^{\frac{\alpha}{2}} \left(1 - \frac{t}{t_f}\right)^{\frac{\gamma}{2}} & \text{si} \quad t \leq t_f \\ 0 & \text{si} \quad t > t_f \end{cases} \tag{2.48}$$

Given an accelerogram, the parameters of the gamma and beta method can easily be obtained using the temporal moments of the record.

$$m_{2k} = \int_0^{t_f} t^k f^2(t) dt = \int_0^{t_f} \psi^2(t) t^k dt \tag{2.49}$$

for $k = 0, 1, \ldots, n$.

2.4.4 Simulation of separable processes

A separable stochastic process can be simulated numerically with the following equation:

$$f(t, \theta) = \psi(t) \sum_{k=1}^{m} \sigma_k [U_k \cos(\omega_k t) + V_k \sin(\omega_k t)] \tag{2.50}$$

where $\psi(t)$ is the modulating function, σ_k is the variance of the process at time step k, which is and can be approximated to:

$$\sigma_k^2 = \int_{\omega_k - \frac{\Delta\omega_k}{2}}^{\omega_k + \frac{\Delta\omega_k}{2}} G(\omega) d\omega \approx G(\omega_k) \Delta\omega_k \tag{2.51}$$

U_k and V_k are independent random variables, that distribute normally, i.e.

$$U_k \sim N(0, 1)$$

$$V_k \sim N(0, 1)$$

$G(\omega) = 2\Phi(\omega)$ is the one sided power spectral density for ω in the positive reals and $G(\omega) = 0$ elsewhere

2.4.5 *Evolutionary stochastic processes*

Different techniques have been used to represent the change of statistical properties as well as the change of frequency content in the time domain, such is the case of Liu [1972], who used the instantaneous power spectral density to incorporate both the frequency and the time domain at the same time in the following way:

$$P = \int_0^{t_f} f^2(t) = \int_0^{t_f} \int_{-\infty}^{+\infty} \varphi(t,\omega) d\omega dt \tag{2.52}$$

Saragoni and Hart [1974] used different spectral functions for different intervals of time, but this did not come out right because the sudden changes in the spectral content affected completely the response of simple single degree of freedom oscillators.

$$f(t) = \psi(t) \sum_{i=1}^{n} (H_t(t_{i-1} - t) - H_t(t_i - t)) s_i(t) \tag{2.53}$$

where $\psi(t)$ is the modulating function, $H_t(t)$ is the heavy side step function, and $s_i(t)$ are the stationary stochastic processes.

Hammond [1968], Shinozuka [1970] and Kameda [1980] used a evolutionary spectral function in time using the Fourier-Stiljes transform.

$$f(t) = \int_{-\infty}^{+\infty} A(t,\omega) e^{-i\omega t} dZ(\omega) \tag{2.54}$$

where $Z(\omega)$ corresponds to stationary processes with orthogonal increments amongst themselves and $A(t,\omega)$ is a sigma oscillatory function, that has a spectral density that varies in the time domain. On the other hand, we have the models proposed by Crempien Laborie and Der Kiureghian [1988], that characterizes a process with non stationary amplitude and frequency content, using the theory of sigma oscillatory processes, that is the characterization of non stationary processes as a sum of independent stochastic processes.

$$f(t) = \sum_{k=1}^{m} \psi_k(t) s_k(t) \tag{2.55}$$

where the evolutionary power spectral density in time is given by:

$$\Phi_{ff}(t,\omega) = \sum_{i=1}^{m} \psi_k^2(t) \Phi_{ss}(\omega) \tag{2.56}$$

Amongst these type of models, Conte and Peng [1997] can be pointed out as an improved and natural consequence of Crempien Laborie [1988]. It must be pointed out that both these models are very complicated, and that there is no study in the literature trying to relate the parameters of these models to the parameters of the physical process of rupture, such as stress drops, area of rupture, etc. These methods enlighten the natural phenomena observed in ground motion, but it is very difficult to reproduce with real conditions.

3. APPROXIMATION AND QUADRATURE OF FUNCTIONS

3.1 THE SPACE OF SQUARE INTEGRABLE FUNCTIONS

Let us consider a deterministic function $g\colon \mathbb{R}^N \to \mathbb{R}$ that holds as argument a random vector $\boldsymbol{\eta}\colon \Omega \to \mathbb{R}^N$ that has a joint cumulative density function (JCDF) $F_\eta(\mathbf{z})$, and a density $p_\eta(\mathbf{z})$. It is clear that g is a random variable with

$$E[g] = \int_{\mathbb{R}^N} g(\mathbf{z}) dF_\eta(\mathbf{z}) \quad \text{and} \quad V[g] = E\left[(g(\boldsymbol{\eta}) - E[g])^2\right] \tag{3.1}$$

Definition 3.1.1. The space of square integrable functions in $\mathbb{R}^N$ is defined as

$$L^2_{p_\eta}(\mathbb{R}^N) = \left\{ g\colon \mathbb{R}^N \to \mathbb{R} \text{ such that } \int_{\mathbb{R}^N} g(\mathbf{z})^2 dF_\eta(\mathbf{z}) < \infty \right\} \tag{3.2}$$

and it is a **Hilbert space** with

- Inner product: $\langle f, g \rangle_{L^2_{p_\eta}} = E[fg] = \int_{\mathbb{R}} f(z) g(z) dF_\eta(z)$
- Norm: $\|g\|_{L^2_{p_\eta}} = \sqrt{E[g^2]}$

$L^2_{p_\eta}(\mathbb{R}^N)$ admits an orthonormal basis ψ_i, $i = 0, 1, \ldots$ such that $E[\psi_i \psi_j] = \delta_{ij}$ for all $i, j \geq 0$. Another feature of the functions that belong to this space is that they can be expanded on this basis in the following manner

$$g(\eta) = \sum_{i=1}^{\infty} g_i \psi_i(\eta) \text{ with } g_i = E[g\psi_i] \tag{3.3}$$

and this expansion satisfies that

$$\lim_{n \to \infty} \|g - \sum_{i=0}^{n} g_i \psi_i(\eta)\|_{L^2_{p_\eta}} = 0 \tag{3.4}$$

3.2 APPROXIMATION OF SQUARE INTEGRABLE FUNCTIONS

3.2.1 Polynomial approximation of functions

(a) Construction of a polynomial basis in $\mathbb{R}$ Orthogonality is defined with respect to an inner product, which in turn involves a measure of integration, dF_η. These measures can be absolutely continuous and it can take the following form:

$$dF_\eta(z) = p_\eta(z)dz \quad on \quad \Omega \tag{3.5}$$

where $p_\eta(z)$ is a positive function in Ω which in turn is referred to as the *support* of dF_η. From now on only support functions that are as well PDF functions will be considered. The moments were previously defined as

$$\mu_p = E[\eta^p],\ p = 1, 2, \dots \tag{3.6}$$

and the assumption for the future is that all of these moments exist and they are of finite value. The inner product of two polynomials p and q relative to the measure dF_η is then well defined as:

$$\langle p, q \rangle_{L^2_{p_\eta}} = \int_{\mathbb{R}} p(z)q(z)dF_\eta = E[p(z)q(z)] \tag{3.7}$$

There are classical weight functions $dF_\eta(z) = p_\eta(z)dz$ where some representative ones are summarized in the following table: Now as it can be noticed, these weight functions are not

Table 3.1: Classical weight functions.

name	$p_\eta(z)$	support	comment
Jacobi	$(1-z)^\alpha(1+z)^\beta$	[-1,1]	$\alpha > -1$ and $\beta > -1$
Laguerre	$z^\alpha e^{-z}$	$[0, \infty]$	$\alpha > -1$
Hermite	$\lvert z\rvert^{2\alpha}e^{-z^2}$	$[-\infty, \infty]$	$\alpha > -\frac{1}{2}$
Legendre	1	[-1,1]	

PDF functions, thus it is necessary to redefine them such that orthonormal polynomials can be obtained from them. The orthonormal polynomials can be computed with the following three term recurrence

$$H_{k+1}(\eta) = (\eta - \alpha_k)H_k(\eta) - \beta_k H_{k-1}(\eta) \tag{3.8}$$

, with $H_0(\eta) = 1$ and $H_{-1}(\eta) = 0$ where

$$\begin{aligned} \alpha_k &= \frac{E[\eta H_k^2]}{E[H_k^2]} \\ \beta_k &= \frac{E[H_k^2]}{E[H_{k-1}^2]} \end{aligned} \tag{3.9}$$

Table 3.2: Modified weight functions.

name	$p_\eta(z)$	support	comment
Modified Jacobi	$\frac{z^{\alpha-1}(1-z)^{\beta-1}}{\int_0^1 y^{\alpha-1}(1-y)^{\beta-1}dy}$	[0,1]	$\alpha > 0$ and $\beta > 0$
Modified Laguerre	$\lambda e^{-\lambda z}$	$[0, \infty]$	$\lambda > 0$
Modified Hermite	$\frac{1}{\sqrt{2\pi}\sigma} e^{-\frac{(z-\mu)^2}{2\sigma^2}}$	$[-\infty, \infty]$	$\sigma > 0$
Modified Legendre	1	[0,1]	

It can be seen in the three-term recurrence relation expressed in equation (3.9), the term that defines the series of β_k is not defined for $k = 0$. In the case when the weights are not representing the PDF of a random variable, then the first term of the recurrence relation will be $H_0 = \int_{\mathbb{R}} p_\eta(z)dz = \beta_0$. it must be noted that in the case of a PDF weight function, $H_0 = 1$ as it was stated before.

Placing the coefficients α_k on the diagonal and $\sqrt{\beta_k}$ on the two side diagonals of a matrix produces what is called the *Jacobi matrix* of the measure dF_η,

$$\mathbf{J}(dF_\eta) = \begin{bmatrix} \alpha_0 & \sqrt{\beta_1} & 0 & \dots & 0 \\ \sqrt{\beta_1} & \alpha_1 & \sqrt{\beta_2} & & \\ 0 & \sqrt{\beta_2} & \alpha_2 & \ddots & \\ \vdots & & \ddots & \ddots & \\ 0 & & & & 0 \end{bmatrix} \tag{3.10}$$

The *Jacobi* matrix is clearly tri-diagonal, real, symmetric of infinite order. With this in mind, then the three term recurrence relation can also be written as

$$\sqrt{\beta_{k+1}}\overline{H}_{k+1}(\eta) = (\eta - \alpha_k)\overline{H}_k(\eta) - \sqrt{\beta_k}\overline{H}_{k-1}(\eta) \tag{3.11}$$

, with $\overline{H}_0(\eta) = \frac{1}{\sqrt{\beta_0}}$ and $\overline{H}_{-1}(\eta) = 0$ and it can also be written as:

$$\eta\mathbf{H}(\eta) = J_n(dF_\eta) + \sqrt{\beta_n}\overline{H}_n(\eta)e_n \tag{3.12}$$

with $\mathbf{H}(\eta) = [\overline{H}_0(\eta), \dots, \overline{H}_{n-1}(\eta)]^T$ and J_n are the eigenvalues of the *Jacobi* which are at the zeros of $\mathbf{H}(\eta)$, and $\mathbf{H}(\overline{\eta})$ are the corresponding eigenvectors where $\overline{\eta}$ are the points of the zeros of $\mathbf{H}(\eta)$.

Example 3.2.1. In the following example, well known orthogonal polynomials will be presented

- Uniform random variables, i.e. $\eta \sim \mathcal{U}(-1, 1)$, which are referred to as Legendre polyno-

mials

$$H_{k+1}(\eta) = \frac{2k+1}{k+1}\eta H_k(\eta) - \frac{k}{k+1}H_{k-1}(\eta)$$
$$E[H_i H_k] = \frac{1}{2(k+\frac{1}{2})}\delta_{ik} \tag{3.13}$$

- Gaussian random variables, i.e. $\eta \sim \mathcal{N}(0,1)$, referred to as Hermite polynomials.

$$H_{k+1}(\eta) = \eta H_k(\eta) - kH_{k-1}(\eta)$$
$$E[H_i H_k] = k!\delta_{ik} \tag{3.14}$$

- Exponential random variable, i.e. $\eta \sim Exp(1)$, called Laguerre polynomials

$$H_{k+1}(\eta) = \frac{2k+1-\eta}{k+1}\eta H_k(\eta) - \frac{k}{k+1}H_{k-1}(\eta)$$
$$E[H_i H_k] = \delta_{ik} \tag{3.15}$$

(b) Lagrange polynomial interpolation Let us consider the recent problem where the n couple values (z_i, y_i), with $i \in [1, \ldots, m]$. We are searching for a polynomial $L_m \in \mathbb{P}_m$, referred to as a interpolatory polynomial, such that

$$L_m(z_i) = a_m z_i^m + \ldots + a_1 z_i + a_0 = y_i, \quad i = 0, \ldots, n \tag{3.16}$$

If $n \neq m$, then the problem will be either overdetermined or underdetermined. If $n+1 = m$, then it can be demonstrated that the problem the following theorem.

Theorem 3.2.2. If there is $n+1$ points with its corresponding values such that (z_i, y_i), then there is a unique polynomial $L_n \in \mathbb{P}_n$ that satisfies $L_n(z_i) = y_i$ for $i = 0, \ldots, n$

There is a specific way to find the polynomial that is given by theorem (3.2.2), and it is a the sum of polynomials making up a base that can the whole space where the interpolation takes place. This polynomial base is referred to in the literature as the Lagrange interpolation polynomial.

Definition 3.2.3. The Lagrange polynomial can be defined as:

$$L_n(z) = \sum_{i=0}^{n} y_i l_i(z) \tag{3.17}$$

where $l_i(z) \in \mathbb{P}_n$ is a family of polynomials of order n, such that they form a base in the space of $\mathbb{P}_n$, and it can be written as:

$$l_i(z) = \prod_{\mathbf{j}} \frac{z - z_j}{z_i - z_j} \tag{3.18}$$

for $i = 0, \ldots, n$ and $\mathbf{j} = 0, 1, \ldots, i-1, i+1, \ldots, n$

It is important to compute the error associated with the use of the interpolating polynomial $L_n f(z)$, a polynomial that is interpolating the values $\{y_i\}$ at the nodes $\{z_i\}$, that are related to the successive evaluations of the function $f(z)$ in the nodes.

Theorem 3.2.4. Let us assume the nodes $z_0, \ldots, z_n$, that are going to be used to interpolate the function $f(z) \in C^{n+1}(I_z)$, where I_z is the smallest interval length associated with the nodal points $z_1, \ldots, z_{n+1}$, then the error at any point z of the domain in which the function $f(z)$ is defined will be given by the following expression:

$$E_n(z) = f(z) - L_n f(z) = \frac{f^{(n+1)}(\xi)}{(n+1)!}\nu_{n+1}(z) \tag{3.19}$$

with $\xi \in I_z$ and $\nu_{n+1}(z) = \prod_{i=0}^{n}(z - z_i)$ is the nodal polynomial of degree $n+1$

Remark 3.2.5. It can be shown that the Lagrange polynomials can be written as:

$$L_n(z) = \sum_{i=0}^{n} \frac{\nu_{n+1}(z)}{(z - z_i)\nu'_{n+1}(z_i)} y_i \tag{3.20}$$

Another way to write the same formula is

$$w_j = \frac{1}{\prod_{\mathbf{j}} z_i - z_j} \tag{3.21}$$

then, this will mean that $w_j = 1/\nu'(z)$, and it is possible to come up with

$$l_j(z) = \nu(z)\frac{w_j}{z - z_j} \tag{3.22}$$

therefore, the polynomial that interpolates the data at the nodes can be expressed as

$$L_n(z) = L(z)\sum_{j=0}^{n} \frac{w_j}{z - z_j} y_j \tag{3.23}$$

this new Lagrange formulation is a formula requiring $O(n^2)$ flops for computing quantities independent of z. Trefethen [2004] shows that it is possible to arrive to a rule that depends on the barycentric weights, thus calling itself the barycentric formula.

$$L_n(z) = \frac{\sum_{j=0}^{n} \frac{w_j}{z - z_j} y_j}{\sum_{j=0}^{n} \frac{w_j}{z - z_j}} \tag{3.24}$$

which also has the advantage of letting new data being incorporated in a very easy way.

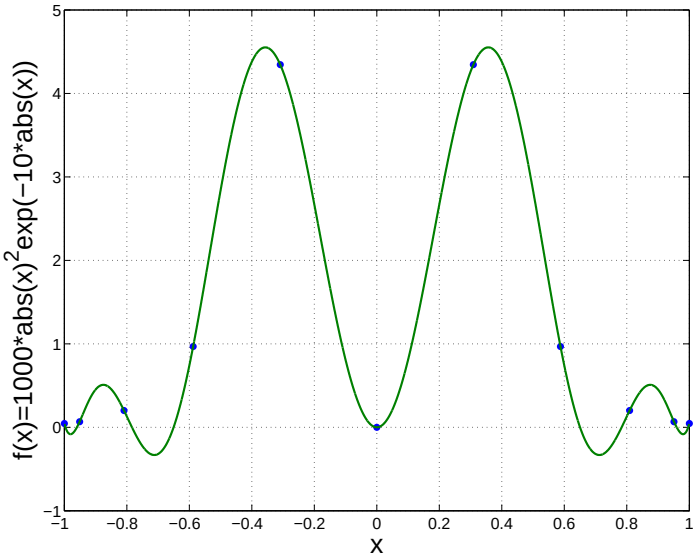

Figure 3.1: Barycentric Lagrange interpolation of a Saragoni function using only 10 CC nodes.

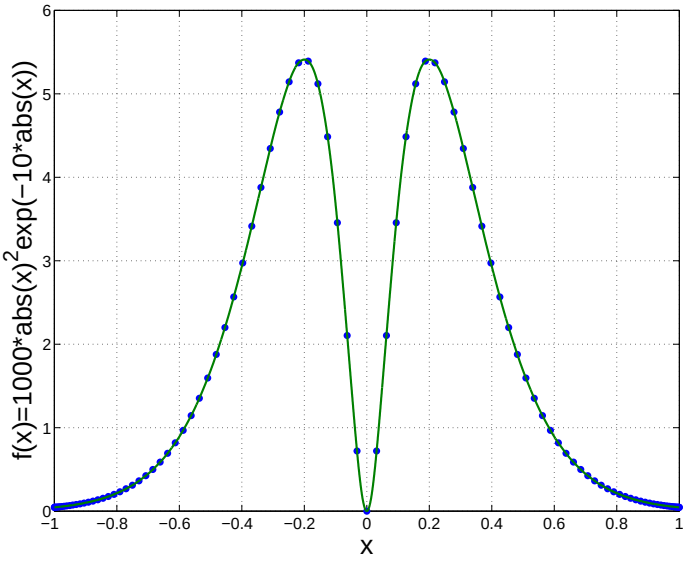

Figure 3.2: Barycentric Lagrange interpolation of a Saragoni function using 100 CC nodes.

In figure (3.1) and (3.2), the Saragoni modulation function is interpolated using 10 and 100 Clenshaw-Curtis nodes. This function has a discontinuity in the first derivative at zero, thus making this function more difficult to approximate, and as it can be seen, the Lagrange interpolation using Clenshaw-Curtis nodes is quite successful.

3.3 QUADRATURE OF SQUARE INTEGRABLE FUNCTIONS IN $\mathbb{R}$

3.3.1 Gauss formula

Given a positive measure dF_η, the n-point Gaussian quadrature formula associated with the measure dF_η is:

$$\int_{\mathbb{R}} f(z)dF_\eta(z) = \sum_{i=1}^{n} \gamma_i f(\tau_i) + R_n(f) \tag{3.25}$$

which has a maximum algebraic exactness of $2n-1$

$$R_n(f) = 0 \quad if \quad f \in \mathbb{P}_{2n-1} \tag{3.26}$$

It is well known that that the nodes τ_i are the zeros of $H(\eta; dF_\eta)$.

3.3.2 Gauss-Radau formula

If there is an interval $[a, \infty]$, $-\infty < a$, containing the support of dF_η, it may be desirable to have an $(n+1)$-point quadrature rule of maximum degree of exactness that has a as a prescribed node,

$$\int_{\mathbb{R}} f(z)dF_\eta(z) = \gamma_0^R f(a) + \sum_{i=1}^{n} \gamma_i^R f(\tau_i^R) + R_n^R(f) \tag{3.27}$$

Here, $R_n^R(f) = 0$ for all $f \in \mathbb{P}_{2n}$ and τ_i^R are the zeros of $H(\eta; dF_{\eta_R})$ where $dF_{\eta_R} = (z-a)dF_\eta$. This is called the *Gauss-Radau* formula.

3.3.3 Gauss-Lobatto formula

If the support of dF_η is contained in the finite interval $[a, b]$, it is more attractive to prescribe 2 nodes, the points a and b. Maximazing the degree of exactness subject to these constrains yields the *Gauss-Lobatto* formula,

$$\int_a^b f(z)dF_\eta(z) = \gamma_0^L f(a) + \sum_{i=1}^{n} \gamma_i^L f(\tau_i^L) + \gamma_{n+1}^L f(b) + R_n^{a,b}(f) \tag{3.28}$$

which is written as an $(n+2)$-point formula; $R_n^L(f) = 0$ for $f \in \mathbb{P}_{2n+1}$. The internal nodes τ_i^L are the zeros of $H(\eta; dF_{\eta_L})$ where $dF_{\eta_L} = (z-a)(b-z)dF_\eta$.

Remark 3.3.1. If there is a domain $\Omega = [a, b]$, then a suitable transformation, $\varphi\colon [a', b'] \to [a, b]$, such that $z = \varphi(\xi) = \frac{b-a}{b'-a'}\xi + \frac{ab'+ba'}{b'-a'}$, which can be used to work in a more simple domain, $\Omega' = [a', b']$

$$\Rightarrow \int_a^b f(z)dz = \frac{b-a}{b'-a'}\int_{a'}^{b'} f(\varphi(\xi))d\xi \tag{3.29}$$

3.3.4 Clenshaw-Curtis formula

This method proposed by Clenshaw and Curtis [1960] consists in a simple change of variable $z = \cos(\iota)$, and withought any loss of generality, if the integration intervale is $[-1, 1]$, then the following integral can also be expressed as

$$\int_{-1}^{1} f(z)dz = \int_0^{\pi} f(\cos(\iota))\sin(\iota)d\iota \tag{3.30}$$

the latter integral can be resolved very efficiently using cosine series

$$f(\cos(\iota)) = \frac{a_0}{2} + \sum_{k=1}^{\infty} a_k \cos(k\iota) \tag{3.31}$$

in which case the integral becomes

$$\int_0^{\pi} f(\cos(\iota))\sin(\iota)d\iota = a_0 + \sum_{k=1}^{\infty} \frac{2a_{2k}}{1-(2k)^2} \tag{3.32}$$

where the cosine coefficients are

$$a_k = \frac{2}{\pi}\int_0^{\pi} f(\cos(\iota))\cos(k\iota)d\iota \tag{3.33}$$

thus, one must perform a numeric integration again, and for periodic functions, Fourier-series integrations are very accurate up to the Nyquist frequency, thus the cosine-series integral can be approximated by the discrete cosine transform (DCT)

$$a_k \approx \frac{2}{N}\left[\frac{f(1)}{2} + \frac{f(-1)}{2}(-1)^k + \sum_{n=1}^{N-1} f\left(\cos\left(\frac{n\pi}{N}\right)\right)\cos\left(\frac{nk\pi}{N}\right)\right] \tag{3.34}$$

for $k = 0, \ldots, N$ to later use the explicit quadrature formula. According to Trefethen [2008], this method might have a theoretical lower polynomial degree of accuracy, but nevertheless, it has great performance anyway, comparable to Gauss integration schemes, with the advantage that the nodes are much faster to compute and they posses the advantage that they are nested

knots. If the integration is required over $\mathbb{R}$, then another type of variable transformation will be needed to respect the original integration limits. Boyd proposed a very simple method based on the following transformation $z = L\cot(\iota)$, thus

$$\int_{-\infty}^{\infty} f(z)dz = L\int_{0}^{\pi} \frac{f(L\cot(\iota))}{\sin^2(\iota)}d\iota \tag{3.35}$$

and this equation can be solved simply by performing a trapezoidal rule integration scheme.

$$\int_{-\infty}^{\infty} f(z)dz \simeq L\sum_{n=1}^{N-1} \frac{f(L\cot(\frac{n\pi}{N}))}{\sin(\frac{n\pi}{N})}d\iota \tag{3.36}$$

This method will also render nested points.

3.4 INTERPOLATION OF SQUARE INTEGRABLE FUNCTIONS IN $\mathbb{R}^N$

3.4.1 Polynomial approximation of functions

(a) Construction of a polynomial basis in multiple dimensions Assuming that the random vector $\boldsymbol{\eta}$, that is obtained after approximating by some specific method the random field of interest, has independent components, the JPDF factorises as

$$p_\eta(\mathbf{z}) = \prod_{i=1}^{M} p_i(z_i) \tag{3.37}$$

Let us consider that for each component of the random vector, η_i, and its corresponding density function p_{η_i}, have associated an orthonormal basis $H_1^{(i)}(z_i), \ldots, H_M^{(i)}(z_i)$ of $L^2_{p_{\eta_i}}$. If a multi-index $\mathbf{i} = [i_1, \ldots, i_M] \in \mathbb{N}^M$ is defined, then the previous can be seen in a more compact way

$$H_{\mathbf{i}}(\mathbf{z}) = H_{i_1}^1(z_1)H_{i_2}^2(z_2)\ldots H_{i_M}^M(z_M) \tag{3.38}$$

and $\{H_{\mathbf{i}}, \forall \mathbf{i} \in \mathbb{N}^M\}$ will be an orthonormal basis in $L^2_{p_\eta}(\mathbb{R}^M)$, it is also referred to as a *tensor product basis*.

(b) Interpolation using tensor product spaces

Definition 3.4.1. A tensor product space is defined as

$$\Xi_N^T = span\{H_{\mathbf{i}}, \forall \mathbf{j}(\mathbf{i}) \leq N\} \tag{3.39}$$

So basically a *tensor product space* is the inclusion of approximating terms in each of the components up to the N^{th} term. If in each of the components there is N basis functions, the dimension of the tensor space Ξ_N^T will be N^M, this means that the dimension of the space grows exponentially fast with M, the number of random variables (*the curse of dimensionality*).

- If Ξ_N^T, the space of polynomials of degree at most N in each component of the random vector, then its dimesion will be

$$dim(\Xi_N^T) = (N+1)^M \tag{3.40}$$

- If the space Ξ_N^T corresponds to a constant piecewise approximation over a cartesian partition of $\mathbb{R}^N$ with N intervals in each component of the random vector, then its dimension is

$$dim(\Xi_n^T) = 2^{NM} \tag{3.41}$$

Because of the *curse of dimensionality*, tensor product approximations can be used with few random variables.

(c) Interpolation using sparse product spaces

Definition 3.4.2. A sparse product space is defined as

$$\Xi_N^S = span\{H_{\mathbf{i}}, \forall |\mathbf{j}(\mathbf{i})| \leq N\} \tag{3.42}$$

These type of spaces overcome partially the *curse of dimensionality* while keeping almost the same approximability properties as tensor product spaces.

- The space Ξ_N^S that corresponds to polynomials of total degree at most of N will have the following dimension

$$dim(\Xi_N^S) = \sum_{|\mathbf{j}(\mathbf{i})| \leq N} 1 = \frac{(M+N)!}{N!M!} = \binom{M+N}{l} \ll (1+N)^M \tag{3.43}$$

- In a sparse wavelet space the dimension will be

$$dim(\Xi_N^S) = \sum_{|\mathbf{j}(\mathbf{i})| \leq N} 1 = 2^N \frac{(M+N)!}{N!M!} = 2^N \binom{M+N}{N} \ll 2^{NM} \tag{3.44}$$

for a large M, these relations behave in an asymptotical way. So a sparse projection using a polynomial basis can be constructed as

$$P_N^S g(\boldsymbol{\eta}) = \sum_{j(k)\leq N} g_{\mathbf{k}} H_{\mathbf{k}}(\boldsymbol{\eta}) \tag{3.45}$$

where $g_{\mathbf{k}} = E[gH_{\mathbf{k}}]$, and the amount of this coefficients is equal to the dimension of the approximating space Ξ_N^S

3.4.2 Sparse interpolation

The difference between 2 levels of interpolation is

$$\Delta_i(g) = \mathcal{I}_i(g) - \mathcal{I}_{i-1}(g) \tag{3.46}$$

where $\mathcal{I}_{-1}(g) = 0$

for integers $w \in \mathbb{N}$, the following sets are defined

$$\begin{aligned} X(w,N) &= \{\mathbf{i} \in \mathbb{N}^N, \mathbf{i} \geq 1 : \textstyle\sum_{k=1}^N (i_k - 1) \leq w\} \\ Y(w,N) &= \{\mathbf{i} \in \mathbb{N}^N, \mathbf{i} \geq 1 : w - N + 1 \leq \textstyle\sum_{k=1}^N (i_k - 1) \leq w\} \end{aligned} \tag{3.47}$$

where $|\mathbf{i}| = i_1 + \cdots + i_N$ for $\mathbf{i} \in \mathbb{N}^N$, then the Smolyak formula reads

$$\mathcal{I}^S(w,N)g(\boldsymbol{\eta}) = \sum_{|\mathbf{i}|\in X(w,N)} \bigotimes_{n=1}^{M} \Delta_{i_n} g(\boldsymbol{\eta}) \tag{3.48}$$

This expression can also be written as

$$\mathcal{I}^S(w,N)g(\boldsymbol{\eta}) = \sum_{|\mathbf{i}|\in Y(w,N)} (-1)^{N-|\mathbf{j}|} \binom{M-1}{N-|\mathbf{i}|} \mathcal{I}^T(N) g(\boldsymbol{\eta}) \tag{3.49}$$

where

$$\mathcal{I}^T(N)g(\boldsymbol{\eta}) = \sum_{j_1=1}^{m_{i_1}} \cdots \sum_{j_N=1}^{m_{i_N}} g(\eta_{i_1 j_1}, \ldots, \eta_{i_N j_N}) l_{j_1}(\eta_{i_1}) \cdots l_{j_N}(\eta_{i_N}) \tag{3.50}$$

Hence the sparse interpolation is obtained as a *linear combination* of tensor product interpolations where the set of points where the function is evaluated will be

$$\mathcal{H}(w,N) = \bigcup_{\mathbf{i}\in Y(w,N)} \left(\vartheta^{i_1} \times \ldots \times \vartheta^{i_N}\right) \tag{3.51}$$

with

$$\vartheta^i = \{\eta_{i1}, \ldots, \eta_{im_i}\} \tag{3.52}$$

is the collection of tensor grids used in sparse interpolation.

3.5 QUADRATURE OF SQUARE INTEGRABLE FUNCTIONS IN $\mathbb{R}^N$

In Barthelmann, Novak, and Ritter [2000], it is possible to find different methods to compute integrals using *cubature* methods (the same as *quadratures* but in multiple dimesions). If our integral is in a N-dimensional cube, Λ^N, then the integral of any function can be expressed as

$$I_N(g) = \int_{\Lambda^N} g(\boldsymbol{\eta}) d\boldsymbol{\eta} \tag{3.53}$$

A tensor product cubature is

$$I_N(g_1 \otimes \cdots \otimes g_N) = I_1(g_1) \otimes \cdots \otimes I_N(g_N) \tag{3.54}$$

then the approximation in the i^{th} component is (using any of the previously described $1d$ approximations methods)

$$U^i(g_i) = \sum_{j=1}^{m_i} f(\eta_{ij}) \cdot \gamma_{ij} \tag{3.55}$$

then using (3.54), it is possible to compute numerically (3.53) as

$$(U^{i_1} \otimes \cdots \otimes U^{i_N})(g) = \sum_{j_1=1}^{m_{i_1}} \cdots \sum_{j_N=1}^{m_{i_N}} g(\eta_{i_1 j_1}, \ldots, \eta_{i_N j_N}) \cdot (\gamma_{i_1 j_1} \otimes \cdots \otimes \gamma_{i_N j_N}) \tag{3.56}$$

, which is a tensor cubature. This has the shortcoming that as the dimension of the integral increases, the number of points increases dramatically, thus not making this method efficient. To overcome this shortcoming, sparse interpolation gives the opportunity to developed sparse numerical integration schemes. Let

$$\Delta^i = U^i - U^{i-1} \tag{3.57}$$

$$A(w, N) = \sum_{|\mathbf{i}| \in X(w,N)} (\Delta^{i_1} \otimes \cdots \otimes \Delta^{i_N}) \tag{3.58}$$

or equivalently it can be written as

$$A(w, N) = \sum_{|\mathbf{i}| \in Y(w,N)} (-1)^{w+N-|\mathbf{i}|} \binom{N-1}{w+N-|\mathbf{i}|} \cdot (U^{i_1} \otimes \cdots \otimes U^{i_N})(g) \tag{3.59}$$

thus simply using for each dimension the desired quadrature method, to later use a method that is proven by Babuška, Nobile, and Tempone [2007] and Nobile, Tempone, and Webster [2008a] to be convergent to the tensor case, which decreases the amount of points needed to compute the integral with respect to the full tensor scheme.

4. DISCRETIZATION OF RANDOM FIELDS

The principal concern is to reduce a infinite amount of information (random variables that belong to a random field) to a finite amount of random variables such that the main information of the random field is well represented. The approximate random field does not only need to be well represented, but also with the minimum amount of random variables to decrease the complexity of calculations. In the literature there are many methods which will be presented.

4.1 SERIES EXPANSION METHODS

Let $\kappa(\mathbf{x}, \theta)\colon \mathcal{D} \times \Omega \longrightarrow \mathbb{R}$ be a random field with a certain autocovariance function $C_{\kappa\kappa}(\mathbf{x}, \mathbf{y}) = C[\kappa(\mathbf{x}, \theta), \kappa(\mathbf{y}, \theta)]$, then an approximation can be

$$\kappa_N(\mathbf{x}, \boldsymbol{\omega}) = \sum_{i=1}^{N} \eta_i \phi_i(\mathbf{x}) \tag{4.1}$$

This can be viewed as an expansion of each possible realization of $\kappa(\mathbf{x}, \theta_0)$ over a basis $\{\phi_i\}$, where $\boldsymbol{\eta}_i(\theta)$ are the coordinates of this expansion. This can be done since this is a Hilbert space (Neveu, don have this paper yet), thus it accepts expansions of the sort.

4.2 KARHUNEN-LOÈVE EXPANSION

The Karhunen-Loève expansion of a random field $\kappa(\mathbf{x}, \theta)$ is a spectral decomposition of the autocovariance function, so that there exists a sequence of values $\lambda_1 \geq \lambda_2 \geq \ldots \lambda_k \ldots \geq 0$, with $\lim_{k\to\infty} \lambda_k = 0$ and a corresponding sequence of functions $\varphi_i(\mathbf{x})\colon \mathcal{D} \to \mathbb{R}$, $i = 1, 2, \ldots$ such that

$$\int_{\mathcal{D}} C_{\kappa\kappa}(\mathbf{x}, \mathbf{y}) \varphi_i(\mathbf{y}) d\mathbf{y} = \lambda_i \varphi_i(\mathbf{x}) \tag{4.2}$$

which is a Fredholm integral equation, where the kernel is the covariance function, being bounded, symmetric and positive definite. The eigenfunctions satisfy $\int_{\mathcal{D}} \varphi_i(\mathbf{x}) b_j(\mathbf{y}) d\mathbf{x} = \delta_{ij}$ where δ_{ij} is the Kronecker delta, thus being orthogonal. Now, it is possible to define a sequence of random variables $\eta_i(\theta)$, $i = 1, 2, \ldots$ such that

$$\eta_i(\theta) = \frac{1}{\sqrt{\lambda_i}} \int_{\mathcal{D}} (\kappa(\mathbf{x}, \theta) - E[\kappa(\mathbf{x})]) \varphi_i(\mathbf{x}) d\mathbf{x} \tag{4.3}$$

and if the covariance between the original random field and the Karhunen-Loève expansion of such random field $C[\kappa(\mathbf{x}, \theta), \hat{\kappa}(\mathbf{x}, \theta)]$ is computed, it is possible to conclude that $E[\eta_i \eta_j] = \delta_{ij} = 0$, thus proving that these variables are uncorrelated with zero mean and unit variance and can be viewed as the coordinates of the expansion and of any possible realization. With all this in mind, the random field $\kappa(\mathbf{x}, \theta)$ can be represented as the infinite series

$$\kappa(\mathbf{x}, \theta) = E[\kappa(\mathbf{x})] + \sum_{i=1}^{\infty} \sqrt{\lambda_i} \varphi_i(\mathbf{x}) \eta_i(\theta) \tag{4.4}$$

thus creating a separation of the space and the random variables of the field $\kappa(\mathbf{x}, \theta)$. The Karhunen-Loève expansion has very interesting properties, such as:

- Due to non accumulation of the eigenvalues around a zero value, it is possible to order the terms of the expansion in descending way, such that if a truncation of the series defined in (4.4) gives an approximated Karhunen-Loève expansion

$$\kappa_N(\mathbf{x}, \boldsymbol{\omega}) = E[\kappa(\mathbf{x})] + \sum_{i=1}^{N} \sqrt{\lambda_i} \varphi_i(\mathbf{x}) \eta_i(\theta) \tag{4.5}$$

- The covariance eigenfunction basis $\{\varphi(\mathbf{x})\}$ is optimal in the sense of the mean square error

$$err = \int_{\mathcal{D}} E[(\kappa(\mathbf{x}, \theta) - \kappa_N(\mathbf{x}, \theta))^2] d\mathbf{x} \tag{4.6}$$

, resulting from the truncation after the N^{th} term is minimized (with respect to the value of any other complete basis $\{\phi_i(\mathbf{x})\}$).

- The closed form solution for each random variable in (4.3) is easy to obtain, and if $\kappa(\mathbf{x}, \theta)$ is a *Gaussian field*, then each random variable η_i is gaussian, and for this specific case, $\{\eta_i\}$ forms a set of independent standard normal random variables. It can also be proven [Loève, 1977] that the expansion of Gaussian random fields is almost surely convergent (I guess this is very important for time stochastic processes).

- The variance error, after truncating the series in the N^{th} term is given by

$$V[\kappa(\mathbf{x}, \theta) - \kappa_N(\mathbf{x}, \theta)] = \sigma^2(\mathbf{x}) - \sum_{i=1}^{N} \lambda_i \varphi_i^2(\mathbf{x}) = V[\kappa(\mathbf{x}, \theta)] - V[\kappa_N(\mathbf{x}, \theta)] \tag{4.7}$$

The right hand side of the previous equation is always positive, hence the truncated Karhunen-Loève expansion always under-represents the variance of the field.

Example 4.2.1. If there is a covariance function

$$C(x,y) = \sigma^2 e^{-|x-y|} \tag{4.8}$$

with $x \in [0,1]$, then the eigenfunctions will be:

$$\varphi_i(x) = \frac{w_i \cos(\theta_i x) + \sin(\theta_i x)}{\sqrt{\frac{\theta^2}{2} + (1 + \frac{\sin(2\theta)}{2\theta}) + \frac{1}{2}(1 - \frac{\sin(2\theta)}{2\theta}) + \sin^2(\theta)}} \tag{4.9}$$

and where θ_i is related to the eigenvalues and can be obtained from the following equation:

$$2\theta\cos(\theta) + (1-\theta^2)\sin(\theta) = 0 \tag{4.10}$$

It is very easy to obtain these roots with any method, such as the Newton scheme. so then it is possible to obtain the eigenvalues from the following relationship:

$$\theta_i^2 = \frac{2-\lambda_i}{\lambda_i}\sigma^2 \tag{4.11}$$

thus making it possible to characterize the random field represented by the covariance in equation (2.33) using the Karhunen-Loève expansion.

This type of expansion has a limited number of closed form solutions for the set of covariance functions, thus it is necessary to perform other types of numerical expansions to have a spectral representation of the random field given a covariance function.

4.3 GALERKIN EXPANSION METHOD

A *Galerkin*-type procedure was suggested by Spanos and Ghanem [1991] and it consists in defining a complete basis of the Hilbert space $\{\phi_i(\mathbf{x})\}_{i=1}^{\infty} \in L^2_{p_\eta}(\mathcal{D})$. Each eigenfunction of $C_{\kappa\kappa}(\mathbf{x},\mathbf{y})$ may be represented by an expansion of the form

$$\varphi_j(\mathbf{x}) = \sum_{i=1}^{\infty} d_{ij}\phi_i(\mathbf{x}) \tag{4.12}$$

where d_{ij} are the unknown coordinates. The Galerkin procedure aims at obtaining the best approximation of φ_j when truncating the above series after the N^{th} term, which is accomplished

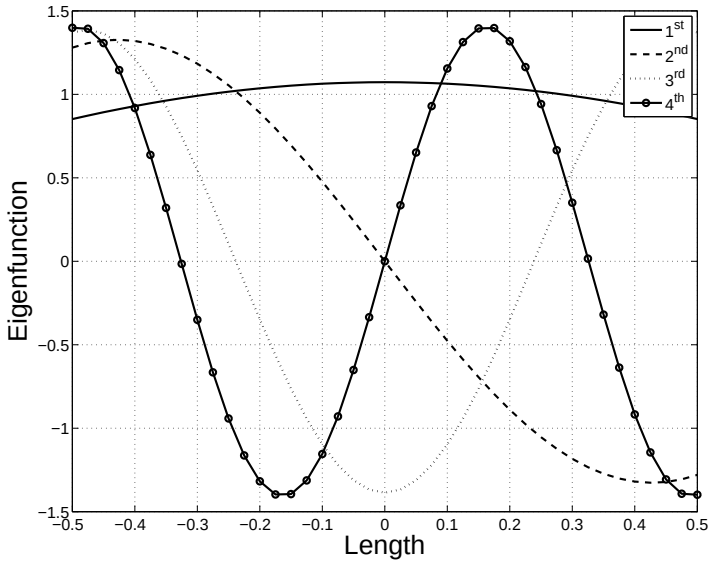

Figure 4.1: The first 4 eigenfunctions are plotted along the domain for a exponential covariance function with a correlation length of 1. This was done using a piecewise Galerkin method.

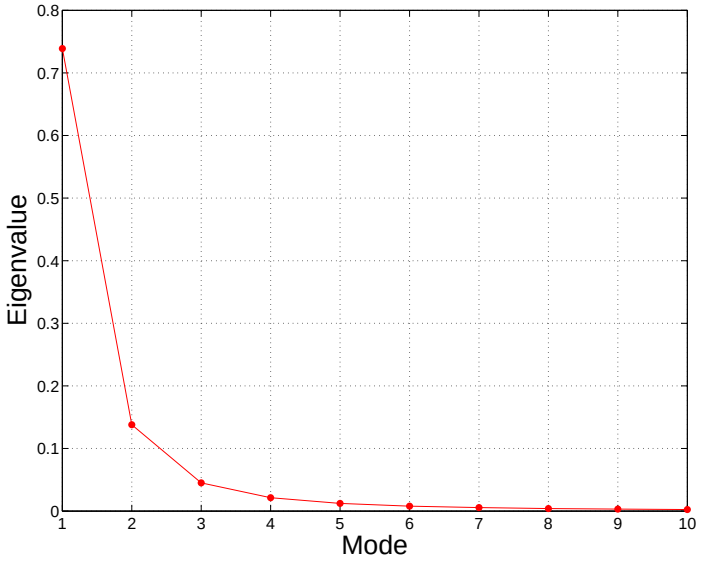

Figure 4.2: The corresponding eigenvalues are plotted for the exponential covariance function with a correlation length of 1.

by projecting φ_j onto the space $\mathcal{H}_N$ spanned by $\{\phi_i\}_{i=1}^N$. The approximation of each eigenfunction is possible because they belong to the space of square integrable functions. The residual can be written as

$$\epsilon_N(\mathbf{x}) = \sum_{i=1}^{N} d_{ij} \left[\int_{\mathcal{D}} C_{\kappa\kappa}(\mathbf{x}, \mathbf{y}) \phi_i(\mathbf{y}) d\mathbf{y} - \lambda_j \phi_i(\mathbf{x}) \right] \tag{4.13}$$

which is orthogonal to $\mathcal{H}_N$, thus the following is true

$$\langle \epsilon_N, \phi_j \rangle \equiv \int_{\mathcal{D}} \epsilon_N(\mathbf{x}) \phi_j(\mathbf{x}) d\mathbf{x} \quad j = 1, \ldots, N \tag{4.14}$$

which leads to a simple linear system

$$\mathbf{CD} = \Lambda \mathbf{BD} \tag{4.15}$$

where the different matrices are defined as follows

$$\begin{gathered} \mathbf{B}_{ij} = \textstyle\int_{\mathcal{D}} \phi_i(\mathbf{x}) \phi_j(\mathbf{x}) d\mathbf{x} \\ \mathbf{C}_{ij} = \textstyle\int_{\mathcal{D}} \int_{\mathcal{D}} C_{\kappa\kappa}(\mathbf{x}, \mathbf{y}) \phi_i(\mathbf{x}) \phi_j(\mathbf{y}) d\mathbf{x} d\mathbf{y} \\ \mathbf{D}_{ij} = d_{ij} \\ \Lambda_{ij} = \delta_{ij} \lambda_j \end{gathered} \tag{4.16}$$

thus rendering a series of linear systems to be solved.

In figures (4.1) and (4.2), the eigenvalues and eigenfunctions of an exponential covariance function are computed, using a piecewise Galerkin method. The discretization of the domain was done using 40 equispaced elements, to assure a good approximation of the first 4 eigenfunctions. The correlation length of the covariance function is equal to 1. In figures (4.3) and (4.4), the same computations where done, with the exception that the covariance function changed to a squared exponential with the same correlation length. From both cases it can be deduced the a rather small amount of terms of the expansion are needed to represent well the random field, where in the exponential case, up to 5 terms are needed, and in the case of the squared exponential, only 2 terms are needed (This is simply done by simple eye inspection).

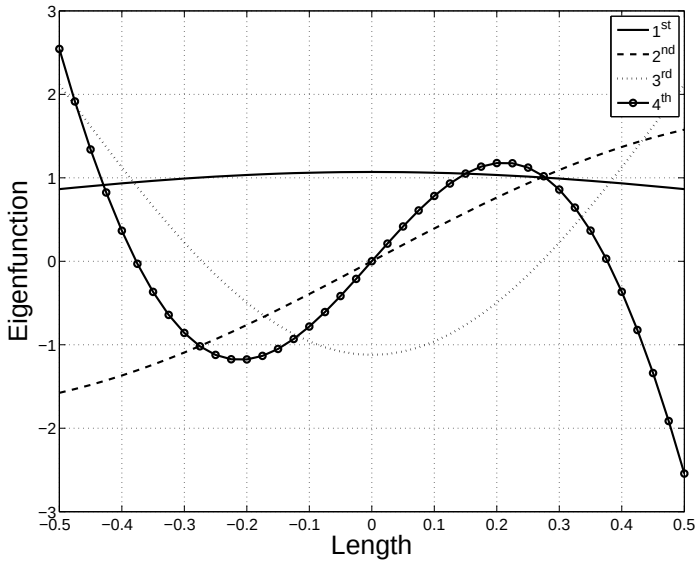

Figure 4.3: The first 4 eigenfunctions are plotted along the domain for a Gaussian covariance function with a correlation length of 1. This was done using a piecewise Galerkin method.

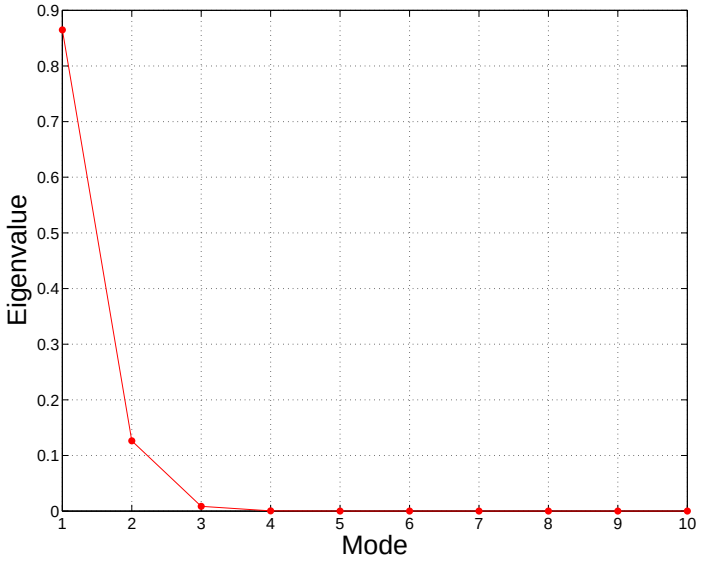

Figure 4.4: The corresponding eigenvalues are plotted for the Gaussian covariance function with a correlation length of 1.

4.4 ORTHOGONAL SERIES EXPANSION METHOD

Often no closed form solution are available to the problem of obtaining eigen-pairs given a kernel function such as the covariance. Taking this into mind, Zhang and Ellingwood [1994] proposed a method to avoid the computation of the eigen-pairs just by selecting prior to any calculation, a complete set of orthogonal functions. A similar idea had been used previously by Lawrence (1987), (don't have this paper). Let $\{\varphi_i(\mathbf{x})\}_{i=1}^{\infty}$ be a family of orthogonal functions forming a basis in L^2, and without any loss of generality, let this family be orthonormal as well

$$\int_{\mathcal{D}} \phi_i(\mathbf{x})\phi_j(\mathbf{x})d\mathbf{x} = \delta_{ij} \tag{4.17}$$

If $\kappa(\mathbf{x}, \theta)$ is a random fields, with a given covariance function $C_{\kappa\kappa}(\mathbf{x}, \mathbf{y})$, any realization of the field is a function of L^2 which can be expanded by means of the previously selected set of orthogonal functions, and this expansion can be

$$\kappa(\mathbf{x}, \theta) = \mu(\mathbf{x}) + \sum_{i=1}^{\infty} \chi_i(\theta)\phi_i(\mathbf{x}) \tag{4.18}$$

where $\chi_i(\theta)$ are zero-mean random variables. Using the orthogonality properties described before, and also with the help of basic algebra, it is possible to show that

$$\chi(\theta) = \int_{\mathcal{D}} \left[\kappa(\mathbf{x}, \theta) - \mu(\mathbf{x})\right] \phi_i(\mathbf{x})d\mathbf{x} \tag{4.19}$$

and

$$(C_{\chi\chi})_{kl} \equiv E[\chi_k\chi_l] = \int_{\mathcal{D}}\int_{\mathcal{D}} C_{\kappa\kappa}(\mathbf{x}, \mathbf{y})h_k(\mathbf{x})h_l(\mathbf{y})d\mathbf{x}d\mathbf{y} \tag{4.20}$$

If $\kappa(\mathbf{x}, \theta)$ is a zero mean Gaussian field, thenit is easy to prove that $\{\chi_i\}_{i=1}^{\infty}$ are zero mean Gaussian random variables, but unfortunately, they might bee correlated, thus it is necessary to construct the covariance matrix of these random variables, and to perform a transformation into uncorrelated random variables using the spectral decomposition method described previously.

4.5 OPTIMAL LINEAR ESTIMATION METHOD

The method was proposed by Li and Der Kiureghian [1993]. It is also mentioned in the literature as *Kriging method* or best linear unbiased estimator (BLUE) in the field of geostatistics. It is a special case of the method of regression on linear functionals, and the approximation has the following form

$$\kappa_N(\mathbf{x}, \theta) = a(\mathbf{x}) + \sum_{i=1}^{N} b_i(\mathbf{x})\chi_i \tag{4.21}$$

where N is the total number of nodal points involved in the approximation. The functions $a(\mathbf{x})$ and $b_i(\mathbf{x})$ are obtained using a nonlinear regression, minimizing in each point $\mathbf{x}$ the error of the variance, subjected to having an unbiased estimator of the real random field in the mean, these consitions are expressed as

$$\begin{array}{ll} \forall \mathbf{x} \in \mathcal{D} & \\ \text{Minimize} & V[\kappa(\mathbf{x},\theta) - \kappa_N(\mathbf{x},\theta)] \\ \text{subjected to} & E[\kappa(\mathbf{x},\theta) - \kappa_N(\mathbf{x},\theta)] = 0 \end{array} \tag{4.22}$$

The condition of problem (4.22) requires that

$$E[\mathbf{x}] = a(\mathbf{x}) + \mathbf{b}^T(\mathbf{x}) \cdot E[\boldsymbol{\chi}] \tag{4.23}$$

then, the error of the variance, which is always a positive value, holds true

$$V[\kappa(\mathbf{x},\theta) - \kappa_N(\mathbf{x},\theta)] = \sigma^2(\mathbf{x}) - 2\sum_{i=1}^{N} b_i(\mathbf{x}) C[\kappa(\mathbf{x},\theta), \chi_i] + \sum_{i=1}^{N}\sum_{j=1}^{N} b_i(\mathbf{x}) b_j(\mathbf{x}) C[\chi_i, \chi_j] \tag{4.24}$$

The minimization problem is solved for each $b_i(\mathbf{x})$, thus requiring that the partial derivatives of $b_i(\mathbf{x})$ be equal to zero for each i yields

$$\forall i = 1, \ldots, N \quad -C[\kappa(\mathbf{x},\theta), \chi_i] + \sum_{j=1}^{N} b_j(\mathbf{x}) C[\chi_i, \chi_j] = 0 \tag{4.25}$$

which can also be written in matricial form

$$-C_{\kappa\chi}(\mathbf{x}) + C_{\chi\chi} \cdot b(\mathbf{x}) = 0 \tag{4.26}$$

with this result, the final estimation is written as

$$\kappa_N(\mathbf{x},\theta) = E[\mathbf{x}] + C^T_{\kappa\chi}(\mathbf{x}) \cdot C^{-1}_{\chi\chi}(\boldsymbol{\chi} - E[\boldsymbol{\chi}]) \tag{4.27}$$

Separating the deterministic terms from the stochastic ones gives

$$\kappa_N(\mathbf{x},\theta) = \left[E[\mathbf{x}] - C^T_{\kappa\chi}(\mathbf{x}) \cdot C^{-1}_{\chi\chi} \cdot E[\boldsymbol{\chi}]\right] + \sum_{i=1}^{N} \chi_i (C^{-1}_{\chi\chi} \cdot C_{\kappa\chi}) \tag{4.28}$$

and since the variance errors are always positive, then this approximation always underestimates the variance.

4.6 EXPANSION OPTIMAL LINEAR ESTIMATION METHOD

The expansion optimal linear estimation method was proposed by Li and Der Kiureghian [1993]. It is an extension of OLE using a spectral vector of nodal variables χ. Assuming that $\kappa(\mathbf{x},\theta)$

is Gaussian, the spectral decomposition of the covariance matrix C_χ, where the random vector $\chi = \{\kappa(x_1, \theta), \ldots, \kappa(x_N, \theta)\}$ is

$$\chi(\theta) = \boldsymbol{\mu}_\chi + \sum_{i=1}^{N} \sqrt{\lambda_i}\zeta_i(\theta)\varphi_i(\mathbf{x}) \tag{4.29}$$

where the set of random variable $\{\zeta_i\}|_i^N$ are independent and standard normal. The pair (λ_i, φ_i) are the eigenvalues and eigenvectors of the covariance matrix $C_{\chi\chi}$ that satisfies

$$C_{\chi\chi}\varphi_i = \lambda_i\varphi_i \tag{4.30}$$

hence, if the substitution of (4.30) into (4.21) and solving the OLE problem yields

$$\kappa_N(\mathbf{x}, \theta) = \mu(\mathbf{x}) + \sum_{i=1}^{N} \frac{\zeta_i(\theta)}{\sqrt{\lambda_i}}\varphi_i^T C_{\kappa\chi} \tag{4.31}$$

As in the Karhunen-Loève expansion, the series can be truncated after r terms, of course after sorting the eigenvalues λ_i in a descending order. The variance error of this methos will be

$$V[\kappa(\mathbf{x}, \theta) - \kappa_N(\mathbf{x}, \theta)] = \sigma^2(\mathbf{x}) - \sum_{i=1}^{r} \frac{1}{\lambda_i}(\varphi_i^T C_{\kappa\chi})^2 \tag{4.32}$$

The problem with this method is the choice of points in the random field, such to assure a good result. This was not aborded by the author of the method.

5. AVAILABLE NUMERICAL METHODS TO SOLVE STOCHASTIC DIFFERENTIAL EQUATIONS

Depending on the type of variability existing in the domain (the operator) of the problem, such as Young's modulus, Poisson's ratio, etc, there are different suitable numerical methods to solve each of these problems. If the variability is very small around the mean value, a simple Neumann expansion around the mean value of the operator is a recommendable solution [Sudret and Der Kiureghian, 2000; Webster, 2007]. It is very easy to use since it only requires the solution of a standard deterministic partial differential equation, and the number of times that this problem needs is exactly the amount of terms that was taken in the Neumann expansion. In the same way, a Taylor expansion technique has been developed in the past, around the mean of the solution [Sudret and Der Kiureghian, 2000]. Jensen [1990]; Jensen and Iwan [1991] showed several dynamical examples in which perturbation method solutions where unsatisfactory. He used highly variable operators and forcing terms. In his study, he did not give convergence properties of any kind. Babuska has shown that the conditions of convergence for perturbation methods depends on the noise level, thus the method does not work for certain levels of noise.

Monte Carlo methods are not restricted by the dimension number or by the variability of the problem. Another advantage of this method is the straightforwardness to parallelize the problem at hand, thus solving M deterministic realizations by sampling the coefficients of the equation with independent identically distributed (iid) approximations of the solution. The deterministic solutions can be solved by any method, such as the Galerkin finite element method, finite differences, etc. With each of these responses, the desired statistical information can be retrieved.

The Galerkin approach dates back to the work of Jensen [1990]; Spanos and Ghanem [1991]; Deb, Babuška, and Oden [2001] among others. The main problem with this approach is that it leads to coupled set of differential equations, thus making it hard to solve, specially for the case of nonlinear problems.

Collocation methods where first introduced by Tatang [1995]; Baldeweck [1999]; Babuška, Nobile, and Tempone [2007], the main idea of these methods is to solve stochastic partial differential equations simply by converting this problem into a decoupled deterministic partial differential equations, thus making the problem completely parallelizable. Another great advantage of this method is that it solves nonlinear problems of all types very easily. The specific approach is to compute in specific realizations of the parameters that represent the operator (the sparse grid points), and with these solutions, to interpolate using sparse interpolation

5.1 STANDARD DEFINITIONS

Let us consider the following problem

$$\mathcal{L}(\kappa)(u) = f \quad in \quad \mathcal{D} \tag{5.1}$$

where $\mathcal{L}$ is an operator of a certain kind withought loss of generality, and it is defined in a domain $\mathcal{D}$. Both $\kappa = \kappa(\mathbf{x}, \theta)$ and $f = f(\mathbf{x}, \theta)$ can be considered as random fields of a certain kind. The latter variables can describe any kind of scalar field, such as the Poisson ratio, Young's modulus or the external forces acting on $\partial\mathcal{D}$. The random field on the right hand side and left hand side of equation (5.1) are considered to be functions of a finite amount of random variables (finite noise) such that it can be written as

$$\begin{aligned} \kappa(\mathbf{x}, \theta) &= \kappa(\mathbf{x}; \eta_1, \ldots, \eta_N) \\ f(\mathbf{x}, \theta) &= f(\mathbf{x}; \eta_1, \ldots, \eta_N) \end{aligned} \tag{5.2}$$

This approximation of a random field using a random vector is possible and it can be done using different methodologies such as the truncation of the Karhunen-Loève expansion, etc. Many assumptions can be made of the chosen random vector that represents the both random fields $\kappa(\mathbf{x}, \theta)$ and $f(\mathbf{x}, \theta)$, such as the correlation between the components of the random vector as $C[\eta_i, \eta_j] = \delta_{ij}$, the type of distribution that each component has, etc.

Sometimes, the uncertain coefficients of the operator $\mathcal{L}$ or the forcing term of equation (5.1) needs to be more specified, an example is illustrated.

Example 5.1.1. If the coefficient $\kappa(\mathbf{x}, \theta)$ is always greater than κ_{min} for it to have physical sense, then the following transformation guarantees that this will always be certain.

$$log(\kappa - \kappa_{min})(\mathbf{x}, \theta) = b_0(\mathbf{x}) + \sum_{i=1}^{N} \sqrt{\lambda_i} b_i(\mathbf{x}) \eta_i(\theta) \tag{5.3}$$

The latter is simple the truncation of the Karhunen-Loève expansion of $log(\kappa - \kappa_{min})$. The same can be done for the forcing term $f(\mathbf{x}, \theta)$

Lemma 5.1.2. Let $\boldsymbol{\eta}$ be an N-dimensional random vector defined on $(\Omega^N, \mathcal{F}, P)$ and let ζ be a σ-measurable random variable defined on the same space. Then $\zeta = g(\boldsymbol{\eta})$ for some Borel measurable $g\colon \mathbb{R}^N \to \mathbb{R}$, this means that ζ will depend only on the components of $\boldsymbol{\eta}$, that is, $\zeta(\eta_1, \ldots, \eta_N)$

This lemma can be extended to problem (5.1) for the case of finite dimensional noise, which can be viewed in the following way:

$$\mathcal{L}(\kappa_N)(u_N) = f_N \quad in \quad \mathcal{D} \tag{5.4}$$

using lemma (5.1.2) it can be concluded that $u_N = u_N(\mathbf{x}; \eta_1, \ldots, \eta_N)$

Remark 5.1.3. It can be noticed that in the definition of the finite noise problem (5.2), for both the forcing term and the term associated with the operator have dependency on the same random variables. It is clear that in most of the real cases this is not, so the problem can be viewed in the following way:

$$\begin{aligned} \kappa(\mathbf{x}, \theta) &= \kappa(\mathbf{x}; \boldsymbol{\eta}_a) \\ f(\mathbf{x}, \theta) &= f(\mathbf{x}; \boldsymbol{\eta}_f) \end{aligned} \tag{5.5}$$

thus $u_N = u_N(\mathbf{x}; \boldsymbol{\eta}_a, \boldsymbol{\eta}_f)$

5.2 STOCHASTIC COLLOCATION APPROXIMATION

Let $u_h(x, \boldsymbol{\eta})$ be the semi-discrete solution of

$$\int_{\mathcal{D}} \kappa(\mathbf{x}, \theta) \nabla u_h(\mathbf{x}, \theta) \cdot \nabla v_h(\mathbf{x}) d\mathbf{x} = \int_{\mathcal{D}} f(\mathbf{x}) v_h(\mathbf{x}) d\mathbf{x} \quad \forall v_h \in V_h \tag{5.6}$$

Consider a sparse interpolation formula $\mathcal{I}_N^S\colon L^2_{p_\eta}(\mathbb{R}^N) \to \Xi_N^S$ that uses a sparse grid $\mathcal{H}_N^S$. The stochastic collocation FEM solution is obtained by simply interpolating the semi-discrete solution on the sparse grid

$$u_h^N(\mathbf{x}, \boldsymbol{\eta}) = \mathcal{I}_N^S u_h(\mathbf{x}, \boldsymbol{\eta}) \in V_h \otimes \Xi_N^S \tag{5.7}$$

This means that if the points in the probability domain are $\boldsymbol{\eta}^{(1)}, \ldots, \boldsymbol{\eta}^{(M)} \in \mathcal{H}_N$ that belong to the sparse grid, then using the pre-defined sparse interpolation, the solution can be achieved simply by computing M deterministic solutions $u_h^{(j)},\ j = 1, \ldots, M$, using the points that belong to the sparse grid, and projecting the solution of these points into the sparse interpolation formula.

5.3 STOCHASTIC GALERKIN APPROXIMATION USING DOUBLE ORTHOGONAL POLYNOMIALS

This method approximates the problem (5.1) with a solution that belongs both to the space of the discretized space in the physical domain, as well as in the discretized probabilistic space with u_h^p such that

$$E\left[B(u_h^p(x,\theta), v_h^p(x,\theta))\right] + E\left[N(u_h^p(x,\theta), v_h^p(x,\theta))\right] = E\left[\langle f_N(x,\theta), v(x,\theta)\rangle_{L_{p_\eta}}\right] \tag{5.8}$$

with $v(x,\theta)$ belonging to the same space as the proposed ansatz for the solution of this problem, B is the bilinear form and N is the term that arises due to nonlinear effects. As an example let us consider the diffusion problem used by Babuška, Tempone, and Zouraris [2004] in their original work, such that there is no nonlinear terms as well as no reaction terms in order to keep the derivations as simple as possible.

$$\begin{cases} \nabla \cdot (\kappa(\mathbf{x},\theta)\nabla u) & \text{in} \quad \mathcal{D} \subset \mathbb{R}^d \\ u = 0 & \text{on} \quad \partial\mathcal{D} \end{cases} \tag{5.9}$$

Babuška, Tempone, and Zouraris [2004] developed an efficient method to solve stochastic finite elements, using a stochastic Galerkin approach, that incorporates double orthogonal polynomials in the probabilistical domain, to obtain a number of undecoupled systems, each of the size of a deterministic realization of the same problem. Using a $p \times h$ finite element version, and withought any loss of generality, attention is focused in finding a solution $u_h^p \in V^h \otimes \Xi_p^S$ such that

$$E\left[\int_{\mathcal{D}} \kappa(\mathbf{x},\theta)\nabla u_h^p(\mathbf{x},\theta) \cdot \nabla v(\mathbf{x},\theta) d\mathbf{x}\right] = E\left[\int_{\mathcal{D}} f(\mathbf{x},\theta) v(\mathbf{x},\theta) d\mathbf{x}\right] \tag{5.10}$$

Up to now, many authors have used this approach, which leads to fully coupled linear systems, which makes it necessary to use highly efficient parallel strategies to find the desired numerical solution. To avoid this problem, a particular basis was chosen by Babuška, Tempone, and Zouraris [2004], double orthogonal polynomials since this choice of basis decouples the problem, but this can only be achieved when the random variables are independent (which is the case for KL expansion with Gaussian fields), and when each of these fields (a_N, f_N) are a linear combination of these random variables. Let $\{H(\boldsymbol{\eta})\}$ be a basis for the subspace $\mathbf{z}^p \subset L^2_{p_\eta}(\Omega)$, and $\{\phi(\mathbf{x})\}$ be a basis for the subspace $V_h \subset H_0^1(\mathcal{D})$. Then an approximation of the solution can be

$$u_h^p(\mathbf{x},\eta) = \sum_{j,i} u_{ij} H_j(\theta)\phi_i(\mathbf{x}) \tag{5.11}$$

and the test functions can be taken as

$$v(\mathbf{x},\theta) = H_k(\theta)\phi_l(\mathbf{x}) \tag{5.12}$$

to find u_{ij} coefficients, then equation (5.3) will be equivalent to

$$\begin{aligned}\sum_{j,i} E\left[H_k(\mathbf{z})H_j(\mathbf{z})\int_{\mathcal{D}}\kappa(\mathbf{x},\theta)\nabla\phi_i(\mathbf{x})\cdot\nabla\phi_l(\mathbf{x})d\mathbf{x}\right]u_{ij}\\ = E\left[H_k(\mathbf{z})\int_{\mathcal{D}} f(\mathbf{x},\mathbf{z})\phi(\mathbf{x})d\mathbf{x}\right]\ \forall k,l\end{aligned} \tag{5.13}$$

defining

$$\begin{aligned}G_{il}(\mathbf{z}) = \int_{\mathcal{D}}\kappa(\mathbf{x},\theta)\nabla\phi_i(\mathbf{x})\nabla\phi_l(\mathbf{x})d\mathbf{x}\\ \text{and } f_l(\mathbf{z}) = \int_{\mathcal{D}} f(\mathbf{x},\mathbf{z})\phi_l(\mathbf{x})d\mathbf{x}\end{aligned} \tag{5.14}$$

If the random field is expanded into a KL expansion, then

$$G_{il}(\mathbf{z}) = \int_{\mathcal{D}}\left(E[\kappa(\mathbf{x},\theta)] + \sum_{p=1}^{N} b_p z_p\right) \tag{5.15}$$

where

$$\begin{aligned}G^0_{il} \equiv \int_{\mathcal{D}} E[\kappa(\mathbf{x},\theta)]\nabla\phi_i(\mathbf{x})\cdot\nabla\phi_l(\mathbf{x})d\mathbf{x}\\ \text{and } G^p_{il} = \int_{\mathcal{D}} b_p(\mathbf{x})\nabla\phi_i(\mathbf{x})\cdot\nabla\phi_l(\mathbf{x})d\mathbf{x}\end{aligned} \tag{5.16}$$

Since $H_k \in \Xi^s_p$, with a multi-index $p = [p_1,\ldots,p_N]$, it is enough to take it as a product

$$H_k(\mathbf{z}) = \prod_{r=1}^{N} H_{kr}(z_r) \tag{5.17}$$

where $H_{kr}\colon \Omega_r \to \mathbb{R}$ is a basis function of the subspace $Z^{p_r} = span\{H_{hr}\colon h = 1,\ldots,p_r+1\}$. Keeping the choice of H_k in mind,

$$\begin{aligned}\int_\Omega p_\eta(\mathbf{z})H_kH_jG_{il}(z)d\mathbf{z} = G^0_{il}\int_\Omega\prod_{m=1}^{N} p_{\eta_m}(z_m)H_{km}(z_m)H_{jm}(z_m)d\mathbf{z}\\ +\sum_{n=1}^{N} G^n_{il}\int_\Omega z_n\prod_{m=1}^{N} p_{\eta_m}(z_m)H_{km}(z_m)H_{jm}(z_m)d\mathbf{z}\end{aligned} \tag{5.18}$$

Now, for every set $\Omega_n,\ n = 1,\ldots,N$, the polynomials $H_j(\mathbf{z}) = \prod_{n=1}^{N} H_{jn}(z_n)$ need to be chose, and they can be selected to satisfy biorthogonality, so that they can satisfy

$$\begin{aligned}\int_{\Omega_n} p_{\eta_n}(z_n)H_{kn}(z_n)H_{jn}(z_n)dz_n = \delta_{kj}\\ \text{and } \int_{\Omega_n} z_n p_{\eta_n}(z_n)H_{kn}(z_n)H_{jn}(z_n)dz_n = c_{kn}\delta_{kj}\end{aligned} \tag{5.19}$$

To find these polynomials, N eigen-problems need to be solved, each of them having a size of $(1+p_n)$. The computational work required by these eigen-problems is negligible compared with the effort to solve for u_{ij} Anyway, there is also the possibility of keeping these polynomials,

for a given support Ω_n, and performing a simple change of variables using the property stated in (2.27) will reduce computational complexity. With this last finding, the right hand side of equation (5.13) will be

$$\begin{aligned} &\sum_{j,i}\left(\int_{\Omega} p_{\eta}(\mathbf{z})H_k(\mathbf{z})H_j(\mathbf{z})G_{il}(\mathbf{z})d\mathbf{z}\right) \\ &= G^0_{il}\int_{\Omega} p_{\eta}(\mathbf{z})H_k(\mathbf{z})H_j(\mathbf{z})d\mathbf{z} + \sum_{n=1}^{N} G^n_{il}\int_{\Omega} z_n p_{\eta}(\mathbf{z})H_k(\mathbf{z})H_j(\mathbf{z})d\mathbf{z} \\ &= \left(G^0_{il} + \sum_{n=1}^{N} c_{kn}G^n_{il}\right)\delta_{kj} \end{aligned} \tag{5.20}$$

thus rendering a N decoupled problem.

5.4 MONTE CARLO APPROXIMATION

The statistical information, such as the response moments of uncertain systems can be computed using the standard Monte Carlo method finite element method $E[u_N(\mathbf{x}, \eta_1, \ldots, \eta_N)^2]$, simply by sample averages of iid realizations of the coefficients that model the governing equation at hand. For each realization, it does not matter what method is used to solve the governing equation, as long as the method converges appropriety at the possible realizations of the random fields that describe the coefficients of the model. This method is quite robust but it lacks speed convergence, since the convergence rate with respect to the number of samples is roughly $O(1/\sqrt{M})$ (Babuska) which is very slow, but on the other hand, it does not depend on the dimension of the problem.

6. NUMERICAL EXAMPLES USING THE SPARSE GRID STOCHASTIC COLLOCATION METHOD FOR STATIC PROBLEMS

In this chapter, a numerical example will be developed and it consists in searching the statistical response of a static mechanical problem. Different source of randomness are incorporated (either in the forcing term or in the operator) and are solved using the sparse grid stochastic collocation method. These solutions are contrasted with the solution given by the standard Monte Carlo method.

6.1 BEAMS WITH UNCERTAIN MECHANICAL PROPERTIES

Let us consider now a beam with uncertain mechanical properties along the length (see figure 6.1). For this a collocation method will be used and the solution of the problem will be expanded

$$\mathcal{I}^S(w,N)\mathbf{g}(\boldsymbol{\eta}) = \sum_{|\mathbf{i}|\in Y(w,N)} (-1)^{N-|\mathbf{j}|}\binom{M-1}{N-|\mathbf{i}|}\mathcal{I}^T(N)\mathbf{g}(\boldsymbol{\eta}) \tag{6.1}$$

where $\mathbf{g} = [\mathbf{u}\ \mathbf{v}\ \boldsymbol{\theta}]^T$ The mechanical properties can be viewed as a random field with the following covariance function

$$C_{\kappa\kappa}(x,y) = e^{-\frac{(x-y)^2}{L^2}} \tag{6.2}$$

for $x, y \in [0,1]$, where L represents the correlation length. The truncated Karhunen Loève expansion of this covariance function is given by

$$\kappa_N(x,\boldsymbol{\eta}) = 1 + \eta_1(\theta)\left(\frac{\sqrt{\pi}L}{2}\right) + \sum_{k=2}^{N}\lambda_k b_k(x)\eta_k(\theta) \tag{6.3}$$

with

$$\lambda_k = \sqrt{\sqrt{\pi}L}e^{\left(-\frac{\lfloor\frac{k}{2}\rfloor^2\pi^2L^2}{8}\right)} \tag{6.4}$$

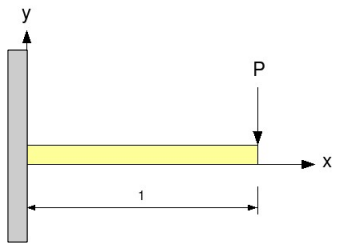

Figure 6.1: The beam has a unit length and is loaded at the tip with a concentrated force P.

$$b_k(x) = \begin{cases} \cos(\lfloor k/2 \rfloor \pi x) & \text{if} \quad k \text{ odd} \\ \sin(\lfloor k/2 \rfloor \pi x) & \text{if} \quad k \text{ even} \end{cases} \tag{6.5}$$

the random coordinates are uniformly distributed in $[-\sqrt{3}, \sqrt{3}]$ with zero mean and unit variance. and $E_N(x, \boldsymbol{\eta}) = 150 + e^{\sigma \kappa_N(x, \boldsymbol{\eta})}$ (GPa) represents the elastic Young modulus along the length of the beam and with $\sigma = 2$. The values of the constants that define the random field will give plausible realizations for the elastic modulus along the length of the beam.

6.1.1 Finite elements for beams using a residual formulation

Since there will be the need to compute the deterministic response for many cases, a Galerkin method is developed to solve each of these deterministic problems. According to the virtual work principal, the external work is equal to the internal work, thus yielding

$$L_v^{int} = L_v^{ext} \tag{6.6}$$

where the internal work is $L_v^{int} = \int_{\mathcal{D}} \sigma \delta \varepsilon dV$. On the other hand, the kinematics of the beam can be stated as

$$\varepsilon = \varepsilon_0 - y\chi = u_{,x} - y v_{,xx} \tag{6.7}$$

which means that plane sections remain plane. Clearly $\delta\varepsilon = \delta u_{,x} - y\delta v_{,xx}$, therefore

$$L_v^{int} = \int_{\mathcal{D}} \sigma(\delta u_{,x} - y\delta v_{,xx}) dV = \int_l (N\delta u_{,x} + M\delta v_{,xx}) dl \tag{6.8}$$

since $N = \int_A \sigma dA$ and $M = -\int_A y\sigma dA$. Using a finite element approximation of the following form for the beam as

$$\begin{array}{ll} u \simeq \mathbf{N}^u \hat{\mathbf{u}} & \hat{\mathbf{u}}_{,x} \simeq \mathbf{B}^u \hat{\mathbf{u}} \\ v \simeq \mathbf{N}^v \hat{\mathbf{v}} & \hat{\mathbf{v}}_{,xx} \simeq \mathbf{B}^v \hat{\mathbf{v}} \end{array} \tag{6.9}$$

introducing these approximations in the equation of virtual work will give a set of equations

$$L_v^{int} = \delta\hat{\mathbf{u}}^T \int_l \mathbf{B}^{uT} N dl + \delta\hat{\mathbf{v}}^T \int_l \mathbf{B}^{vT} M dl \tag{6.10}$$

which can also be written as

$$L_v^{int} = \delta\hat{\mathbf{u}}^T \mathbf{F}_{axi}^{int} + \delta\hat{\mathbf{v}}^T \mathbf{F}_{bend}^{int} \tag{6.11}$$

and recalling that

$$L_v^{ext} = \delta\hat{\mathbf{u}}^T \mathbf{F}_{axi}^{ext} + \delta\hat{\mathbf{v}}^T \mathbf{F}_{bend}^{ext} \tag{6.12}$$

the principal of virtual work implies that

$$\mathbf{R}(\hat{\mathbf{u}}, \hat{\mathbf{v}}) = [\mathbf{R}_{axi}(\hat{\mathbf{u}})\ \mathbf{R}_{bend}(\hat{\mathbf{v}})]^T = 0 \tag{6.13}$$

There are many algorithms available in the literature to solve this kind of system of equations, for instance the Newton-Raphson scheme. For the sake of simplicity, the integration rule for each cross section is done using a composite midpoint rule over n_s horizontal stripes of width b and height h/n_s.

$$\Rightarrow N = \int_A \sigma dA \simeq \frac{bh}{n_s} \sum_{i=1}^{n_s} \sigma_i \tag{6.14}$$

and

$$M = -\int_A \sigma y dA \simeq -\frac{bh}{n_s} \sum_{i=1}^{n_s} \sigma_i y_i \tag{6.15}$$

where $y_i = \frac{h}{2}\left(\frac{2i-1}{n_s} - 1\right)$. To compute the internal forces a simple 3 point Simpson quadrature is more than enough, using the first end, the midpoint and the end of the element as $P1$, $P2$ and $P3$, thus the expression for the internal force reduces to

$$\mathbf{F}^{int} = \int_l \begin{bmatrix} \mathbf{B}^{uT} N \\ \mathbf{B}^{vT} M \end{bmatrix} dl \tag{6.16}$$

where also, $\mathbf{R} = \mathbf{F}^{int} - \mathbf{F}^{ext}$ and the integral can be solved with many quadrature schemes, such as Simpson and Gauss. For this numerical example a 3 point Simpson rule was used. To obtain the consistent tangent, the residual needs to be differentiated.

$$d\mathbf{R} = d\mathbf{F}^{int} = \begin{bmatrix} \mathbf{F}^{int}_{,\hat{\mathbf{u}}} & \mathbf{F}^{int}_{,\hat{\mathbf{v}}} \end{bmatrix} \begin{bmatrix} \hat{\mathbf{u}} \\ \hat{\mathbf{v}} \end{bmatrix} = \mathbf{K}_T \begin{bmatrix} \hat{\mathbf{u}} \\ \hat{\mathbf{v}} \end{bmatrix} \tag{6.17}$$

Defining the tangent modulus as $E_T = \sigma_{,\varepsilon}$, and remembering that $\varepsilon_{,\hat{\mathbf{u}}} = \mathbf{B}^u$, $\varepsilon_{,\hat{\mathbf{v}}} = -y\mathbf{B}^v$, it is possible to compute the derivatives in the consistent tangent as follows (using the chain rule)

$$\begin{aligned}
N_{,\hat{\mathbf{u}}} &= \mathbf{B}^u \textstyle\int_A E_T dA &&\simeq \mathbf{B}^u \tfrac{bh}{n_s} \textstyle\sum_{i=1}^{n_s} E_{Ti} \\
N_{,\hat{\mathbf{v}}} &= -\mathbf{B}^v \textstyle\int_A E_T y dA &&\simeq -\mathbf{B}^v \tfrac{bh}{n_s} \textstyle\sum_{i=1}^{n_s} E_{Ti} y_i \\
M_{,\hat{\mathbf{u}}} &= -\mathbf{B}^u \textstyle\int_A E_T y dA &&\simeq -\mathbf{B}^u \tfrac{bh}{n_s} \textstyle\sum_{i=1}^{n_s} E_{Ti} y_i \\
M_{,\hat{\mathbf{v}}} &= \mathbf{B}^v \textstyle\int_A E_T y^2 dA &&\simeq \mathbf{B}^v \tfrac{bh}{n_s} \textstyle\sum_{i=1}^{n_s} E_{Ti} y_i^2
\end{aligned} \tag{6.18}$$

In the end, the consistent tangent can be computed along the element using any quadrature rule, like the Simpson rule that was used for this example.

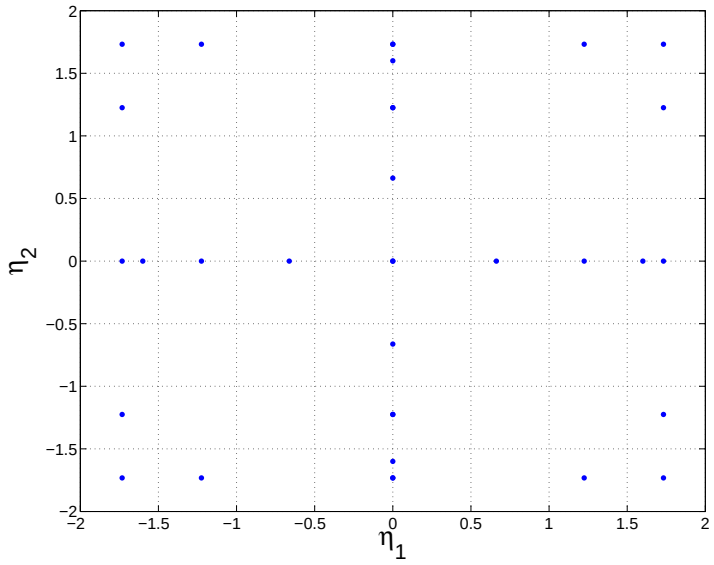

Figure 6.2: The sparse grid using Clenshaw-Curtis nodes for $N = 2$, $L = 2$, $w = 3$.

The equations (6.14) and (6.15) can be a set of nonlinear equations due to the nonlinearity of the constitutive equations. In the case of linear elastic constitutive relationships, equations (6.14) and (6.15) shall become a set of nonlinear equations. In the following numerical examples, both linear elastic and elastic perfectly plastic constitutive relationships are approached.

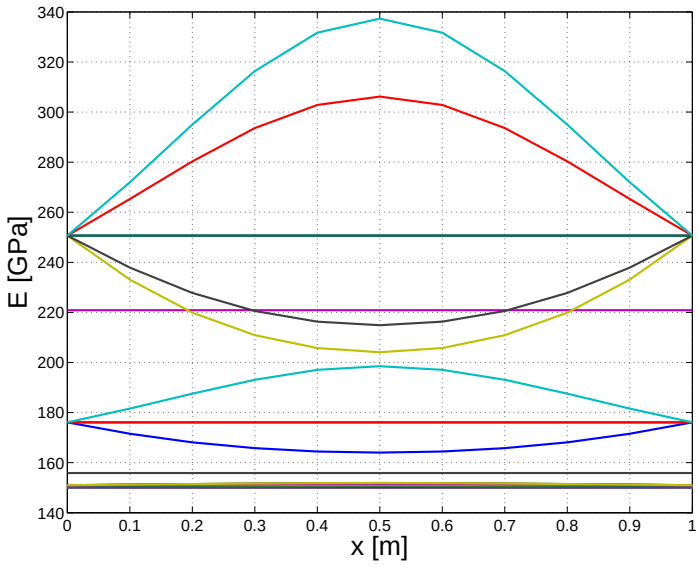

Figure 6.3: The realization of the elastic Young modulus along the length of the beam of each point of the previous sparse grid is shown.

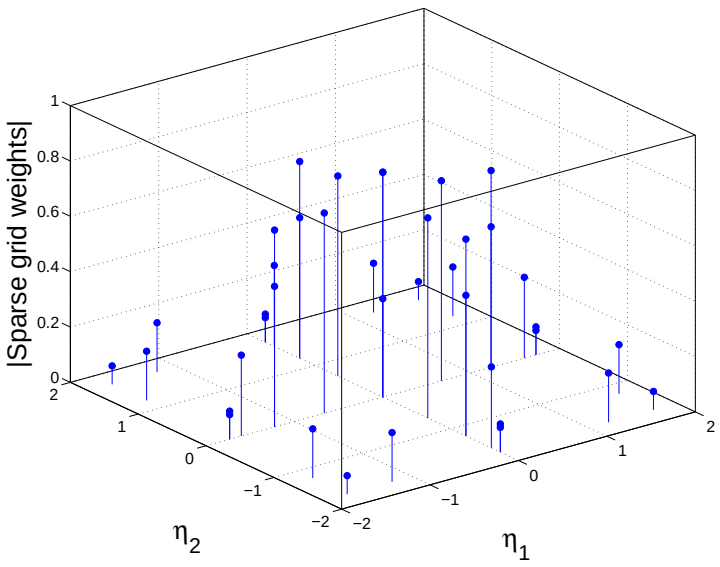

Figure 6.4: The absolute value of the weights assigned to each sparse grid point used before.

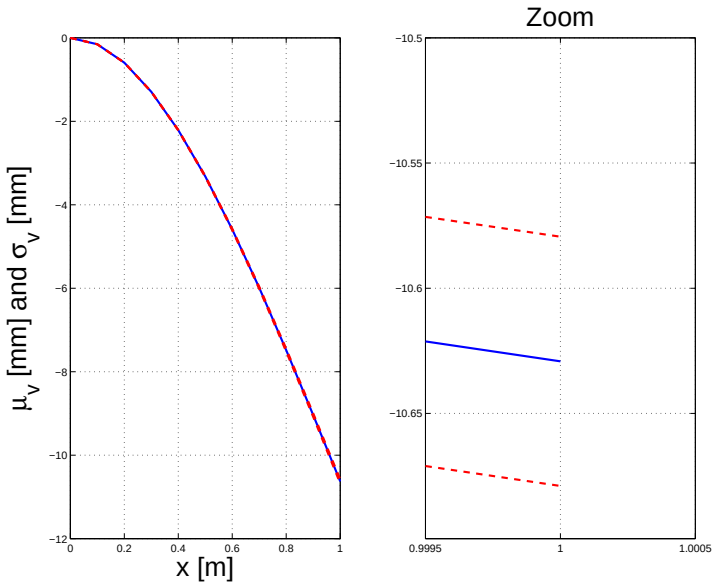

Figure 6.5: Mean (in solid blue) plus minus the standard deviation (in red dashed) of the deflection at the tip of the beam due to a load of $P = 1.5$ (MN). the beam is considered to be elastic.

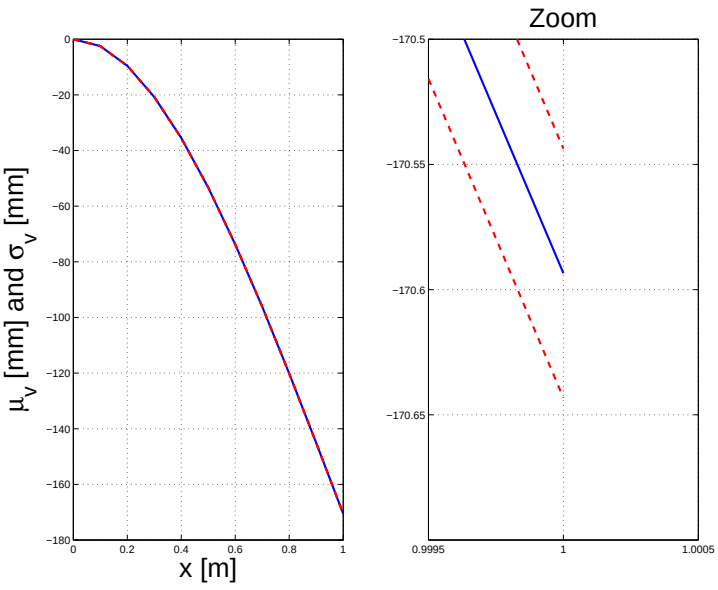

Figure 6.6: Mean (in solid blue) plus minus the standard deviation (in red dashed) of the deflection at the tip of the beam due to a load of $P = 1.5$ (MN). the beam is considered to be inelastic, with $\sigma_y = 250$ (MPa).

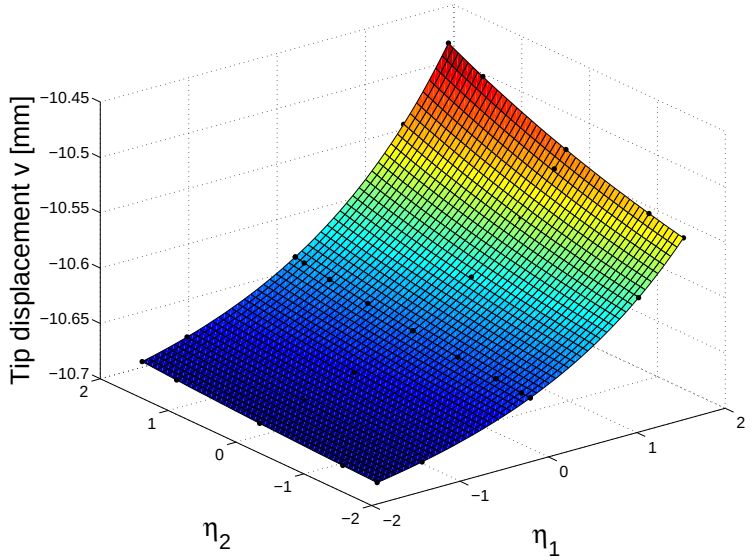

Figure 6.7: The surface response of the deflection of the tip of the beam with a load of $P = 1.5$ (MN) for the elastic case. This surface was computed using sparse interpolation techniques and the previous sparse grid where the black dots are the realizations of the sparse grid points.

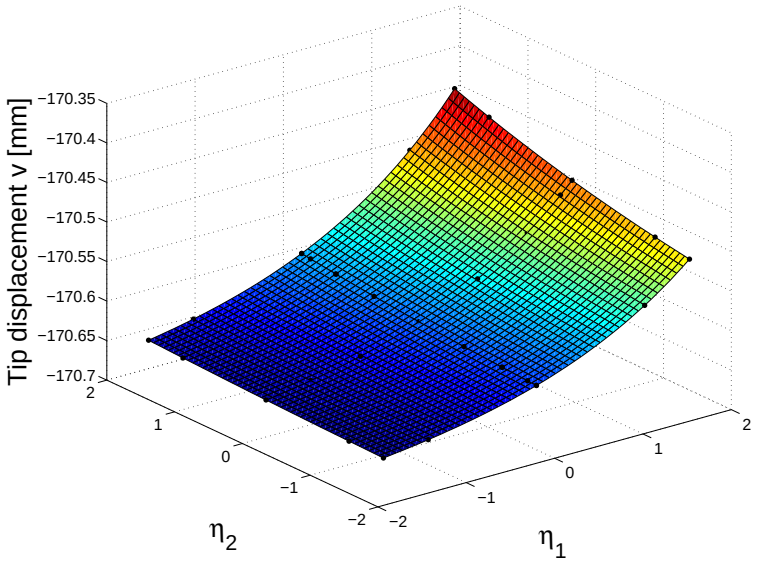

Figure 6.8: The surface response of the deflection of the tip of the beam with a load of $P = 1.5$ (MN) for the inelastic case, with $\sigma_y = 250$ (MPa). This surface was computed using sparse interpolation techniques and the previous sparse grid where the black dots are the realizations of the sparse grid points.

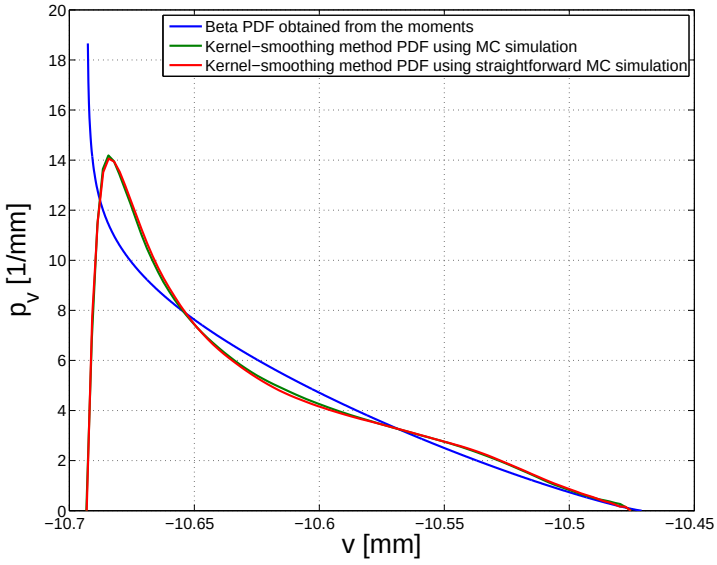

Figure 6.9: The PDF of the deflection at the tip of the beam using a fitting scheme with Beta function with the moments and limits, the K-S density estimation with Monte Carlo simulation using the response surface and finally a Monte Carlo simulation from scratch, also using K-S density estimation. All of these for the elastic case and loaded with $P = 1.5$ (MN).

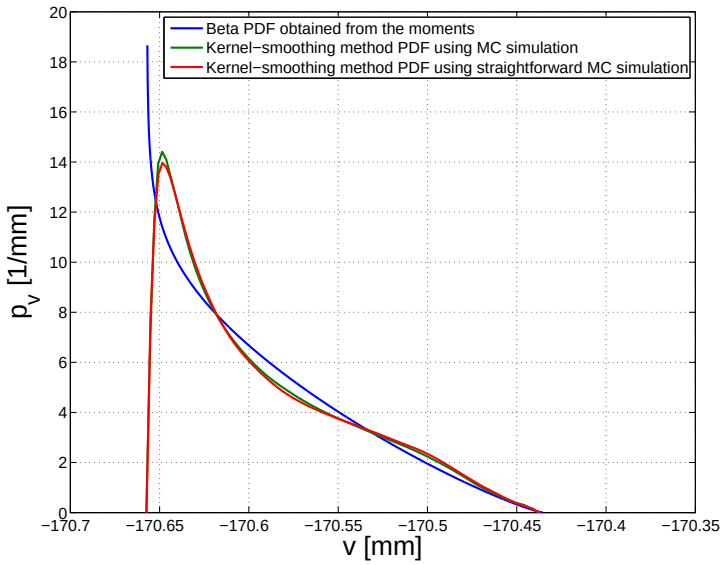

Figure 6.10: The PDF of the deflection at the tip of the beam using a fitting scheme with Beta function with the moments and limits, the K-S density estimation with Monte Carlo simulation using the response surface and finally a Monte Carlo simulation from scratch, also using K-S density estimation. All of these for the inelastic case and loaded with $P = 1.5$ (MN) and $\sigma_y = 250$ (MPa).

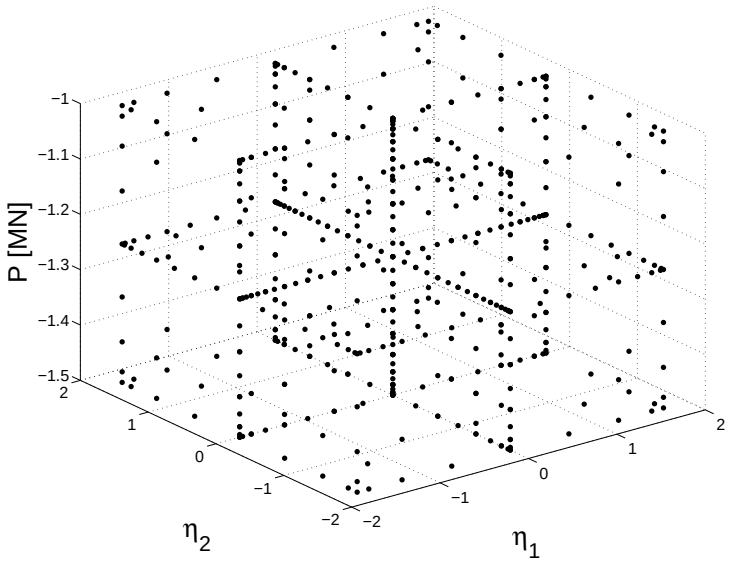

Figure 6.11: The 3d sparse grid for the previous problem with the addition of uncertain loading, the load $P \sim \mathcal{U}$ between the values of 1 and 1.5 (MN). $N = 3$ and $w = 5$.

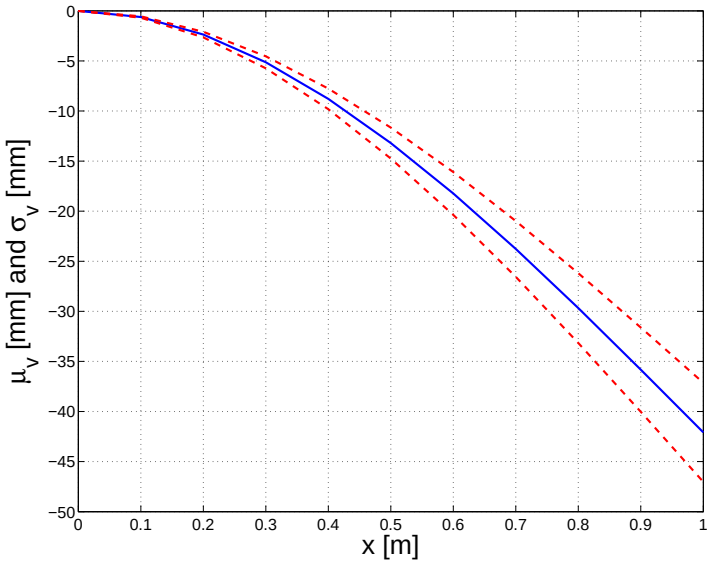

Figure 6.12: Expected value (solid blue line) plus minus the standard deviation (dashed red line) of the tip deflection.

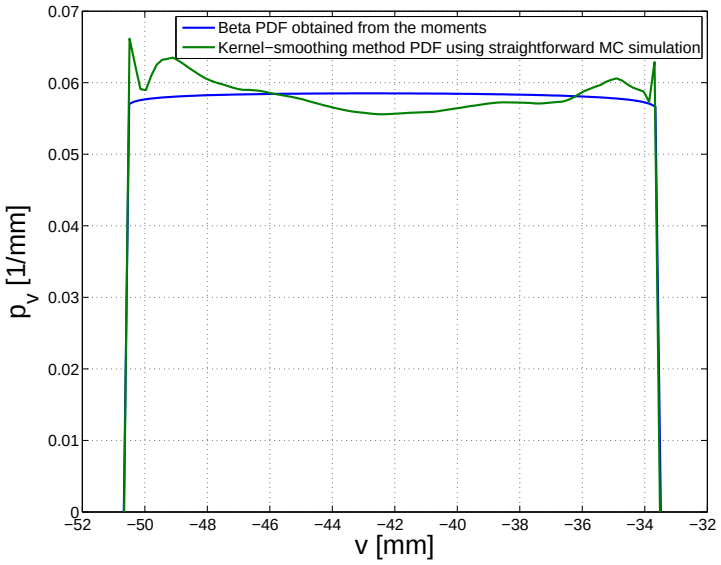

Figure 6.13: Beta PDF estimation, using the first 2 moments as well as the limits and K-S density estimation with the straight forward Monte Carlo simulation, the inelastic case, with $\sigma_y = 250$ (MPa).

It is worth mentioning that the tip load that was chosen is under the ultimate value for which all of the fibers in the section reach the plastic region, considering a yielding stress of $\sigma_y = 250$ (MPa). It can be seen in figures (6.5) and (6.6), that the variability is very small. This is due to the small variability that was taken in the original random field for the respresentation of the elastic modulus. Figure (6.3) might be misleading since there are sparse grid points the yield very variable realizations of the elastic modulus along the length of the beam. Figure (6.4) shows the absolute value of the weights for each sparse grid point, and as it can be seen, there are many of this nodes that do not contribute to the final response in mean and standard deviation, specially for the points in the extreme part of the grid, which are the ones that escape the mean values, thus giving a small variability to the response of the beam problem for both the elastic and inelastic case.

Another important issue to be mentioned is that the random field that was used in this case is nonstationary, and this can be seen in figure (6.3), since the variability concentrates more in the middle of the beam, rather that the extremes, thus giving nonstationarity to the problem.

For this problem, the amount of sparse grid points that was used was very small in comparison with the exactitude of the results shown in figures (6.9) and (6.10). For this case, the number of flops used in the sparse grid computation plus the Monte Carlo simulation was far less than the case of full Monte Carlo simulation. For both cases, 10000 points where used in the Monte Carlo simulations. In the case of the beta estimation, it can be said that it is not a very good approximation. Beta estimation is relatively exact for the third case of the beam, where the tip load distributes uniformly, but still it is not recommendable to use this approach.

7. NUMERICAL EXAMPLES USING THE SPARSE GRID STOCHASTIC COLLOCATION METHOD FOR DYNAMIC PROBLEMS

In this chapter, several dynamical examples will be presented, to show that the proposed method produces satisfactory results also in dynamics. For this purpose, a Bouc-Wen model has been selected, subjected to random pulses, as well as the response of a 1d soil column using the spectral element method (SEM), considering a medium that is modelled as a piecewise constant random field. Later, the treatment of the random SDOF random oscillator in the parameters and subjected to a stochastic Gaussian process is studied in detail.

7.1 RESPONSE OF LINEAR SYSTEMS SUBJECTED TO STOCHASTIC GAUSSIAN PROCESSES

Many authors have worked on this specific problem with different angles of approach. Such is the case of Lin [1965], who is one of the first to work on this field. Lin studied the response of linear systems, subjected to aleatory pulse sequences. Roberts [1965] used the same approach to solve the problem, and in both cases, a non-stationary noise method, developed by Parzen [1962] was used which is quite similar to the one developed by Rice [1944]. This same methodology was used by Wen [1974] to study the of lightweight equipment joined to structural systems. Hammond [1968] studied the response of systems subjected to base excitation by stochastic processes that have a evolutionary power spectral density function with the principal aim of including in the structural response the variation of the frequency content in time.

Roberts [1965] used relations in the frequency domain, assuming that the excitation was periodical and non-stationary. He was careful to define a period of time larger than the duration of the duration of the external loading to avoid aliasing in the signal. This method however presents problems for the computation of the response, if the selected period of time is not long enough.

Holman and Hart [1974] computed the response of linear systems excited by segmented and modulated stationary processes. They considered that the frequency content was invariant in each time segment. Corotis and Vanmarcke [1975] proposed a method to compute the response of linear structural systems subjected to sudden white noise.

Crempien Laborie and Saragoni [1978] studied the influence of strong ground motion duration in the response of linear structural systems. For this they assumed a time segment of the excitation to be stationary. This proved the necessity to study the response of non-stationary response of structural systems.

Spanos and Lutes [1980] also used an evolutionary power spectral density function to compute the response assuming that the response can be modelled as a Markov process.

The approach that will be developed now considering that the excitation is of Gaussian nature, both non-stationary in time and in frequency and the structural system is linear.

7.1.1 Response of a simple oscillator

The response of a simple linear, SDOF (single degree of freedom) oscillator can be deduced from its ordinary differential equation that is stated as

$$m\ddot{u}(t) + c\dot{u}(t) + ku(t) = -mF(t) \tag{7.1}$$

where m is the mass of the oscillator, c is the viscous damping and k is the elastic rigidity of the oscillator. u is the displacement of the oscillator. u is the displacement of the oscillator, considering the location were the oscillator is at rest as the reference state position. The external excitation is considered as a basal acceleration $F(t)$ which later on will be considered as a stochastic process. The problem stated in (7.1) has an equivalent formulation when normalizing my the mass m

$$\ddot{u}(t) + 2\xi\omega_n\dot{u}(t) + \omega_n^2 u(t) = f(t) \tag{7.2}$$

In this last equation, $2\xi\omega_n = \frac{c}{m}$ and $\omega_n^2 = \frac{k}{m}$ where ω_n is the circular natural frequency of the system and ξ is the critical damping ratio of the system. With these 2 constants, the dynamical behavior of the system can be characterized. The response of the system can be written as a Duhammel integral solution, which is simply a convolution integral given by

$$u(t) = \int_{-\infty}^{+\infty} h(t-\tau)f(\tau)d\tau \tag{7.3}$$

where $h(t)$ is the response of the system to an unitary impulse excitation, that can be considered as a delta Dirac function, thus yielding

$$h(t) = \begin{cases} \frac{1}{\omega_a} e^{-\xi\omega_n t}\sin(\omega_a t) & \text{si} \quad t \geq 0 \\ 0 & \text{si} \quad t < 0 \end{cases} \tag{7.4}$$

where $\omega_a = \omega_n\sqrt{1-\xi^2}$ If the expected value of the response is taken, then

$$E[u(t)] = \int_{-\infty}^{+\infty} h(t-\tau)E[f(\tau)]d\tau \tag{7.5}$$

and since the expected value of $E[f(t)] = 0$ is equal to zero, then equation (7.5) will become

$$E[u(t)] = 0 \tag{7.6}$$

To compute the autocorrelation of the response, the following can be done

$$R_{uu}(t_1,t_2) = E\left[\int_{-\infty}^{+\infty} h(t_1-\tau_1)f(\tau_1)d\tau_1 \int_{-\infty}^{+\infty} h(t_2-\tau_2)f(\tau_2)d\tau_2\right] \tag{7.7}$$

using the properties of commutativity , then

$$R_{uu}(t_1,t_2) = \int_{-\infty}^{+\infty}\int_{-\infty}^{+\infty} h(t_1-\tau_1)h(t_2-\tau_2)E[f(\tau_1)f(\tau_2)]d\tau_1 d\tau_2 \tag{7.8}$$

$$R_{uu}(t_1,t_2) = \int_{-\infty}^{+\infty}\int_{-\infty}^{+\infty} h(t_1-\tau_1)h(t_2-\tau_2)R_{ff}(\tau_1,\tau_2)d\tau_1 d\tau_2 \tag{7.9}$$

And in this last equation, the autocorrelation of the response has been computed, in function of the autocorrelation of the process.

7.1.2 Response to a stationary process

A stationary stochastic process which has a autocorrelation function that depends only on the difference between two instances of time t_1 and t_2

$$R_{ff}(t_1,t_2) = R_{ff}(t_2-t_1) \tag{7.10}$$

which can be related to the power spectral density function (PSD) $S_{ff}(\omega)$ through the Wiener-Kchinchine theorem

$$R_{ff}(t_2-t_1) = \int_{-\infty}^{+\infty} S_{ff}(\omega)e^{i\omega(t_2-t_1)}d\omega \tag{7.11}$$

replacing this last equation in (7.9) and alternating the order in the integral yields

$$R_{uu}(t_1,t_2) = \int_{-\infty}^{+\infty} S_{ff}(\omega)\int_{-\infty}^{+\infty} h(t_1-\tau_1)e^{-i\omega\tau_1}d\tau_1 \int_{-\infty}^{+\infty} h(t_2-\tau_2)e^{i\omega\tau_2}d\tau_2 d\omega \tag{7.12}$$

and with a proper variable change as $\xi_1 = t_1 - \tau_1$, $\xi_2 = t_2 - \tau_2$, $\tau = t_2 - t_1$, it is possible to obtain

$$R_{uu}(\tau) = \int_{-\infty}^{+\infty} S_{ff}(\omega) e^{-i\omega\tau} \int_{-\infty}^{+\infty} h(\xi_1) e^{-i\omega\xi_1} d\xi_1 \int_{-\infty}^{+\infty} h(\xi_2) e^{i\omega\xi_2} d\xi_2 d\omega \tag{7.13}$$

and the integral becomes

$$\int_{-\infty}^{+\infty} h(\tau) e^{-i\omega\xi_i} d\xi_i = 2\pi \hat{h}(\omega) \tag{7.14}$$

where $\hat{h}(\omega)$ is the Fourier transform of $h(t)$, given by

$$\hat{h}(\omega) = \frac{1}{2\pi} \int_{-\infty}^{+\infty} h(\tau) e^{-i\omega\xi_i} d\xi_i = \frac{1}{2\pi((\omega_n^2 - \omega^2) - 2i\xi\omega_n\omega)} \tag{7.15}$$

therefore, the autocorrelation function can be written as

$$R_{uu}(\tau) = \int_{-\infty}^{+\infty} S_{ff}(\omega) e^{-i\omega\tau} \hat{h}(\omega) \hat{h}^*(\omega) d\omega \tag{7.16}$$

If $t_1 = t_2$, then $\tau = 0$. This corresponds to the mean square response

$$R_{uu}(0) = E[u^2(t)] = \int_{-\infty}^{+\infty} \|\hat{h}(\omega)\|^2 S_{ff}(\omega) d\omega \tag{7.17}$$

If S_{ff} varies slowly with respect to $\|\hat{h}(\omega)\|$, then the system will behave like a narrow band filter, this means that the highest contribution of the excitation of the process will be around the natural frequency ω_n [Caughey and Stumpf, 1961], thus equation (7.17) will take the following form

$$E[u^2(t)] = S_{ff}(\omega_n) \int_{-\infty}^{+\infty} \|\hat{h}(\omega)\|^2 d\omega \tag{7.18}$$

Caughey and Stumpf [1961], among many, use the residual theorem to solve equation (7.18), leaving the following equation

$$E[u^2(t)] = \frac{\pi S_{ff}(\omega_n)}{2\xi\omega_n^3} \tag{7.19}$$

If the mean value is considered to be zero, then equation (7.19 completes the probabilistical structure of the response in the case of an Gaussian excitation.

7.1.3 Response of a non-stationary separable process

if f is considered to be a non-stationary separable process, then using the property stated in equation (7.8), the autocorrelation function can be found, which is given by

$$R_{ff}(t_1, t_2) = \psi(t_1)\psi(t_2) R_{ss}(t_1, t_2) \tag{7.20}$$

now equation (7.9) can be used to find the autocorrelation of the response

$$R_{uu}(t_1,t_2)=\int_{-\infty}^{+\infty}\int_{-\infty}^{+\infty}h(t_1-\tau_1)h(t_2-\tau_2)\psi(\tau_1)\psi(\tau_2)R_{ss}(\tau_1,\tau_2)d\tau_1 d\tau_2 \tag{7.21}$$

Using the Wiener-Kchinchine relationship, the autocorrelation function can be expressed in terms of the autocorrelation of the stationary process, an the latter, can be expressed in terms of the power spectral density function of the stationary process as follows

$$R_{ss}(\tau_1,\tau_2)=\int_{-\infty}^{+\infty}S(\omega)e^{i\omega(\tau_2-\tau_1)}d\omega \tag{7.22}$$

making some algebraic arrangements the next expression can be obtained

$$R_{uu}(t_1,t_2)=\int_{-\infty}^{+\infty}S(\omega)\int_{-\infty}^{+\infty}h(t_1-\tau_1)\psi(\tau_1)e^{-i\omega\tau_1}d\tau_1\int_{-\infty}^{+\infty}h(t_2-\tau_2)\psi(\tau_2)e^{i\omega\tau_2}d\tau_2 d\omega \tag{7.23}$$

Calling non-stationary transfer function to

$$\Upsilon(t,\omega)=\int_{-\infty}^{+\infty}h(t-\tau)\psi(\tau)e^{-i\omega\tau}d\tau \tag{7.24}$$

and replacing this term in equation (7.23), it is possible to obtain

$$R_{uu}(t_1,t_2)=\int_{-\infty}^{+\infty}\Upsilon(t_1,\omega)\Upsilon^*(t_2,\omega)S(\omega)d\omega \tag{7.25}$$

where $\Upsilon^*(t,\omega)$ is the complex conjugate of $\Upsilon(t,\omega)$. In the case that $t_1=t_2=t$, then the mean square response will be

$$E[u^2(t)]=\int_{-\infty}^{+\infty}\|\Upsilon(t,\omega)\|^2S(\omega)d\omega \tag{7.26}$$

To obtain the probabilistical structure of the response, it is convenient to have the correlation functions of the displacement-velocity, $E[\dot{u}(t)u(t)]$ and the mean square response of the velocity $E[\dot{u}^2(t)]$. To obtain these functions, the methodology used by Crempien Laborie and Crempien de la Carrera [2005] can be used, this is achieved derivating with respect to time equation (7.26), and developing these expressions, the correlation between u y $\dot{u}$ can be obtained.

$$\frac{\partial}{\partial t}(E[u^2(t)])=\frac{\partial}{\partial t}\int_{-\infty}^{+\infty}\Upsilon(t,\omega)\Upsilon^*(t,\omega)S(\omega)d\omega \tag{7.27}$$

The partial derivative can be taken into the integral

$$\frac{\partial}{\partial t}(E[u^2(t)])=\int_{-\infty}^{+\infty}\left[\dot{\Upsilon}(t,\omega)\Upsilon^*(t,\omega)+\dot{\Upsilon}^*(t,\omega)\Upsilon(t,\omega)\right]S(\omega)d\omega \tag{7.28}$$

The same with the expected operator

$$E[2\dot{u}(t)u(t)]=\int_{-\infty}^{+\infty}\left[\dot{\Upsilon}(t,\omega)\Upsilon^*(t,\omega)+\left(\dot{\Upsilon}(t,\omega)\Upsilon^*(t,\omega)\right)^*\right]S(\omega)d\omega \tag{7.29}$$

If this expression is further manipulated, the correlation can be reached

$$2E[\dot{u}(t)u(t)] = 2\int_{-\infty}^{+\infty} \text{Real}\left[\dot{\Upsilon}(t,\omega)\Upsilon^*(t,\omega)\right] S(\omega)d\omega \tag{7.30}$$

$$E[\dot{u}(t)u(t)] = \int_{-\infty}^{+\infty} \text{Real}\left[\dot{\Upsilon}(t,\omega)\Upsilon^*(t,\omega)\right] S(\omega)d\omega \tag{7.31}$$

If equation (7.25) is partially derived with respect to any two different instances of time, then

$$\frac{\partial^2}{\partial t_1 \partial t_2} R_{uu}(t_1,t_2) = \frac{\partial^2}{\partial t_1 \partial t_2} \int_{-\infty}^{+\infty} \Upsilon(t_1,\omega)\Upsilon^*(t_2,\omega)S(\omega)d\omega \tag{7.32}$$

The partial derivatives can enter the integral in the following way

$$\frac{\partial^2}{\partial t_1 \partial t_2} R_{uu}(t_1,t_2) = \int_{-\infty}^{+\infty} \dot{\Upsilon}(t_1,\omega)\dot{\Upsilon}^*(t_2,\omega)S(\omega)d\omega \tag{7.33}$$

If $t_1 = t_2 = t$, then the mean square of the velocity will be obtained

$$E[\dot{u}^2(t)] = \int_{-\infty}^{+\infty} \|\dot{\Upsilon}(t,\omega)\|^2 S(\omega)d\omega \tag{7.34}$$

expression that can be a analytical in certain cases.

Using equation (7.24), it is possible to see that it is also the solution of a simple SDOF subjected to $\psi(t)\exp(-i\omega t)$, thus it can be solved using any numerical integration scheme such as Newmark family for deterministic cases of ω_n and ξ. To take into account the variability of the natural frequency and the damping ratio the *Law of Total Expectation* can be used. This law states that $E[u^2] = E[E[u^2|\boldsymbol{\eta}]]$, where $\boldsymbol{\eta}$ is a vector representing other uncertain parameters in equation (7.2).

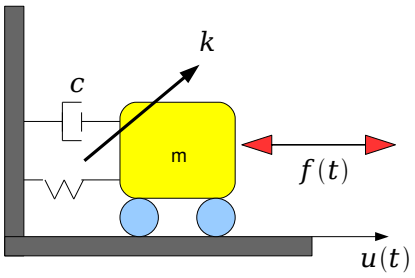

Figure 7.1: SDOF subjected to a dynamic force modelled as a stochastic process.

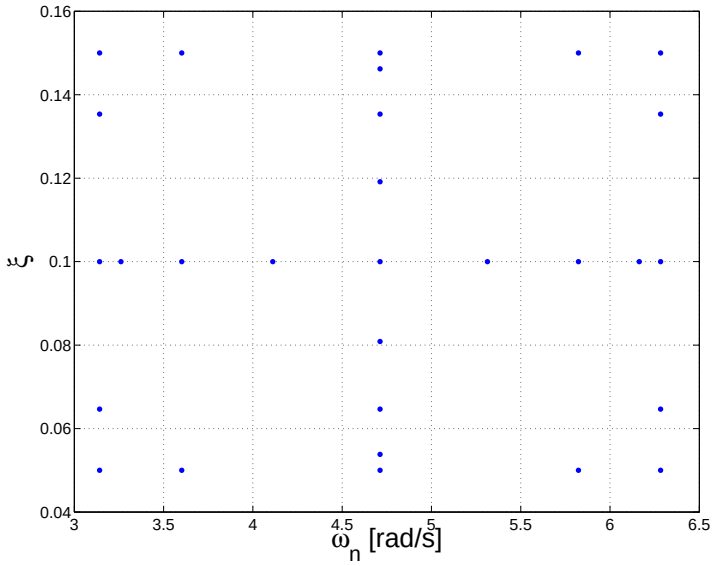

Figure 7.2: Sparse grid plot for the possible values of the circular natural frequency and the critical damping ratio with $N = 2$ and $w = 3$.

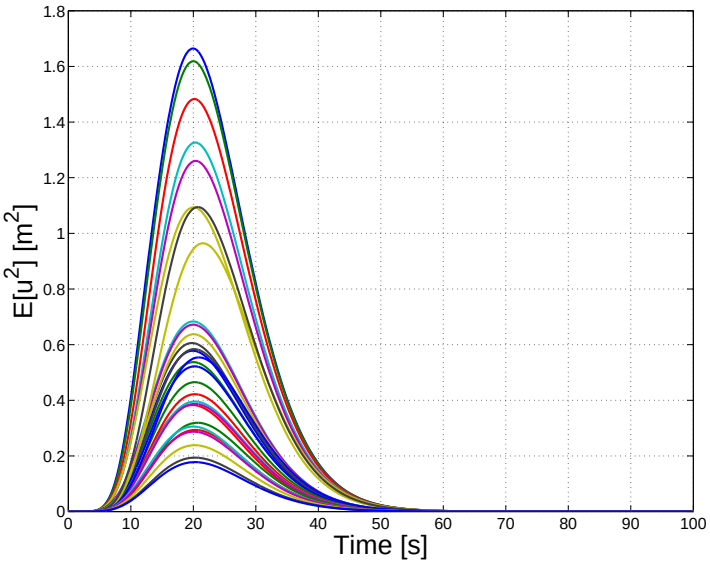

Figure 7.3: Realizations of the mean square displacement response in time for each point in the previous sparse grid where the linear oscillator was subjected to a Gaussian process with a gamma envelope. The coefficients of the envelope are $\alpha = 0.18$, $\beta = 0.5$ and $\gamma = 3.55$.

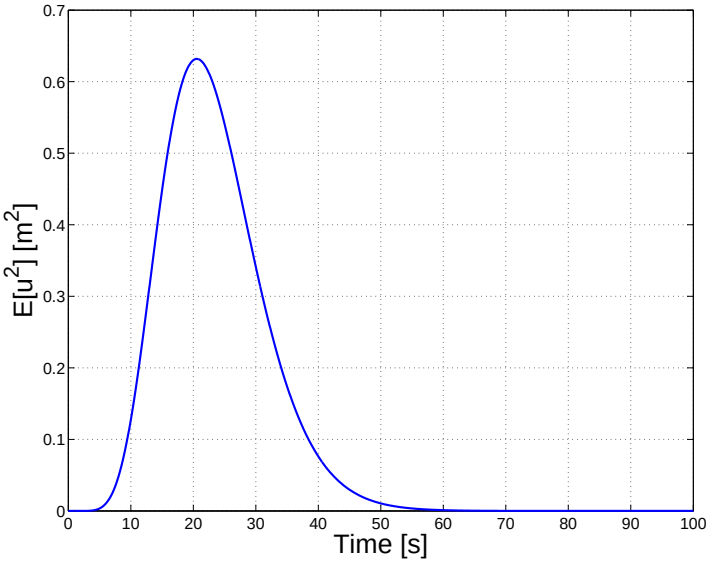

Figure 7.4: Mean square displacement response in time of a linear SDOF subjected to a non-stationary Gaussian process with uncertain circular natural frequency and critical damping ratio (both distribute uniformly). The coefficients of the gamma envelope are $\alpha = 0.18$, $\beta = 0.5$ and $\gamma = 3.55$.

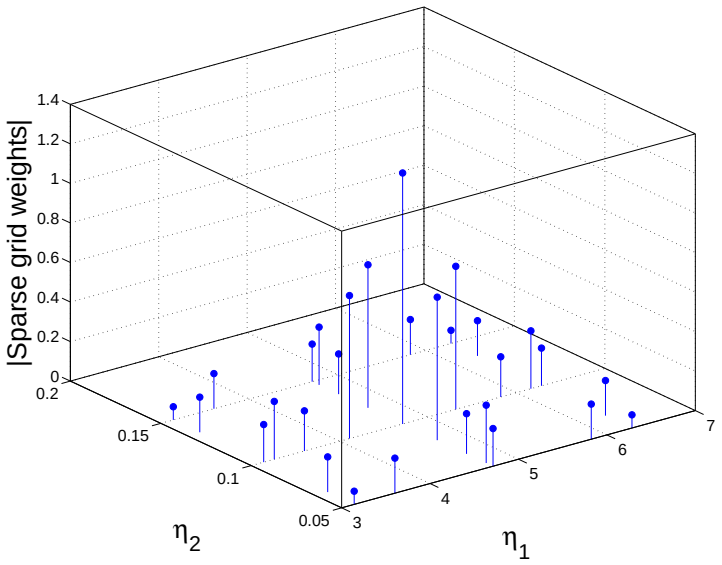

Figure 7.5: The absolute value of the weights for every sparse grid point that was considered in the original grid.

After solving (7.24), equation (7.26) needs to be solved, and for this case, a quadrature based on the Laguerre quadrature rule. It is clear that the solution of this method is based on the positive reals, and the problem at hand is in the whole real domain, but since the integrand of (7.26) is a even function, then

$$E[u^2(t)] = 2\int_0^{+\infty} \|\Upsilon(t,\omega)\|^2 S(\omega) d\omega \tag{7.35}$$

and since $S(\omega)$ can be taken as a weight function, then the corresponding Jacobi matrix is formed, and the nodes and weights are computed.

It is also important to mention that the response is also a Gaussian process, since it was originally subjected to a Gaussian process in the first place, and because of the linearity of the operator.

In figure (7.2) we can see a sparse grid plot of natural frequencies versus the damping ratio of the linear elastic SDOF in figure (7.1). The natural frequency and the damping ratio are considered to distribute uniformly between the range of values seen in figure (7.2. The mean square response of the SDOF subjected to a Gaussian process for each point of the sparse grid in figure (7.2) can be seen if figure (7.3). The final mean square response considering uncertainty in the damping and in the natural frequency can be seen in figure (7.4) and the absolute value of the weights for each sparse grid point is showed in figure (7.5) with η_1 is the natural frequency ω_n and η_2 is the damping ratio ξ.

7.2 RESPONSE OF BOUC-WEN SDOF TO RANDOM PULSES

Let us consider the Bouc-Wen model for a SDOF that uses k_1 and k_2 as the stiffnesses that try to capture the bilinear behavior of a lead bearing or other more general cases [Bouc, 1967]. The change of stiffness occurs at a deformation u_y. If we take the ratio of the stiffnesses $\alpha = \frac{k_2}{k_1}$, then it is possible to use the following model

$$p(t) = \alpha k_1 u(t) + (1-\alpha) k_1 u_y z(t) \tag{7.36}$$

which is the total restoring force of the system, and the differential equation that determines $z(t)$ is given by

$$u_y \dot{z}(t) + \gamma |\dot{u}(t)| z(t) |z(t)|^{n-1} + \beta \dot{u}(t) |z(t)|^n - \dot{u}(t) = 0 \tag{7.37}$$

where β and γ are dimensionless quantities that control the shape of the hysteresis loops. The dimensionless parameter n, can be viewed as a controller of the degree of smoothness of the curves during the transition of the stiffness and $z(t)$ is a dimensionless function of time. As it can be seen, the last 2 equations are dimensionally correct. As it can be seen clearly, if $k_2 = 0$

and $n = 0$, then the Bouc-Wen model reduces to a simple elastic perfectly plastic hysteresis rule. These equations can be incorporated in the equation of motion as follows

$$m\ddot{u}(t) + p(t) = -m\ddot{u}_g(t) \tag{7.38}$$

which does not have terms of velocity damping, but it can be included in the following manner

$$m\ddot{u}(t) + c\dot{u}(t) + p(t) = -m\ddot{u}_g(t) \tag{7.39}$$

and this equation takes into account viscous and hysteretic behavior, and it can be solved using a state-space formulation.

$$\ddot{u}(t) + 2\xi\omega_1\dot{u}(t) + \alpha\omega_1^2 u(t) + (1-\alpha)\omega_1^2 u_y z(t) = -\ddot{u}_g(t) \tag{7.40}$$

To solve this set of nonlinear differential equations, the matlab function ode15s was used, which is a variable order solver that is based on the numerical differentiation formulas. It also uses alternately the backward differentiation formulas, that are also known as Gear's method [Shampine and Reichelt, 1997], which are very efficient for these kind of problems. dissipated energy

$$W_D = \int_0^\infty F(t)du = \int_0^\infty F(t)\dot{u}dt \tag{7.41}$$

where

$$F(t) = c\dot{u}(t) + p(t) \tag{7.42}$$

The advantage of this parameter that depends in time, is that it is a relatively smooth function, thus it is more or less easy to characterize.

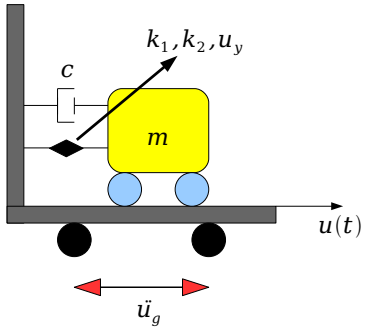

Figure 7.6: A SDOF with a bilinear Bouc Wen model of hysteresis subjected to random pulses.

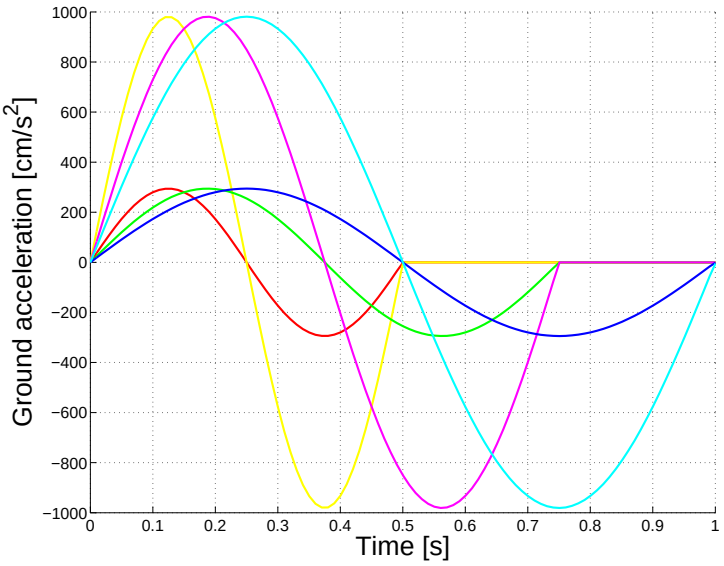

Figure 7.7: Possible acceleration pulses applied at the base of the SDOF in figure (7.6).

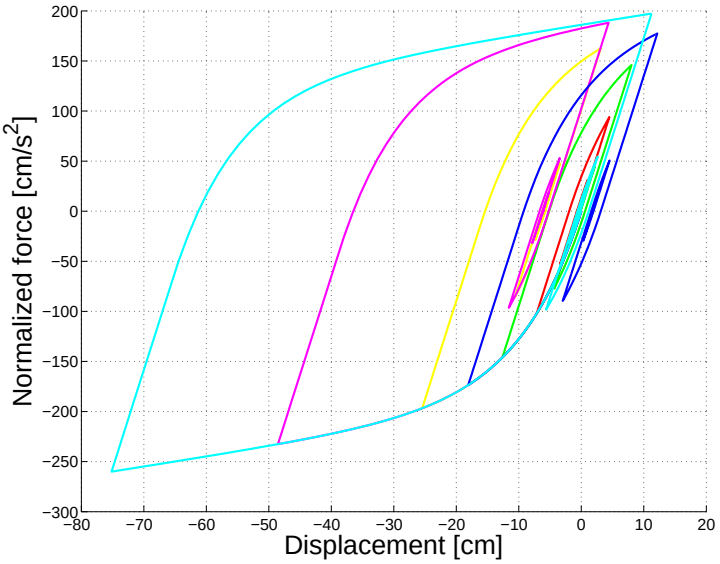

Figure 7.8: Normalized force-displacement curves of a SDOF oscillator with a Bouc-Wen nonlinear rule due to the previous pulses (in accordance by colors).

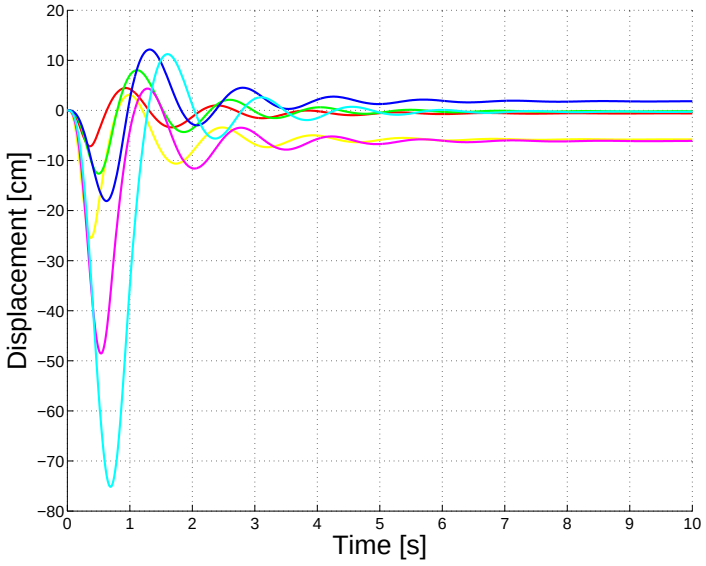

Figure 7.9: Displacement response in time of a SDOF oscillator with a Bouc-Wen nonlinear rule due to the previous pulses (in accordance by colors).

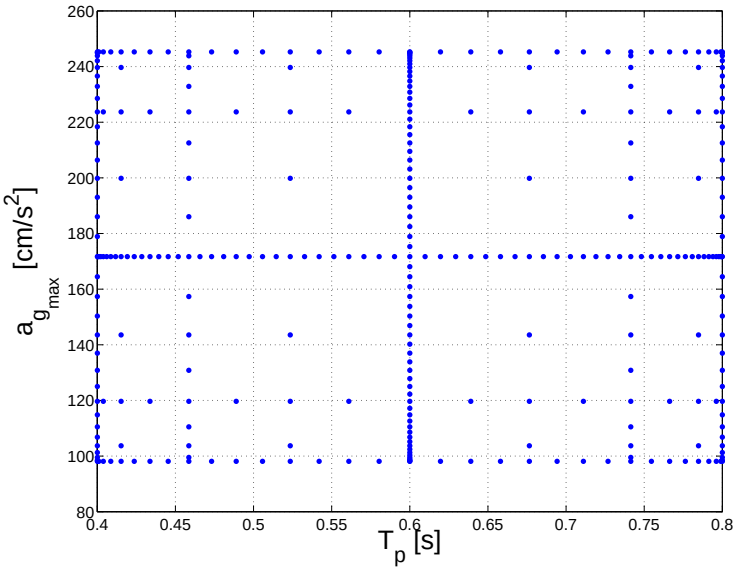

Figure 7.10: Sparse grid plot of the possible maximum amplitudes and pulse durations using $N = 2$ and $w = 6$.

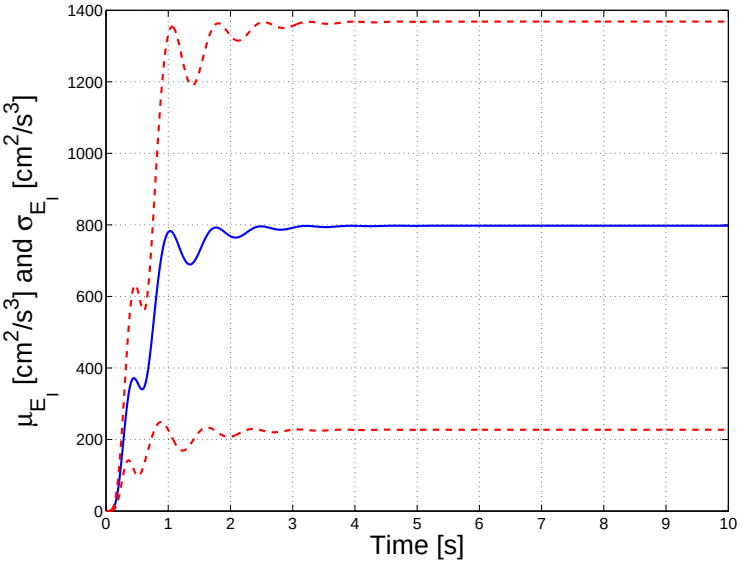

Figure 7.11: The expected value (solid blue line), plus minus the standard deviation (dashed red line) of the normalized internal energy due to the random pulses stated before.

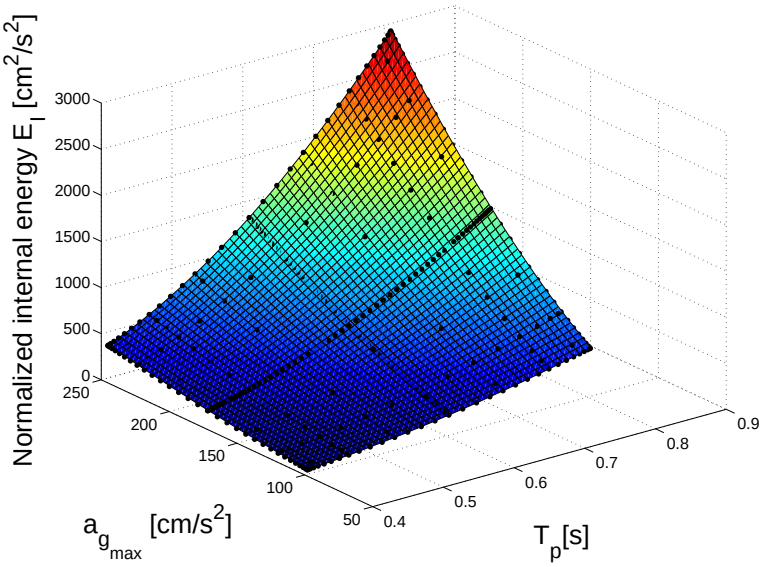

Figure 7.12: Sparse interpolation of the final normalized internal energy where the black dots are the realizations of the sparse grid points.

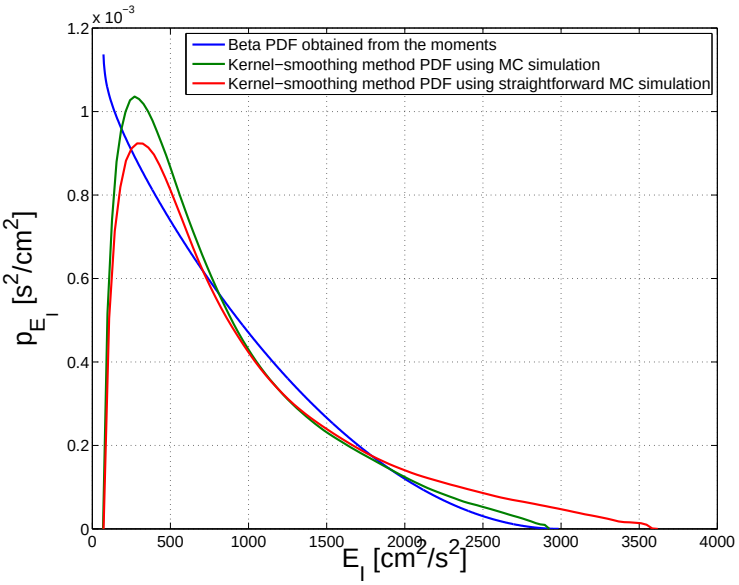

Figure 7.13: The estimation of PDF using a Beta fitting method, K-S density estimation combined with Monte Carlo simulation with the response surface and K-S density estimation with straightforward Monte Carlo simulation for the normalized internal energy.

Plot (7.7) are simply possible acceleration pulses, which are applied to the nonlinear SDOF of figure (7.6). The normalized force displacement curves due to the acceleration pulses are presented in plot (7.8) as well as the displacement plots which are shown in figure (7.9). From these plots it is clear that time duration is an important factor to take into account, just as peak ground acceleration.

Figures (7.10), (7.11) and (7.12) are respectively the sparse grid plot considering the peak ground acceleration and the pulse duration, the expected value plus minus the standard deviation and finally the response surface of the normalized internal energy. In figure (7.10) a great variability can be observed as time evolves.

In graph (7.13) the method does not compare favorably to the straightforward Monte Carlo simulation. There are events which cannot be found by the sparse grid interpolation thus giving relatively different PDF functions. There must be a very local maxima or minima in the response function that cannot be represented by the sparse interpolation, and to find this irregularity it is necessary to turn to other methods. But for this kind of problem, there is not much in the literature to start with, and it can be said that it is an open problem for the field.

7.3 SITE RESPONSE USING 1D SEM

The spectral element method is a numerical method that is formulated based on the weak form of a partial differential equation. Basically it is a higher order finite element method. It was introduced into the field of computational seismology in the late 90's and the main contributors are Komatitsch and Vilotte [1998]; Komatitsch and Tromp [1999]; Chaljub, Komatitsch, Vilotte, Capdeville, Valette, and Festa [2007]; Faccioli, Maggio, Paolucci, and Quarteroni [1997]. In this section the 1d wave equation will be presented, as well as the weak form of this equation. Later the ansatz of this equation will be presented and the final solution will be derived.

The 1d wave equation can be stated as the following partial differential equation defined in a physical domain $\Omega = [-H, 0]$.

$$\rho(z)u_{,tt}(z,t) - [\mu(z)u_{,z}(z,t)]_{,z} = f(z,t) \tag{7.43}$$

where u is the displacement field, ρ is the mass density, μ is the shear modulus and f is the forcing term. The traction along the depth of the physical domain Ω will always be $\mathbf{t}(z,t) = \mu(z)u_{,z}(z,t)$. It is obvious that the traction on the free surface will always be zero $\mathbf{t}(0,t) = 0$ at all times, this property will be useful as the derivation of this problem advances. At the bottom, an absorbing condition will be imposed such that $\mathbf{t}(-H,t) = \mathbf{t}_{abs}(-H,t)$, so that the

downgoing waves do not reflect upwards again at the bottom condition. To solve this equation using the spectral element method it is necessary to take it to it's weak form, for this purpose the wave equation is multiplied by an arbitrary displacement field $v(z)$, to later integrate in the whole domain

$$\int_{\Omega} \left[\rho(z)u_{,tt}(z,t) - \left[\mu(z)u_{,z}(z,t)\right]_{,z} - f(z,t)\right] v(z)dz = 0 \tag{7.44}$$

As it was mentioned before, this equation holds for any admissible displacement field $v(z)$ where admissible means that this function does posses a certain level of continuity over the domain Ω. This last equation can be integrated by parts to obtain

$$\begin{aligned} &\int_{\Omega} \rho(z)u_{,tt}(z,t)v(z)dz + \int_{\Omega} \mu(z)u_{,z}(z,t)v_{,z}(z)dz \\ &= \int_{\Omega} f(z,t)v(z)dz + \left[\mathbf{t}(0,t)v(0) - \mathbf{t}(-H,t)v(-H)\right] \end{aligned} \tag{7.45}$$

continuing the derivation and as it was mentioned before, $\mathbf{t}(0,t) = 0$, so the weak form finally is

$$\begin{aligned} &\int_{\Omega} \rho(z)u_{,tt}(z,t)v(z)dz + \int_{\Omega} \mu(z)u_{,z}(z,t)v_{,z}(z)dz \\ &\quad = \int_{\Omega} f(z,t)v(z)dz - \mathbf{t}_{abs}(-H,t)v(-H) \end{aligned} \tag{7.46}$$

Now it is possible to divide the spatial domain Ω in elements Ω_e, such that $\Omega = \cup_{e=1}^{E}\Omega_e$. After this consideration the previous equation can be rewritten as

$$\begin{aligned} &\sum_{e=1}^{E} \int_{\Omega_e} \rho(z)u_{,tt}(z,t)v(z)dz + \sum_{e=1}^{E} \int_{\Omega_e} \mu(z)u_{,z}(z,t)v_{,z}(z)dz \\ &\quad = \sum_{e=1}^{E} \int_{\Omega_e} f(z,t)v(z)dz - \mathbf{t}_{abs}(-H,t)v(-H) \end{aligned} \tag{7.47}$$

The displacement field can be expanded in series as

$$u(z,t) = u(F^e(\xi),t) \approx \sum_{i=0}^{N} u(F^e(\xi_i),t)l_i(\xi) \tag{7.48}$$

where $F^e(\xi)$ is a transformation into the isoparametric space (in this case $[-1,1]$), such that quadrature turns out to be much more simple. ξ_i are the quadrature nodes that for computational purposes, it is very attractive to choose Gauss Lobatto Legendre nodes, because in this way, the mass matrix turns out to be diagonal. $l_i(\xi)$ are the components of the Lagrange interpolation that are used to characterize the solution in each element by enriching the polynomial degree. With this approximation, the final system of equations is

$$\mathbf{M}\ddot{\mathbf{U}} + \mathbf{K}\mathbf{U} = \mathbf{S}\mathbf{F}(t)$$

Which is possible to solve with different numerical methods such as the Newmark family.

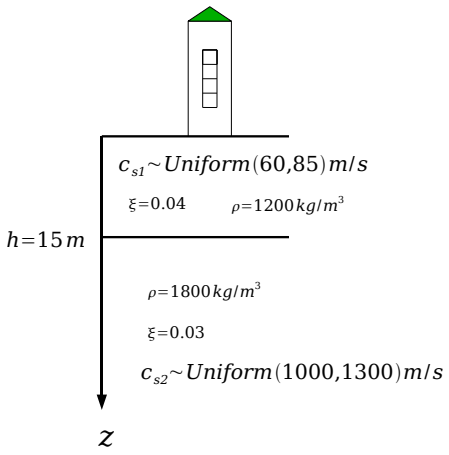

Figure 7.14: The 1d site conditions and the respective uncertainty in the shear wave speed of each layer.

The problem that is analyzed is a medium with 2 layers as seen in figure (7.14). Both of these layers have a shear wave velocity which is modelled as a uniform random variable, and the distribute between $60\ [m/s]$ and $85\ [m/s]$ for the upper layer, and $1000\ [m/s]$ and $1300\ [m/s]$. The 1d soil column is subjected to a deterministic Ricker wavelet that can be appreciated in figure (7.15). The parameter of interest will be the Arias intensity [Arias, 1970], which is given by the following equation

$$I_a = \frac{\pi}{2g} \int_0^{\infty} \ddot{U}^2(top) dt \tag{7.49}$$

This quantity of interest is also relatively smooth, thus easy to characterize.

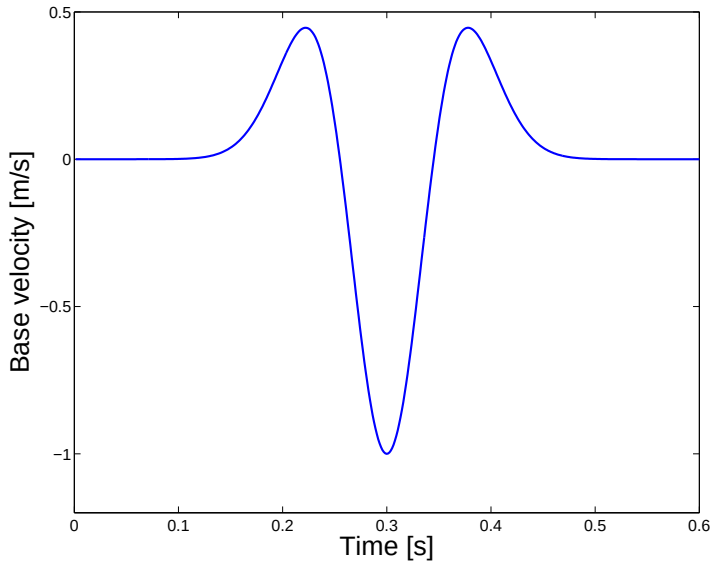

Figure 7.15: The 1d soil column is subjected to this Ricker wavelet at the base.

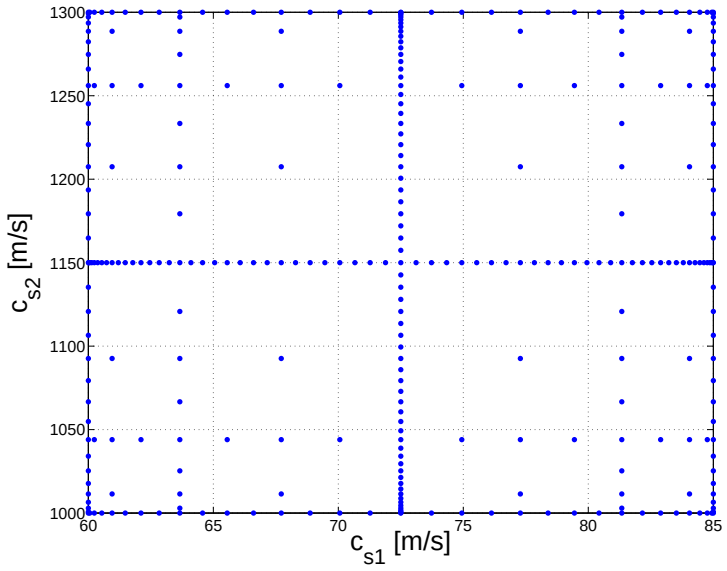

Figure 7.16: Sparse grid for the possible shear wave velocities of the bi-medium 1d soil column with $N = 2$ and $w = 6$.

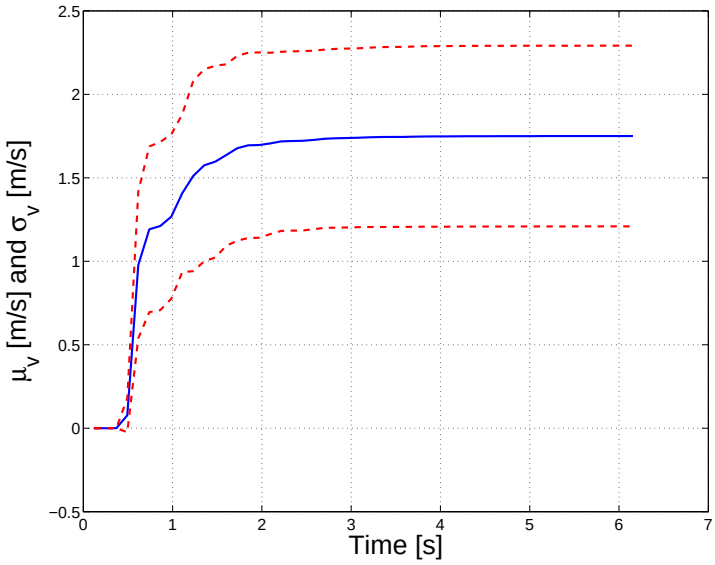

Figure 7.17: Mean (solid blue line), plus minus the standard deviation (dashed red line) of the evolutionary Arias intensity at the free surface due to a Ricker wavelet at the base of the medium.

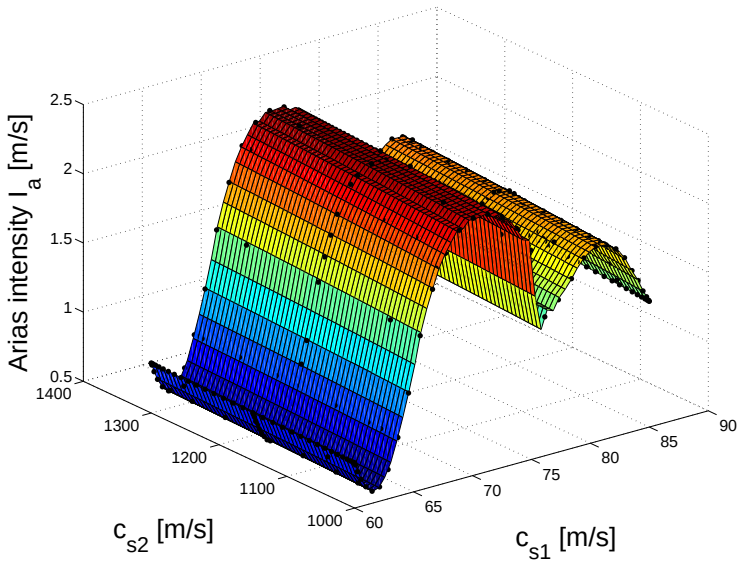

Figure 7.18: Response surface of the Arias intensity at the free end using sparse interpolation where the black dots are the realizations of the sparse grid points.

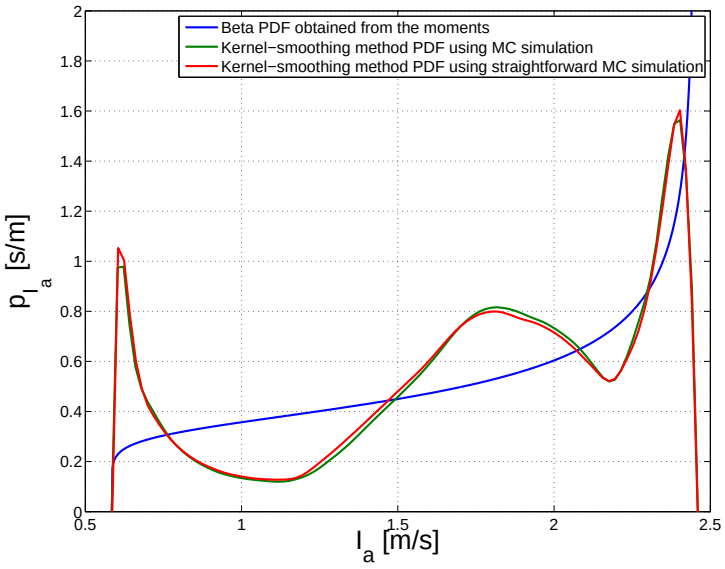

Figure 7.19: PDF estimation using a Beta fitting method using the first 2 moments and the limits, Monte Carlo simulation combined with K-S density estimation using both the response surface and simulation from scratch. All of witch are due to a Ricker wavelet at the base of the medium.

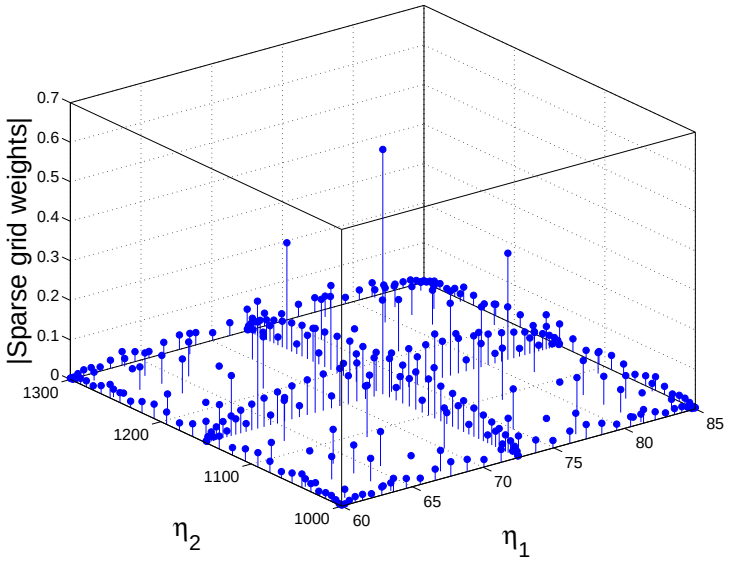

Figure 7.20: Absolute value of the weights for each sparse grid point.

Figure (7.16) shows the sparse grid using Clenshaw-Curtis nodes and in figure (7.17), the mean plus minus one standard deviation of the evolutionary Arias intensity is obtained. The plots show that the sparse grid interpolation and subsequent Monte Carlo simulation are very much precise, and is almost comparable to the full Monte Carlo simulation. In figure (7.18) it is clear that the shear wave velocity of the bottom medium in not an important factor, i.e. the final response has no great variations if this parameter if changed, thus there is a waste of computational effort due to the evaluation of points along the variation of c_{s2}. An interesting approach to solve this problem would be to use anisotropic parse grids [Nobile, Tempone, and Webster, 2008b]. The explanation of this phenomena is due to the high contrast between the two mediums, which allows an incoming wave from the bottom to the upper layer to be trapped in the low velocity medium for a long while, thus not letting the high velocity medium to be used to propagate the SH waves in comparison with the low velocity medium. In figure (7.19), the final PDF for the beta fitting using the moments is plotted as well as the K-S density estimation using the results of the Monte Carlo simulation for both the straightforward case and the sparse grid approach. There is a remarkable similitude between both of the K-S density estimations (straightforward and sparse grod approach). The beta estimation method using the moments is quite far from the actual solution. Finally the absolute values of the weights are shown in figure (7.20).

8. CONCLUDING REMARKS AND FUTURE RESEARCH

8.1 CONCLUDING REMARKS

The sparse grid stochastic collocation methods are shown to be regular for problems in which the solution is smooth, and irregular with irregular response. It is also not a good idea to use this method for problems in which the noise level is very high, since this will lead to the necessity to include many terms in the Karhunen Loève expansion, thus increasing the dimension of the problem. There will be a point in which if the dimension increases too much, the best approach will be the use of Monte Carlo simulation, because as mentioned before, Monte Carlo simulation does not depend on the dimension number, though it converges rather slow.

The moments are not enough for engineering applications, at least not combined with beta functions, though these computed with the moments and boundaries are maximizing the information entropy [Harr, 1989]. But still they seem far off with respect to the two Monte Carlo simulation based techniques that where exposed. It must be pointed out that there are other methods that are present in the literature that estimate PDF functions using the first four moments which were not explored in this work, the reader is referred to Johnson [1949].

8.2 FUTURE RESEARCH

There should be a different approach for dynamical/hyperbolic problems, to find the solution of quantities of interest in time. For linear problems this can be done with the approach that was used in chapter (7), but there is still an open question in the field of nonlinear response of systems (only Fokker-Planck solutions and linearized methods that do not hold convergence properties). A similar approach to the elastic case should be used.

A special effort direct towards improving of a priori anisotropic sparse grid collocation methods

should be done since it is a computational effort saver.

Problems with localized maxima and minima should be addressed using adaptive schemes to find this singular points.

Another interesting problem is the correct characterization-discretization of random fields using the Galerkin approach, but with wavelets to make the matrices of the problem as sparse as possible [Phoon, Huang, and Quek, 2004], thus reducing the computational effort that needs to be done to solve the eigenvalue and eigenvector problem. It would also be interesting to do this considering that for different zones withing the domain of interest, a different covariance function, which can be a realistic way to model a large domain.

REFERENCES

Amin, M. and H. S. Ang (1966). A Nonstationary Stochastic Model for Strong Motion Earthquake. Technical report, University of Illinois, Urbana, Illinois.

Arias, A. (1970). *A Measure of Earthquake Intensity*. New York: MIT Press, Cambridge, Massachusetts.

Arias, A., A. Holzapfel, and G. R. Saragoni (1976). An Approximation Expression for the Mean Square Acceleration of Earthquake Ground Motions. In *Proceedings of Fith World Conference on Earthquake Engineering*.

Babuška, I., F. Nobile, and R. Tempone (2007). A stochastic collocation method for elliptic partial differential equations with random input data. *SIAM Journal of Num. Anal. 43 (3)*, 1005–1034.

Babuška, I., R. Tempone, and G. Zouraris (2004). Galerkin finite element approximation of stochastic partial differential equations. *SIAM Journal of Num. Anal. 42 (2)*, 800–825.

Baldeweck, H. (1999). *Métodes aux éléments finis stochastiques - applications á la géotechnique et á la mécanique de la rupture*. Ph. D. thesis, Université d'Evry-Val d'Essone, France.

Baroth, J., L. Bodé, P. Bressolette, and M. Fogli (2006). SFE method using Hermite polynomials: An approach for solving nonlinear mechanical problems with uncertain parameters. *Computer methods in applied mechanics and engineering 195*, 6497–6501.

Baroth, J., P. Bressolette, C. Chauviére, and M. Fogli (2007). An efficient SFE method using Lagrange polynomials: Application to nonlinear mechanical problems with uncertain parameters. *Computer methods in applied mechanics and engineering 196*, 4419–4429.

Barthelmann, V., E. Novak, and K. Ritter (2000). High dimensional polynomial interpolation on sparse grids. *Adv. Comput. Math 12 (4)*, 273–288.

Bogdanoff, J. L. and F. Kosin (1961). Comment on Reliability of Structures in Resisting Chance Failure. *Operations Research 9*, 123–126.

Bolotin, V. V. (1960). Statistical Theory of the Aseismic Design of Strucutres. In J. Science

Council of Japan (Ed.), *Proceedings of Second World Conference on Earthquake Engineering, 1960*, pp. 1365–1374. Science Council of Japan. Volume 2.

Bolotin, V. V. (1984). *Random Vibrations of Elastic Systems*. The Hauge, Holland: Martinus Nijhoff.

Bouc, R. (1967). Forced vibration of mechanical system with hysteresisStatistical Method of Determining the Maximum Response of a Building Structure During a Earthquake. In *Proceedings 4th Conference on Nonlinear Oscillation, Prague, Czechoslovakia*.

Brady, A. G. (1966). Studies of Response to Earthquake Ground Motions. Technical report, California Institute of Technology, Pasadena.

Bycroft, G. N. (1960). White Noise Representation of Earthquakes. *Journal of Engineering Mechanics Division, ASCE 86*, 1–16.

Caughey, T. K. and H. J. Stumpf (1961). Transient Response of Dynamic Systems under Random Excitations. *Journal of Applied Mechanics 28*, 563–566.

Chaljub, E., D. Komatitsch, J.-P. Vilotte, Y. Capdeville, B. Valette, and G. Festa (2007). Spectral element analysis in seismology. In R.-S. Wu and V. Maupin (Eds.), *Advances in Wave Propagation in Heterogeneous Media*, Volume 48 of *Advances in Geophysics*, pp. 365–419. Elsevier - Academic Press.

Clenshaw, C. W. and A. R. Curtis (1960). A method for numerical integration on an automatic computer. *Numerische Mathematik 2*, 197–205.

Conte, J. P. and B. F. Peng (1997). Fully Nonstationary Analytical Earthquake Ground-Motion Model. *Journal of Engineering Mechanics, ASCE 123*, 15–24.

Corotis, R. B. and E. H. Vanmarcke (1975). Time Dependant Spectral Content of a System Response. *Journal of Engineering Mechanics Division, ASCE 101*, 623–637.

Cox, R. T. (1946). Probability, frequency, and reasonable expectation. *American Journal of Physics 14*, 1–13.

Crempien Laborie, J. E. (1988). *A Time-Frequency Model for Earthquake Motion and Structural Response*. Ph. D. thesis, University of California, Berkeley.

Crempien Laborie, J. E. and J. G. F. Crempien de la Carrera (2005). Failure Probability of a Simple SDOF Elastic Structure Subyected to an Evolutionary Model of Ground Motion. *AMCA, Mecnica Computacional 25*, 721–741.

Crempien Laborie, J. E. and A. Der Kiureghian (1988). A Time-Frequency Evolutionary Model for Earthquake Motion and Structural Response. *Structural Safety 6*, 235–246.

Crempien Laborie, J. E. and G. R. Saragoni (1978). Influence of the Duration of Earthquake Ground Motion in Average Response Spectra. In *Proceedings of Sixth European Conference on Earthquake Engineering, Dubrovnic, Jugoslavia*, pp. 143–150. Volume 2.

Deb, M. K., I. M. Babuška, and J. T. Oden (2001). Solution of stochastic partial differential equations using Galerkin finite element techniques. *Comput. Methods Appl. Mech. Engrg. 190*, 6359–6372.

E.H.Vanmarcke (1977). Probabilistic modeling of soil profiles. *Journal of Geotechnical Engineering Division 103*(11), 1227–1246.

Faccioli, E. F., F. Maggio, R. Paolucci, and A. Quarteroni (1997). 2d and 3d elastic wave propagation by pseudo-spectral domain decomposition method. *Journal of Seismology 1*, 237–251.

Ghanem, R. G. (1998). Probabilistic characterization of transport in heterogeneous media. *Journal of Engineering Mechanics Division, ASCE 158*, 199–220.

Ghanem, R. G. and P. D. Spanos (1991). Spectral stochastic finite-element formulation for reliability analysis. *Journal of Engineering Mechanics Division, ASCE 117, 10*, 2351–2372.

Ghiocel, D. and R. Ghanem (2002). Stochastic finite element analysis of seismic soil-structure interaction. *ASCE, Journal of Engineering Mechanics 128*(1), 66–77.

Goldberg, J. E., J. L. Bogdanoff, and D. R. Sharpe (1964). The Response of Simple Non-Linear Structures to a Random Disturbance of Earthquake Type. *Bulletin of the Seismological Society of America 54*, 263–276.

Graham, L. L. and S. Baxter (2000). Characterization of random composite materials using the moving-window generalized method of cells technique. *ASCE Journal of Engineering Mechanics 126*(4), 389–397.

Hammond, J. (1968). On the Response of Single and Multidegree of Freedom Systems to Non-Stationary Random Excitations. *Journal of Sound and Vibration 7*, 393–416.

Harr, M. E. (1989). Probabilistic Estimates for Multivariate Analyses. *Applied Math. Modelling 13*, 313–318.

Haukaas, T. and A. Der Kiureghian (2005). Parameter sensitivity and importance measures in nonlinear finite element reliability analysis. *Journal of Engineering Mechanics, ASCE 131 (10)*, 1013–1026.

Holman, R. E. and G. C. Hart (1974). Nonstationary Response of Structural Systems. *Journal of Engineering Mechanics Division, ASCE 100*, 415–431.

Housner, G. W. (1947). Characteristics of Strong-Motion Earthquakes. *Bulletin of the Seismological Society of America 37*, 19–31.

Housner, G. W. and P. C. Jennings (1964). Generation of Artificial Earthquakes. *Journal of Engineering Mechanics Division, ASCE 90*, 113–150.

Huang, S., S. Mahadevan, and R. Rebba (2007). Collocation-based stochastic finite element analysis for random field problems. *Probabilistic Engineering Mechanics 22*, 194–205.

Iyengar, R. N. and K. T. Iyengar (1969). A Nonstationary Random Process Model for Earthquake Accelerations. *Bulletin of the Seismological Society of America 59*, 1163–1188.

Jennings, P. C. and G. W. Housner (1968). Simulated Earthquake Motions. Technical report, California Institute of Technology, Pasadena.

Jensen, H. and W. D. Iwan (1991). Response variability in structural dynamics. *Earthquake Engineering and Structural Dynamics 20*, 949–959.

Jensen, H. A. (1990). *Dynamic Response of Structures with Uncertain Parameters*. Ph. D. thesis, California Institute of Technology, Pasadena.

Johnson, N. L. (1949). System of frequency curves generated by methods of translation. *Biometrika 36*(1), 149–176.

Kameda, H. (1980). Evolutionary Spectra of Seismogram by Multifilter. *Journal of Engineering Mechanics Division, ASCE 101*, 787–801.

Keese, A. and H. G. Matthies (2003). Parallel Computation of Stochastic Groundwater Flow. Technical report, Institute of Scientific Computing, Technical University Braunshweig, Brunswick, Germany.

Kolmogorov, A. N. (1956). *Foundations of the theory of probability*. New York: Chelsea Publishing Company, New York.

Komatitsch, D. and J. Tromp (1999). Introduction to the spectral-element method for 3-D seismic wave propagation. *139*(3), 806–822.

Komatitsch, D. and J. P. Vilotte (1998). The spectral-element method: an efficient tool to simulate the seismic response of 2D and 3D geological structures. *88*(2), 368–392.

Lai, C. G., S. Foti, and G. Rix (2002). Propagation of data uncertainty in surface wave inversion. *Journal of Environmental and Engineering Geophysics 10*(2), 219–228.

Li, C. C. and A. Der Kiureghian (1993). Optimal discretization of random fields. *Journal of Engineering Mechanics Division, ASCE 119, 6*, 1136–1154.

Lin, Y. K. (1965). Nonstationary Excitation and Response in Linear Systems Treated as Sequences of Random Pulses. *Journal of Acustical Society of America 38*, 453–461.

Liu, S. C. (1972). An Aproach to Time-Varying Spectral Analysis. *Journal of Engineering Mechanics Division, ASCE 98*, 243–253.

Loève, M. (1977). *Probability theory*. New York: Springer-Verlag.

Nobile, F., R. Tempone, and C. Webster (2008a). An anisotropic sparse grid stochastic collocation method for partial differential equations with random input data. *SIAM Journal of Num. Anal. 46 (5)*, 2411–2442.

Nobile, F., R. Tempone, and C. Webster (2008b). An anisotropic sparse grid stochastic collocation method for partial differential equations with random input data. *SIAM Journal on Numerical Analysis 46*(5), 2411–2442.

Ostoja-Starzewski, M. and C. Wang (1989). Linear elasticity of planar delaunay networks: Random field characterization of effective moduli. *ASCE Journal of Engineering Mechanics 80*(1-2), 61–80.

Paez, T. L. (2006). The history of random vibrations through 1958. *Mechanical Systems and Signal Processing 20*, 1783–1818.

Parzen, E. (1962). *Stochastic Processes*. San Francisco, California: Holden-Day.

Phoon, K., H. Huang, and S. Quek (2004). Comparison between KarhunenLoeve and wavelet expansions for simulation of Gaussian processes. *Computers and Structures 82*, 985–991.

Rice, S. O. (1944). Mathematical Analysis of Random Noise. *Bell Systems Technical Journal 23*, 282–332.

Roberts, J. B. (1965). The Response of Linear Vibratory Systems to Random Impulses. *Journal of Sound and Vibration 2*, 375–390.

Rosenblatt, M. (1952). Remarks on a multivariate transformation. *Ann. Math. Stat. 23*, 470–472.

Saragoni, G. R. and G. C. Hart (1974). Simulation of Artificial Earthquakes. *Earthquake Engineering and Structural Dynamics 2*, 249–267.

Sett, K., B. Jeremić, and L. Kavvas (2007). The role of nonlinear hardening-softening in probabilistic elasto-plasticity. *International Journal for Numerical and Analytical Methods in Geomechanics 31*, 953–975.

Shampine, L. F. and M. W. Reichelt (1997). The Matlab ODE Suite. *SIAM J. SCI. COMPUT 18*, 1–22.

Shinozuka, M. (1970). Random Process with Evolutionary Power. *Journal of Engineering Mechanics Division, ASCE 96*, 543–545.

Shinozuka, M. and Y. Sato (1967). Simulation of Nonstationary Random Process. *Journal of Engineering Mechanics Division, ASCE 93*, 11–40.

Spanos, P. D. and R. G. Ghanem (1991). *Stochastic finite elements, A spectral approach*. New York: Springer-Verlag.

Spanos, P. D. and L. Lutes (1980). Probability Response to Evolutionary Processes. *Journal of Engineering Mechanics Division, ASCE 106*, 213–224.

Sudret, B. and A. Der Kiureghian (2000). Stochastic Finite Element Methods and Reliability. Technical report, University of California, Berkeley.

Tajimi, H. (1960). A Statistical Method of Determining the Maximum Response of a Building Structure During a Earthquake. In J. Science Council of Japan (Ed.), *Proceedings of Second World Conference on Earthquake Engineering, 1960*, pp. 781–797. Science Council of Japan. Volume 2.

Tatang, M. (1995). *Direct incorporation of uncertainty in chemical and environmental engineering systems*. Ph. D. thesis, MIT.

Trefethen, L. N. (2004). Barycentric Lagrange Interpolation. *SIAM REVIEW 46*, 501–517.

Trefethen, L. N. (2008). Is Gauss quadrature better than Clenshaw-Curtis? *SIAM REVIEW 50*, 67–87.

Webster, C. G. (2007). *Sparse Grid Stochastic Collocation Techniques for the Numerical Solution OF Partial Differential Equations With Random Input Data*. Ph. D. thesis, The Florida State University, U.S.A.

Wen, Y. K. (1974). Nonstationary Seismic Response of Light Equipment. *Journal of Engineering Mechanics Division, ASCE 103*, 1035–1048.

Zhang, J. and B. Ellingwood (1994). Orthogonal series expansion of random fields in reliability analysis. *Journal of Engineering Mechanics Division, ASCE 120, 12*, 2660–2677.

Zhang, Y. and A. Der Kiureghian (1993). Dynamic response sensitivity of inelastic structures. *Comp. Methods Appl. Mech. Engrg. 108 (1)*, 23–36.